

CORRELATION OF MATERIAL CHARACTERISTICS AND WEAR OF POWDER METALLURGICAL METAL MATRIX COMPOSITES

Päivi Kivikytö-Reponen

Dissertation for the degree of Doctor of Science in Technology to be presented with due permission of the Department of Materials Science and Engineering for public examination and debate in Auditorium 1 at Helsinki University of Technology (Espoo, Finland) on the 1st of December, 2006, at 12 o'clock noon.

Helsinki University of Technology
Laboratory of Materials Science
P.O. Box 6200
FI-02015 TKK

Available in pdf-format at <http://lib.hut.fi/Diss/>

© Päivi Kivikytö-Reponen

Cover:

The WC/Co reinforcements of the tool steel based composite are classified by size.
Micrograph is processed with image analysis tool.

ISBN-13 978-951-22-8478-8

ISBN-10 951-22-8478-2

ISBN-13 978-951-22-8479-5 (electronic)

ISBN-10 951-22-8479-0 (electronic)

ISSN 1795-0074

Picaset Oy
Helsinki 2006

ABSTRACT

The wear of materials is a major and widely recognised industrial problem. The direct costs of wear failures, i.e., wear part failures and replacements, increased work and time, loss of productivity, as well as indirect losses of energy and the increased environmental burden, are real problems in everyday work and business.

In this study, the materials of interest are wear-resistant powder metallurgical metal matrix composites, MMCs. Powder metallurgical, P/M, production of material, involving, for example, hot isostatic pressing (HIPing), offers considerable potential for enhanced wear resistance because it has a larger capacity to modify microstructures than conventional production technologies. Martensitic- and tool-steel-based composites were studied with reference to the needs of the mineral industry, while the wear of austenitic- or duplex-steel-based composites was evaluated with reference to those of the energy industry. The wear was studied both in functional wear tests involving a small-scale cone crusher, as well as in laboratory tests, such as the dry sand rubber wheel and erofuge tests.

The correlation between the wear behaviour and the material-related parameters of the steel-based metal matrix composites was investigated. The material-related parameters were microstructural parameters, such as the volume fraction of the reinforcements and hard particles, the size of the reinforcements, the true carbide size of the hard particles and spacing between the reinforcement particles. These parameters are evaluated by varying the matrix material of the composite and by varying the reinforcements in the fixed matrix material. The significantly important parameters that have an effect on the material wear rate were identified. The most important reinforcement-related parameters in these wear environments were the total volume fraction of the hard phase, the spacing between hard particles and the type of the hard phase.

PREFACE

This study was undertaken at the Graduate School on Metallurgy and Metals Technology financed by the Ministry of Education and the Academy of Finland. The first part of the study was carried out during the period 1998 to 2001 at the Laboratory of Physical Metallurgy and Materials Science, Helsinki University of Technology. In the second part of the study, undertaken during the period 2003-2005, the author was located at Metso Powdermet Oy in Tampere. The final work for the thesis was undertaken while working at Metso Powdermet Oy as an employee. I would like to give special thanks to Metso Powdermet Oy for all the experimental materials, as well as agreeing to the subject of study. All parties are acknowledged for their financial support for the work.

I would like to thank the Graduate School Board and, in particular, Professor Tuomo Tiainen from Tampere University of Technology and Professor Pentti Karjalainen from University of Oulu. All my colleagues in graduate school are thanked for their support and comments on the work. Also, my colleagues at Helsinki University of Technology and Metso are thanked with much gratitude.

Professor Simo-Pekka Hannula from Helsinki University of Technology is gratefully thanked for his supervision. I would like to thank my earlier supervisor Emeritus Professor Veikko Lindroos for introducing the field of metal matrix composites. With reference to the laboratory work, my special thanks go to Mr. Jussi Hellman for his help, to Ms. Pirjo Korpiala for all her help, and to Doctor Outi Söderberg and Ms. Ulla Nyman for their invaluable advice. Thanks go to Ms. Sanna Ala-Kleme for her friendship and help during this work and to Mr. Sakari Siipilehto who showed great interest in my field of study. Most of this study was completed at Metso Powdermet Oy. I would like to thank all the personnel, and especially my advisor Doctor Jari Liimatainen, for their helpful conversations and constant support, and President Jouko Pulliainen for making my work financially possible. I would also like to thank Metso Minerals for the experimental practices and all the personnel there who helped in this study. Special thanks go to the experts working in the field: Mr. Jussi Hellman, Mr. Jussi Järvinen, Mr. Jouni Mähönen, and all the operators of the experimental tests who kept the simulative wear tests running. For his scientific advice, I would like to thank Metso specialist Mr. Pekka Siitonen. I also thank my advisor in postgraduate studies and my supervisor in my Master's Degree work, Professor Veli-Tapani Kuokkala of Tampere University of Technology, for his scientific advice and encouragement during the work, and for his help in focussing on the things that matter. Special thanks to Mr. Mikko Hokka and Mr. Tuomo Saarinen.

Very special thanks go to my family. The love and patience of Petri made this work possible and the encouragement of my parents and the joy of my children greatly helped me in my work for this thesis. Friends and other relatives also are thanked gratefully.

Tampere, 3.6.2006

Päivi Kivikytö-Reponen

TABLE OF CONTENTS

ABSTRACT.....	i
PREFACE	v
TABLE OF CONTENTS	vii
1 INTRODUCTION	1
1.1 Abrasive wear phenomenon	3
1.2 Evaluation of the abrasive wear rate or resistance of the material	7
1.3 Improving wear resistance by strengthening and toughening.....	13
1.4 Abrasive wear models and maps	20
1.5 Aim of the study	24
2 EXPERIMENTAL MATERIALS AND METHODS.....	25
2.1 Materials	25
2.1.1 Tested metal matrix composite sets.....	26
2.1.2 Characteristics of selected metal matrix composite materials	28
2.2 Experimental methods.....	35
2.2.1 Dry sand rubber wheel test and erofuge test.....	35
2.2.2 Cone crusher test	35
2.2.3 Other experimental methods.....	38
3 RESULTS.....	39
3.1 Abrasive and erosive wear of steel-based composites.....	39
3.1.1 Abrasive wear rates	39
3.1.2 Erosive wear rates.....	40
3.1.3 Hardness values	42
3.1.4 Worn surfaces after erosive wear laboratory tests.....	43
3.2 Laboratory-scale cone crusher wear tests	45
3.2.1 Wear of the composites with different matrices	45
3.2.2 Wear of the composites with different particle reinforcements.....	47
3.2.3 Wear surfaces after laboratory cone crusher tests	48
4 DISCUSSION	51
4.1 The reliability of data.....	51
4.1.1 The reliability of the wear experiments	51
4.1.2 The scatter and defects of the composite structure.....	54
4.2 Abrasive and erosive wear performance of steel-based composites	56
4.2.1 Dependence of abrasive wear on reinforcement-related parameters.....	56
4.2.2 Dependence of erosive wear rate on reinforcement-related parameters ..	62
4.3 Dependence of cone crusher wear rate on internal material parameters of composite materials	67
4.3.1 Dependence of wear rate on the material carbide type and content.....	67
4.3.2 Dependence of wear rate on the sizes of the reinforcement particles and hard particles.....	73
4.3.3 Dependence of the wear rate on the hardness of SET2 composites	76
4.4 Correlation between cone crusher wear test data and modified split Hopkinson pressure bar test and surface fatigue wear test data.....	78
5 SUMMARY AND CONCLUSIONS.....	83
REFERENCES	87

LIST OF SYMBOLS AND ABBREVIATIONS

A	contact area
A_p	contact area of the particle
A_m	contact area of the matrix
C_1	the sliding wear coefficient
C_2	the squeezing wear coefficient
d	particle size, the carbide/oxide size diameter
d_{HP}	hard particle size
d_{MM}	metal matrix powder particle size
E	elastic modulus
F_N	total applied normal load
F	load
f	volume content
f_{HP}	volume content of the hard particles
f_{MM}	volume content of the metal matrix
H	hardness of material
H_A	abrasive hardness
H_S	surface hardness
HP	hard particle
K	constant in Archard equation
K_c	fracture toughness, critical stress intensity factor
K_{Ic}	fracture toughness of the material in loading type I
MM	metal matrix
N	number of particles
p	pressure
p_{max}	maximum pressure
p_{normal}	normal component of the pressure
p_{shear}	shear component of the pressure
Q	the total volume removed by sliding for a specific distance
R^2	correlation coefficient
R_b	bending strength
s^{-1}	1/second
sp	spacing between reinforcement particles
v	sliding velocity
v_c	carbide volume fraction
Vol.%	volume percent
w	wear per crushing stroke
W_v	wear rate
W_v^{-1}	wear resistance
Wt.%	weight percent
α	symbol for constant in equations
α_3	material-independent constant
α_4	constant
λ	mean free path in the matrix
σ_y	yield strength

AISI	American Iron and Steel Institute
ASM	American Society for Metals
ASTM	American Society of Testing and Materials
AVE	average
B90	Nordberg laboratory cone crusher
BSE	backscattered electron
CIP	cold isostatic pressing
COV	coefficient of variation, standard deviation divided by average and multiplied by 100
CSS	close side setting, CSS is the minimum distance between mantle and the concave at the outlet of the crushing cavity
DC	double cemented
DSRW	dry sand rubber wheel
EP	equal pressure of the phases - wear mode
EW	equal wear rate of the phases - wear mode
HIP	hot isostatic pressing
HP	hard particle
HRC	Rockwell hardness
HV	Vickers hardness
MM	metal matrix
MMC	metal matrix composite
P/M	powder metallurgy
PTA	plasma transferred arc
SEM	scanning electron microscope
SHPB	split Hopkinson pressure bar
SFW	surface fatigue wear
STDEV	standard deviation
UCS	ultimate compressive strength
WCI	white cast iron

1 INTRODUCTION

A progressive loss of material from its surface is called wear. It is a material response to the external stimulus and can be mechanical or chemical in nature. Mechanical abrasive wear is damage of the solid surface due to relative motion between a contacting substance or substances and the solid surface. In this study, industrial wear, i.e., extreme abrasive wear, is examined. It is “multi-mode” wear typical of a specific industrial process such as compressive mineral crushing, involving possibly several “sub-modes” of abrasive wear.

Wear is unwanted and the effect of wear on the reliability of industrial components is recognised widely; also, the cost of abrasive wear has been recognised to be high. Systematic efforts in wear research were started in the 1960’s in industrial countries. The direct costs of wear failures, i.e., wear part replacements, increased work and time, loss of productivity, as well as indirect losses of energy and the increased environmental burden, are real problems in everyday work and business. In catastrophic failures, there is also the possibility of human losses.

Although wear has been extensively studied scientifically, in the 21st century there are still wear problems present in industrial applications. This actually reveals the complexity of the wear phenomenon. Wear can be divided into different wear modes. In the simplest case, only one wear mode is present. In multi-mode wear, more aspects have to be taken into consideration regarding the materials than in single mode wear. However, these circumstances are more difficult to investigate from the scientific point of view.

In this study, materials of interest are wear-resistant powder metallurgical metal matrix composites, MMCs. Important in composite material design is the relationship between external abrasive wear parameters and the microstructural factors of the wearing material, i.e., the spacing between hard particles or hard particle size of the wear surfaces. The use of tailored material microstructures in specific industrial environments could still be more common; however, knowledge of how to design a multi-phase composite for a specific wear system is needed. Powder metallurgical (P/M) production of material, for example, by hot isostatic pressing (HIPing), offers considerable potential for enhanced wear resistance because it has a larger capacity to modify microstructures than conventional production technologies. The multiphase microstructure can consist of several phases, their tailored orientations, volume fractions, shapes, sizes, spacing etc., i.e., the typical design parameters of composite materials.

The benefits of wear-resistant composite material structures have been recognised, and the so-called “double dispersion” type structure in metal matrix composites and hardmetals has been introduced by some research groups [*Berns95a, Berns97a, Berns98a, Berns98b, Berns98c, Berns99a, Berns99b, Berns03a*][*Deng01a, Deng02a*][*Kulu02a*][*Theisen01a, Theisen04a*].

Besides the relationship between wear environment and material structure, there are always other aspects – mechanical reliability of the construction, geometry of the design or the machine, the costs etc. – that are equally important in a wear situation.

Furthermore, when changing the material in a wear environment, other wear-related factors also should be re-evaluated and possibly changed. In many cases, wear-resistant materials may be used as coatings or functionally graded materials (surfaces) because of the cost or unreliability of mechanical properties other than wear resistance. As a conclusion, by combining in material design the *mechanical, chemical and thermal* demands, improved, or possibly optimum, wear resistance could be achieved.

1.1 Abrasive wear phenomenon

According to the ASM handbook [Blau92a], wear can be “1) damage to a solid surface, generally involving progressive loss of material, which is due to relative motion between that surface and a contacting substance or substances. 2) The progressive loss of substance from the operating surface of a body occurring as a result of relative motion at the surface.” In the first definition, surface material may be displaced but not removed. In the second definition, the substance is required to be removed in order to be considered as wear. Surface damage is referred to as “a solid surface resulting from mechanical contact with another substance, surface, or surfaces moving relatively to it and involving the displacement or removal of material” [Blau92a].

The nomenclature of general wear modes differs in the literature. Wear modes recognised as fundamental and major are adhesive wear, abrasive wear, fatigue wear and corrosive wear/tribochemical reaction [Kato01a, ZumGahr87a]. Sub-modes of wear have been introduced, and, in the case of the possible wear phenomenon, the classification into four modes seems to be quite limited, remembering the large variety of different wear environments in reality.

For example, the terminology related to earthmoving, mining and minerals processing, which are all subjects close to this study, has many forms. The dominant wear mode/mechanism is said to be abrasion. In this field, the abrasive wear classifications usually cited include the following sub-modes [Hawk01a]:

- gouging abrasion (the removal of large volumes of material per event from the wear surface),
- high-stress grinding abrasion (i.e., the abrasive particle is crushed during the wear interaction),
- low-stress scratching abrasion (i.e., the abrasive particle remains intact as it moves freely across the wear surface),
- erosion (low-stress scratching),
- erosion-corrosion (low-stress scratching abrasion in a corrosive environment).

According to the ASM Handbook [Blau92a], abrasive wear/abrasion is either

- 1) wear by displacement of material caused by hard particles or hard protuberances or
- 2) wear due to hard particles or hard protuberances forced against and moving along a solid surface.

Abrasive wear is divided sometimes into two-body and three-body abrasive wear, as illustrated in *Figure 1*. Two-body abrasive wear is caused by hard protuberances on the counter face. In three-body abrasive wear, particles are free to roll and slide between two sliding surfaces [Hutchings92a].

Erosive wear/erosion is either [Blau92a]

- 1) loss of material from a solid surface due to relative motion in contact with a fluid that contains solid particles, or
- 2) progressive loss of original material from a solid surface due to mechanical interaction between that surface and a fluid, a multi-component fluid, and impinging liquid, or solid particles.

Erosive wear in which the relative motion of particles is nearly parallel to the solid surface is called abrasive erosion. Additionally, erosive wear in which the relative motion of the solid particles is nearly normal to the solid surface is called impingement erosion or impact erosion [Blau92a]. Erosive wear is in many contexts a sub-mode of abrasive wear. The term *impact wear* has also been used in specific applications where material is under dynamic loading conditions. Wear in the mineral industry case in the present study, i.e., in a cone crusher, is referred to here as multi-mode wear containing the sub-modes of abrasive wear.

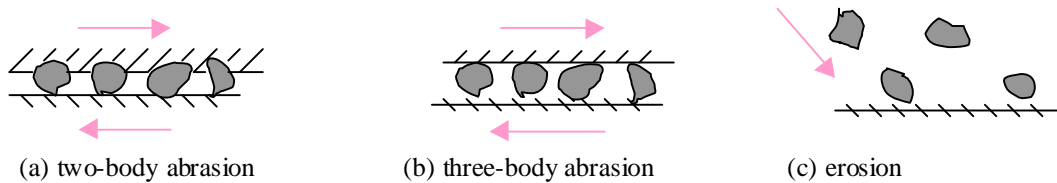


Figure 1 Illustrations of the differences between (a) two-body abrasion, (b) three-body abrasion and (c) erosion, after [Hutchings92a].

The first question in wear research is always how to approach the wear phenomenon. Often wear is considered as a system property [Kato01a]. This is because even slight changes in wear environments (loads, particle size, shape, velocity etc.) may cause changes in the wear rate of a material. In this study, the behaviour of the different materials is evaluated in the particular wear environments, i.e., the wear rate or wear resistance of the material is considered here to be a material-related property.

The definition of abrasive wear is based on the existence of the system with particles and the surface(s); it does not represent wear mechanisms in the scientific way. Mechanisms of abrasive wear on a material surface have been observed to be

- microploughing,
- microcutting,
- microcracking or
- microfatigue

when considering the physical interaction between abrasive particles and surface material [ZumGahr87a]. Principally the same four mechanisms of abrasive wear have been presented by Jacobson and Hogmark [Jacobson96a]: microploughing, microcutting, microflaking and microfatigue. (In Swedish, microplogning, microspånbildning, microflagnig, microutmattning.) The first two mechanisms are the results of ductile material behaviour, while cracking is typical for brittle material behaviour. In microscale, fundamental mechanisms of plastic deformation, crack initiation and crack propagation in materials are widely studied in the field of material science.

Firstly, abrasive wear by *plastic deformation* may involve in principle the first two mechanisms. In ploughing mode, “a ridge of deformed material is pushed along ahead of the particle and no material is removed from the surface.” [Hutchings92a] In cutting mode, material is “deflected through a shear zone and flows up the front face of the (abrasive) particle to form a chip” and all the material is removed in the chip [Hutchings92a]. In the case of ploughing, material is said to flow down the front face

of the (abrasive) particle, while, in the case of cutting, material is said to flow up the front face of the particle. Material may also behave in intermediate mode, called *wedge formation* [Hutchings92a], where “limited slip, or even complete adhesion, occurs between the front face of the particle and a raised prow of material.” This mode leads to the removal of the material.

Secondly, there is the idealised concept of abrasive wear that involves *brittle fracture* (no plastic flow present), brought about through the mechanism of microcracking. Different crack types are formed under different load contacts on the surface. Hertzian conical cracks are formed under blunt, spherical bodies when contact stresses remain elastic. Under point load, high stresses will occur and the indenter generates an elastic-plastic stress field. Under the point load, a median vent crack will form in the brittle material; following this lateral vent crack formation may be observed during unloading. These lateral cracks can directly lead to wear [Hutchings92a]. The angular particles in abrasive or erosive wear will probably result in point loads on the surface of the material.

In surface *fatigue*, material failure can be “characterised by crack formation and flaking of material caused by repeated alternating loading of solid surfaces” [ZumGahr87a], while the single wear event is expected to cause material loss in microploughing, microcutting or microcracking. In abrasive or erosive wear, the repeated sliding or impacting contacts are always present, so the environment for surface fatigue is apparent.

In erosive wear, three basic material-removal mechanisms are classified by Jacobson and Hogmark [Jacobson96a]. These mechanisms can be referred to as follows:

- cutting or chipping erosion (Swedish spånaskiljande erosion),
- fatigue erosion (Swedish utmattningserosion) and
- flaking erosion (Swedish avflagningserosion).

The first two reflect ductile material behaviour, while flaking is a result of brittle material behaviour. In erosive wear by plastic deformation, the dominant wear mode depends on the attack angle and on the shear strength of the interface between the particle and the surface. Differences between ploughing and cutting after Hutchings [Hutchings92a] are shown in the illustrations of erosive wear in *Figure 2*.

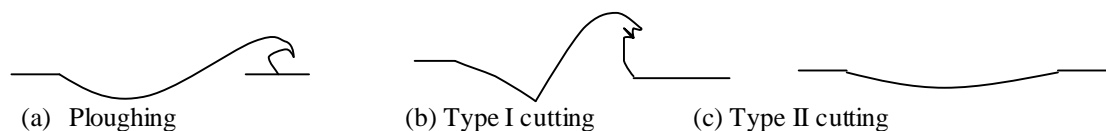


Figure 2 Sections through impact sites formed by hard particles on a ductile metal show typical shapes in erosive wear: (a) ploughing deformation by a sphere, (b) type I cutting by an angular particle rotating forwards during impact and (c) type II cutting by angular particle rotating backwards during impact. The impact direction is from left to right, after [Hutchings79a].

Parameters influencing material wear performance can basically be divided into two groups: *external* parameters, such as type of motion, abrasive velocity, abrasive size, abrasive shape, temperature, atmosphere, external load conditions of the material etc.

and *internal* material properties, i.e., microstructure, hardness, toughness etc. of the wearing material. The material response on the external stimulus, wear, depends on both groups of influencing factors, external and internal, shown in *Figure 3*. Influencing parameters of abrasive wear are discussed in more detail in the next Section, 1.2.

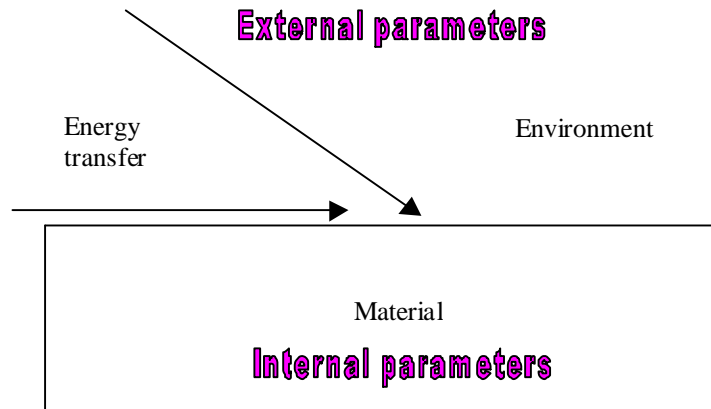


Figure 3 Wear phenomenon with external and internal parameters. The material response on the external stimulus, wear, depends on both groups of influencing factors.

Fundamentally, material can be removed from a solid surface in only three ways: by melting, by chemical dissolution, or by physical separation of atoms from the surface. In mechanical wear, the final degeneration of material and loss of material always involves the fracture of atomic bonds on the surface area. These lead inevitably to the structural evaluation of the materials. The structure and the type of material have a fundamental influence on the deformation and fracture behaviour. Dependence of the tendency for brittle fracture on the electron bond, crystal structure and degree of order is shown in *Table 1*.

Table 1 Relation between basic structure of solids and brittle behaviour after [Hertzberg 96a].

Basic characteristic	Increasing tendency for brittle fracture		
	→		
Electron bond	Metallic	Ionic	Covalent
Crystal structure	Close-packed crystals	Low-symmetry crystals	
Degree of order	Random solid solution	Short-range order	Long-range order

The influence of internal parameters on material wear performance is discussed later in Section 1.3.

1.2 Evaluation of the abrasive wear rate or resistance of the material

The evaluation of material wear rate or resistance is a demanding task because of the endless number of possible wear environments, materials, influencing parameters and variations of them. The material performance may be evaluated through wear tests, which can be categorised as follows:

- single wear event tests, and
- wear tests – for evaluation of steady-state wear behaviour.

Wear tests can be classified as model tests, simplified component tests, component tests, sub-system tests, bench tests or field tests [Jacobson96a]. The degree of realism and the costs of the tests increase from a single wear event test towards field tests and real operations in industry.

Single wear event tests are important in order to understand the material behaviour and basic wear mechanisms involved in the wear system, but they can seldom predict the so-called *steady-state* wear rate. Wear rates and mechanisms can be very different on the virgin surface as compared to those on the worn surface, depending on the materials and their characteristics, for example, work hardening rate. *Wear tests*, i.e., *steady-state wear tests* do have a higher degree of realism in order to estimate material behaviour in a wear environment.

A number of wear tests have been *standardised* in order to obtain reliable or comparable wear results. Nevertheless, slight changes in testing parameters can still have an effect on wear rates and the scatter of them; therefore, results of even standardised tests from different testing laboratories have to be compared with care. A natural sand abrasive having different shapes and compositions is one possible source of the wear test result variation. In a practical wear situation, the applied load might be unknown and various wear modes or sub-modes may act simultaneously with several wear mechanisms present, the relative importance of which cannot be evaluated. Then a practical solution may be *simulative wear testing*. The final reliability of the materials may be found in *field tests* or in the actual wear part usage; however, the costs (and time) increase with the degree of realism and therefore all the wear test levels serve their own purposes. Both wear test types, single wear event tests and steady-state wear tests, are important from the scientific point of view in order to gain a fundamental understanding of wear mechanisms of materials, as well as practical information about the material's performance.

Beside the laboratory abrasive and erosive wear tests, material wear resistance under a cone crusher wear environment is evaluated in this study. A cone crusher can be classified as a compressive crusher type of jaw and gyratory crushers. The basic principle of the cone crusher is presented in *Figure 4*. The principle of crushing relates to more of a kind of compressive crushing motion than that of impactors, where the crushing occurs through impact action. The impact wear of selected materials (including similar types of MMCs than in this study) has been studied by Osara [Osara01a, Osara03a] earlier with an impact hammer device.

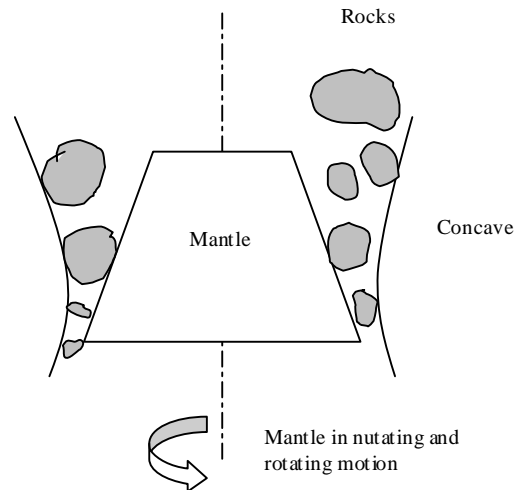


Figure 4 Principle of the cone crusher.

In the cone crusher, the rocks (also called feed) are crushed into the required size fractions by compression in the cavity between the concave and mantle, which is in eccentric rotating motion. Typically, cone crushers are secondary crushers (feed size 100-400 mm) or tertiary/fine crushers (feed size 10-100 mm) in the crushing process, while jaws and gyratories are typical primary crushers with feed size 500-2000 mm [Eloranta95a].

Concerning rock processing, crushing chamber performance is influenced by the following factors [Eloranta95a]:

- shape of the crushing cavity,
- stroke,
- cone shaft speed,
- crusher setting, close side setting CSS,
- crushing force and ratio, and
- feed gradation and moisture.

Evidently, these operating factors, *external* parameters, will affect the wear of the liners beside the used feed/rock. The exact *individual particle* movement in the cavity is unknown, and the particles have variation in sizes and shapes. However, the movement and crushing of the feed is characterised well by the crusher manufacturers. Load patterns in the crushing chamber can be characterised by a load wave rotating around the crushing cavity due to the eccentric rotation [Eloranta95a]. In the present study, the velocities of mantle in the stroke vary between 10 mm/s to 100 mm/s in the laboratory cone crusher, as estimated by the crusher manufacturer.

The geometry of the liners or wear parts (mantle and concave) has been optimised in relation to the final product, crushed stone. When liners are worn and the geometry is changed, the shape of the cavity is also changed. There have been extensive studies and predictions of the worn geometry of wear parts in crushing environments by Lindqvist [Lindqvist 03a, Lindqvist03b, Lindqvist05a]. The material in the liner was manganese steel (1,2% C, 12,5% Mn, 0,6% Si and 1,5% Cr) [Lindqvist03b] and the

work hardening of the wear surface occurred. Also, Ruuskanen [Ruuskanen06a] studied in his doctoral thesis the influence of operating parameters of the cone crusher on the chamber performance and liner wear. The crusher liner materials were manganese steels.

The composite materials studied in this study are new in the present application; it must be remembered that it does take time to launch new materials into the field. According to Berns [Berns03a], the change from ductile manganese steel to white cast iron (WCI) required more than a decade and was accompanied by numerous failures in production and service. A similar period is expected with metal matrix composites (MMCs). In industrial crushing applications other than the cone crusher, the powder metallurgical composite materials have achieved greater resistance to wear than conventional materials [Theisen01a]. The wear protection concept is called HEXADUR[®], and designed for rock grinding, where abrasive (sliding) and indentation movement of the crusher feed is detected.

According to general classification, the wear system is three-body abrasive wear in a cone crusher. In earlier studies, the wear situation is defined as squeezing wear in a cone crusher situation, with small sliding motion [Lindqvist03b]. In the cone crusher wear system, many external (parameters) load directions and load values exist on the wearing material surface caused by the type of rock bed motion. Both sliding and indentation/compression (squeezing) movement of the rocks are expected to occur. Beside the resistance of material to load inputs by indentation/compression, optimisation of the sliding/scratching abrasive wear is important. The wear mechanisms present can be all forms of abrasive wear, i.e., microploughing, microcutting, microcracking and microfatigue, depending on the material.

Influencing parameters in abrasive wear

Several independent parameters related to abrasive particles, wearing environment and target material have an effect on abrasive and erosive wear phenomena. The general factors affecting abrasive wear are summarised in *Tables 2 and 3*, based on [Hawk01a] and [ZumGahr87a], respectively. The effect of separate (influencing) parameters listed in the tables may not be independent of each other. For instance, the change in values of the microstructure-related parameters would change the values of mechanical properties of materials.

External parameters

The *external* parameters have been quite extensively investigated in the field of wear. The wear rate of the material has been observed to be sensitive to the abrasive contact-related, design-related, operating-related and environment-related parameters, classified in *Tables 2 and 3*. The classification of these parameters differs, but all are external parameters from the material point of view. All these parameters describe the transfer of load to the material surface in a certain environment. Notable is that also chemical components are present in so called mechanical wear in real life, e.g., moisture, rain and frost.

Table 2 The factors that influence wear behaviour after [Hawk01a].

Abrasive Properties	Contact Conditions	Wear Material Properties
Particle size	Force/impact level	Hardness
Particle shape	Velocity	Yield strength
Hardness	Impact/impingement angle	Elastic modulus
Yield strength	Sliding/rolling	Ductility
Fracture properties	Temperature	Toughness
Concentration	Wet/dry	Work-hardening characteristics
	pH	Fracture toughness
		Microstructure
		Corrosion resistance

Table 3 Factors of tribological system which influence abrasive wear after [ZumGahr87a].

Design properties	Operating conditions	Type of abrasive	Material Properties
Transmission of load	Contact area	Hardness	Alloy composition
Type of motion	Contact pressure	Acuteness	Alloy microstructure
Shape of the structural parts	Surface condition of the structural parts	Shape	Surface hardening
Degree of lubrication	Degree of lubrication	Size	Coating
Temperature and environment	Temperature and environment	Ductility	
		Wear resistance	

Many “classical” correlations or trends between external parameters and material wear rate have been formed. Abrasive particles with hardness lower than the wearing surface cause much less wear than harder particles, for example. Above a certain hardness ratio, H_A/H_B (H_A is hardness of the abrasive and H_S is hardness of the test surface), the particle can cause plastic deformation. When the observed value is $H_A/H_S > \sim 1.2$, this situation is called hard abrasion, and when $H_A/H_S < \sim 1.2$, the situation is called soft abrasion. The wear rate also depends strongly on the shapes of the abrasive particles. Angular particles generally cause more wear than round ones, for example [Hutchings92a]. In solid particle erosion, the response of the material is traditionally characterised by the impact angle of the particles; material response divides materials into ductile and brittle. Ductile materials commonly show a peak of erosion rate at small impact angles, while the brittle materials often show maximum wear behaviour for normal incidence [Finnie95a].

Internal parameters

Concerning *internal* parameters, wear performance of a material has been widely explained through basic material parameters such as strength and toughness or directly through the structural characteristics of the material. Three material properties, the elastic modulus E , the yield strength σ_y and the fracture toughness K_{Ic} , are most important in low-temperature mechanical design [Courtney00a]. Material properties have been widely correlated with wear [Tylchak92a] and properties like elastic modulus E , hardness H and the fracture toughness K_{Ic} , are generally present in the wear models discussed later in Section 1.4.

In abrasive wear of metals, a good correlation between hardness and wear rate has been reported with many metals, but this may not be the case in all wear modes or even sub-modes of abrasive wear, for example, in erosive wear. The mechanical properties of materials are commonly tested in standard tensile testing machines at the quasi-static strain rate regime [Nemat-Nasser01a], while the wear of material in some cases happens in high strain rate regimes. The material behaviour and the mechanical

properties do change with the strain rate (s^{-1}), because of the differences in dislocation motion at different strain rates based on thermal effects, increasing the dislocation density, re-arrangement of the dislocation structure etc. or phase transformations and twinning. In some wear modes or sub-modes, for example, erosive or impact wear, materials can deform locally under high strain rates. At those the mechanical behaviour of the material has been observed to differ considerably from the situation in quasi-static strain rate regimes [Courtney00a]. The estimated strain rates of materials in erosion of mild steels can be over $10^3 s^{-1}$, depending on the impacting particle size and velocity [Hutchings92a]. Material (wear) behaviour at high strain rates has been investigated with, among others, dynamic impact experiments [Tirupataiah91a] [Sundararajan91a], or, more recently, with dynamic single scratch events [Kuokkala04a] [Hokka04, Hokka04b].

In the case of composites, the material itself is inhomogeneous. There can be several types of second phases with varying properties (size, shape, hardness toughness etc.), and they may also vary in volume fraction and distribution. The microstructural characteristics become exceptionally important as compared to those of conventional materials. This is because the general material properties of the surface, such as hardness, are only “average” values of the surface, while the single wear events are always local. This also means that, in the material’s surface, the local material response to the external wear event differs locally. Some of the phases may behave in the brittle way, some can be ductile during the wear process, while the total material response is the combined effect of the whole microstructure.

Combining external and internal parameters

The material performance depends on the wear conditions, as well as on the internal structure of materials. The homogeneity of the material is highly dependent on the perspective of the viewpoint. In wear, the contact area of the abrasive particle largely defines the homogeneity of the material. A contact area that is large compared to the scale of the material microstructure defines material as homogeneous and vice versa; a contact area of the abrasive that is small as compared to the scale of the material microstructure leads to inhomogeneous behaviour of the material concerning wear. Same material can be defined as homogeneous or inhomogeneous depending on the scale of the wear attack, *Figure 5*.

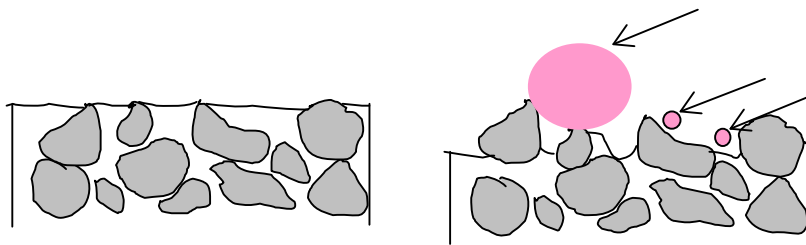


Figure 5 Composite microstructure in relation to abrasive particle size.

In the case of sliding abrasive or erosive wear of a heterogeneous composite, when the abrasive particle is small enough as compared to the scale of composite

microstructure, the binder phase will wear, and eventually the hard particles will fall out of the matrix. In the case of a homogeneous composite, overall abrasion or erosion of the hard phase and binder will occur [*Hutchings92a*]. However, all the wear cases are unique and the wear circumstances, as well as the multiphase materials, may differ. Numerous parameters may influence the wear situation, so the comparison of different wear performances in the literature is unfortunately extremely difficult.

1.3 Improving wear resistance by strengthening and toughening

In many circumstances, wear resistance of material is combined with both optimum material strength (hardness) and toughness properties. The increasing strength (in metallic materials with sufficient toughness) has generally been observed to increase wear resistance in many wear environments. However, increasing strength generally results in loss of toughness. In order to achieve the higher strength and toughness of metallic material, refinement of the microstructure or composite structure is suggested, *Figure 6*.

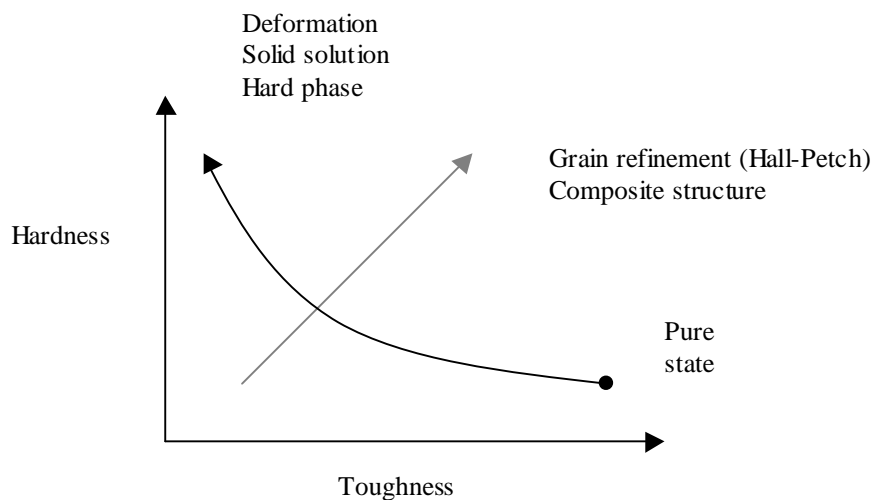


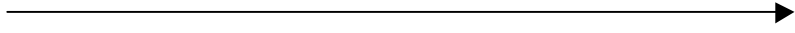
Figure 6 The general hardness vs. toughness relationship of metallic materials, and the effect of the commonly used strengthening mechanisms on this relationship, after [Hogmark01a].

The *strength* of material is, in practise, resistance to plastic flow. Also, *hardness* of metals and alloys is inherently related to plastic flow resistance. Firstly, strength depends mainly on both the atomic structure and microstructure of the alloy. In *Table 4*, the influence of atomic bonding type on the yield strength and ease of dislocation motion in the material is illustrated. Secondly, there are several microstructural ways to improve strength, toughness and wear resistance of materials:

- work hardening,
- boundary strengthening,
- solid-solution strengthening,
- particle hardening (precipitation, dispersion, reinforcements),
- two phase aggregates,
- ductile binder phase,
- double dispersion structures in “Deutsche Zweistufiges Disperiongefüge” [Berns98a], and also
- extrinsic crack-tip shielding mechanism (deflection and meandering, zone and contact shielding).

The efficiency of these strengthening methods in improving the wear resistance depends on the external wear conditions.

Table 4 Influence of bonding type on yield strength after [Roberts04a].
Increasing directionality of bonding: increasing yield stress and hardness



Close-packed metals	Other metals	Ionic compounds	Intermetallic compounds	Covalent bonds
Nearly non-directional bonding	Some directionality in bonding	Bonding by electrostatic attraction: not directional but slip moves strongly charged ions past each other	Ordered structures with fairly directional bonding.	Ceramics: very strongly directional bonding.
Dislocation motion easy	Dislocation motion fairly easy (varies with temperature)	Dislocation motion fairly difficult	Dislocation motion difficult	Dislocation motion very difficult.
Copper, aluminium	Iron, tungsten	NaCl, MgO	CuAl ₂ , TiAl, Ni ₃ Al	Diamond, SiC, Al ₂ O ₃

Hardness of the material has been shown experimentally and theoretically to correlate with *abrasion* rate in pure metals. It is generally thought that the surface of a material is work hardened during abrasion and it has been found that the wear resistance of the metal is proportional to the hardness of the worn surface. However, there are also cases where an increase of the material strength (hardness) does not improve the wear resistance, i.e., there might be a lack of material toughness.

Toughness is resistance of a material against the propagation of a crack. It shows inherently how plastic flow is easy near cracks [Roberts04a]. The area under the stress-strain curve can define toughness. It would be highest, when an optimum combination of strength and ductility is developed [Hertzberg96a]. Toughening mechanisms can be *intrinsic* (basic differences in material ductility and ease of plastic flow) or *extrinsic* (focus in the wake of the crack or ahead of the advancing crack front) [Hertzberg96a].

Improving wear resistance with composite structure

Generally, metallic materials for wear applications have been work-hardening materials or materials with hard phases or particles: manganese steels, white cast irons, steels with precipitated carbides. Other classes of materials, ceramics and polymers are also used. Multiphase materials or composites have been widely noticed to be beneficial in improving wear resistance. The materials combining metallic and ceramic material classes are called metal matrix composites, hardmetals (cemented carbides) or cermets. Different coatings also follow these principles of hard/ductile phase mixtures. The wear resistance of composites and other multiphase materials is generally considered to depend both on strength and toughness.

The microstructure of a composite basically consists of matrix materials and reinforcement(s) in the form of continuous fibre, short fibre, particle or particulate, and the interfaces between the matrix and reinforcements. The variations of the structures consisting of two phases are diverse, *Figure 7*. The composite (dispersion

of two materials) itself can be brittle or ductile. More complicated structures, for instance, those consisting of several types of homogeneous particles or “composite” particles, are called hybrid composites, dual dispersions or double dispersions, for example.

The wear mechanisms and behaviour of the composite structure depend on the combination of the matrix, reinforcing particles or “composite” particles and interfaces. The relationship between structure, matrix and hard particles, and wear environment is highly sensitive. In the present thesis, the matrix is metallic (higher toughness) and reinforcements are ceramic or cermets (higher strength). Basically, the material performance can depend on the weakest link of the structure. Depending on the wear situation and the material, the wear performance can depend mostly on one of the three factors: *matrix, reinforcements or interfaces*, i.e., which one is the “weakest link” in the structure concerning wear. The possible structures of two phases, ductile metal and brittle hard particles, are presented in *Figure 7*.

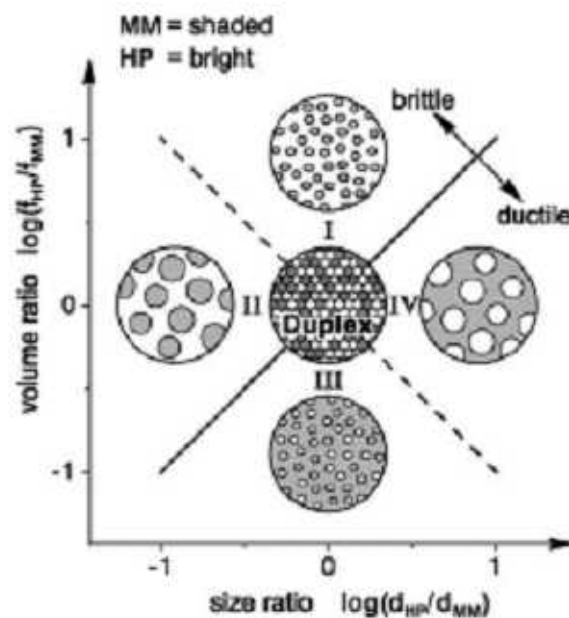


Figure 7 Schematic representation of microstructure of MMC derived from mixtures of near-globular hard particles (HP) and metal matrix (MM) powders of volume content f and size d . I and II are brittle dispersions of MM in HP. III and IV are ductile dispersions of HP in MM. [Berns03a]

Reprinted from an article in WEAR, Vol. number 254 (2003), Hans Berns, Comparison of wear resistant MMC and white cast iron, Pages 47-54, Year 2003, with permission from Elsevier.

In case of *matrix or reinforcements*, the material selection, hard phase distribution or other properties can be carried out so that, at the point of wear, this part of the structure will fail first; this point is then critical concerning wear. The same parameter can both increase or decrease wear resistance of the material. The structure is in the present case a combination of hard and tough phases. A structure that is too hard will

lead to brittle behaviour, and if it is too soft it will lack wear resistance in certain wear environment.

Interfaces represent discontinuities in elastic modulus and thermodynamic parameters, i.e., chemical potential and the coefficient of the thermal expansion. Discontinuity in chemical potential leads to the chemical interaction, i.e., the inter-diffusion zone or a chemical compound formation. When there is a thermal mismatch between the phases in the composite, there will be biaxial or triaxial stress fields present. The role of the bonding between matrix and the interface has been reported to be important. If the interface is weak enough, e.g., if the brittle phases are formed at the interfaces, the reinforcements will “drop” rapidly during wear. The role of the interface may be crucial in that case.

The design of the composite structure is possible with powder metallurgical production technology, which widens and opens new possibilities to design controlled multiphase structures, impossible with conventional technologies. Another practical advantage of the powder metallurgy approach is near net shape manufacturing, especially in the case of wear-resistant materials, which can be very difficult to machine. In a reported application, the composite structure of a roller surface in a high compressive wear system has been shown to have a five to ten times longer service life than traditional surface systems [Theisen01a]. This structure is powder metallurgical multi-material with multi-phase structures of hard and soft components [Theisen04a], having both hard structural groove barriers and ductile environment for cracks to stop.

Powder metallurgical techniques generally are

- sintering,
- powder forging,
- cold isostatic pressing (CIP),
- hot isostatic pressing (HIP),
- spray forming,
- plasma transferred arc (PTA) welding and
- different coating technologies.

Concerning *abrasive wear*, *hard particles* have for a long time been known to impede the wear that occurs by grooving or indenting, while metallic matrix has provided sufficient toughness. The addition of hard particles means an increase in material hardness and/or addition of sliding barriers. In the case of composite materials, wear resistance is often influenced by the microstructure-related factors, such as the volume fraction, the size and the orientation of the particle reinforcements.

One of the widely used parameters in determining the effect of the microstructure on the wear behaviour is *the volume fraction of the hard phase*, v_c , (or binder content). The use of this parameter in case of multiphase materials, metal matrix composites, hardmetals or cermets with material wear behaviour is reported in several studies of abrasive wear [Axen94a, Axen95a] [Colaco03a] [ZumGahr87a] [Lee02a] [Pagounis96a] [Dogan01a] [Pirso04a] [Kubarsepp01a] and in erosive wear [Hovis86a] [Hussainova03a] [Kulu04a] [Levin00a] [Stack97a, Stack99a] [Shin87a].

The importance of *hard particle size*, d , as well as *spacing*, sp , is concerned in wear. The improvement of wear resistance against grooving requires that the hard particles are at least as large as the grooving width. In rough abrasion, the metal matrix composites with 50 to 100 μm reinforcement particle size have shown good performance [Berns95a]. In addition to the erosive wear dependence on material characteristics, the erosive wear of material is strongly dependent on the direction of applied force, which may be oblique (small or medium angle) or normal. The variation of impacting angles of abrasive particles/force leads to different micromechanisms of wear, verified with MMCs recently by Veinthal [Veinthal05a].

One important parameter in the wear of composite materials is the scale of the individual contacts, which can be expressed either as the ratio between *the area of the contact zone that the abrasive particle makes with the wearing surface and the reinforcement/hard particle size or the spacing between the reinforcement/hard particles*. This ratio also takes into consideration to some extent the impact angle of erosive particles, supposing that the particles make different contact zones at different impact angles.

The mechanical properties of composite materials are highly dependent on *hard particle size* and *spacing*. Mechanical failure of metal matrix composites has been investigated e.g. by Broeckmann [Broeckmann96a]. Hard phase cleavage and decohesion are the primary failure mechanisms observed under external load. Theoretically, bending strength, R_b , decreases with the increasing mean hard particle size, d_{HP} [Berns98b], *Figure 8a*. The ease of cracking increases with the hard particle diameter, thus lowering the fracture strength.

The *toughness* properties of the composites are also highly dependent on the structure of the materials. The toughness of metal matrix composites depends on, among other properties, the size, the amount and the distribution of the hard particles [Berns98c]. Earlier studies of microstructures of MMCs in wear environments [Berns 97a] have revealed that contacts between hard particles in duplex or net-like distribution lower the fracture toughness. It is assumed that, if hard particle spacing is larger than the size of the stressed zone at the crack tip, the fracture toughness is improved, *Figure 8b*. The fracture toughness increases with the reinforcement size in a particulate reinforced composite. This will lead to double dispersion microstructure discussed later (the benefit of the larger reinforcements, however, keeping the actual/true hard particle size small, without the loss of the fracture toughness and bending strength values). [Berns03a]

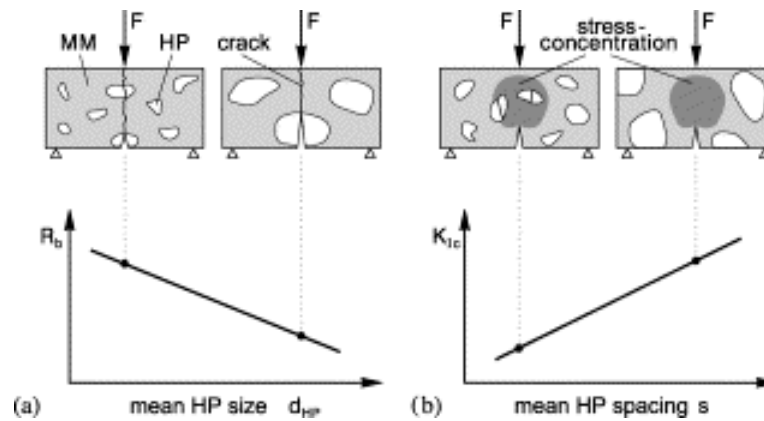


Figure 8 Schematic presentation of bending strength R_b and fracture toughness K_{Ic} in dependence on the HP size and spacing at a given HP content. [Berns03a]

Reprinted from article in WEAR, Vol. number 254 (2003), Hans Berns, Comparison of wear resistant MMC and white cast iron, Pages No. 47-54, year 2003, with permission from Elsevier.

One of the most interesting parameter-related microstructural factors is a *distribution* of the phases, visualised in *Figure 9*. Modification of the distribution has certain advantages in wear environments where, besides the grooving, toughness is needed. With the modification of distribution, keeping the volume fraction of the harder phase constant, the properties and performance of the material can be changed. The properties, microstructure and wear of steel matrix composites, especially so-called *double dispersion* have been investigated systematically by Berns et al. [Berns95a, Berns97a, Berns98a, Berns98b, Berns98c, Berns99a, Berns99b, Berns03a]. Kulu et al. [Kulu02a] have studied similar double dispersion structures of the cermets, hardmetals, composite alloys and coatings. Double dispersion structure of WC/Co, called dual composite, hybrid composite or double cemented, DC, has been studied by Deng et al. [Deng01a][Deng02a]. It is pointed out by Jacobson and Hogmark [Jacobson96a] that double dispersion type distribution of the small hard particles behaves similarly to bigger reinforcements in abrasive grooving action, while evenly distributed small particles will not hinder bigger abrasive particles. In the structure of clustered small hard particles, the catastrophic brittle fracture is not as easy as in the structure of the large solid reinforcements in the matrix. Osara [Osara01a,] among others, studied the wear behaviour of materials of a type similar to those in the present study in several environments: abrasive, impact abrasive and impact. In pure abrasion, double dispersion type composite behaved well among the other composites. In impact type tests, the wear behaviour was highly dependent on abrasive mineral, type of mineral and size.

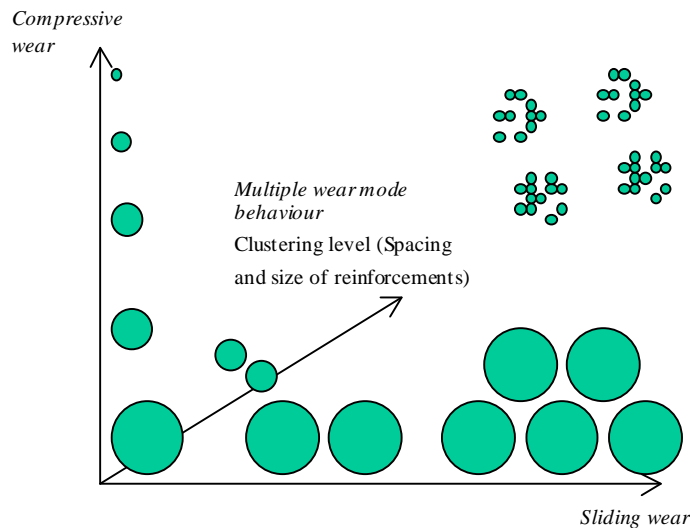


Figure 9 Schematic presentation for optimising the structure of the composites for specific wear environment. The example deals with combined compressive and sliding wear.

The structural idea of double dispersion structure of metal matrix composite was proposed by Berns [Berns98b, Berns98c, Berns03a] for increased toughness in, for example, metal forming tools. This structure has also been proposed to be beneficial for certain applications in the crushing industry [Theisen01a, Theisen04a] and in earth-boring applications [Fang01a]. In these applications, both an increase in strength and toughness is achieved. Hardmetals are known as wear (abrasion and erosion) resistant materials consisting of the small hard particles in the soft metallic binder phase. Concerning hardmetals, the dependence of the impact angle on wear in erosion has been studied by Kulu et al. [Kulu02a]. In the case of impact erosion at an oblique angle, the hard phase should exceed 50% (in cermet coatings). At normal (90°) impact angles, the microcracking, or fatigue, may dominate, and here the role of toughness becomes more important. For these situations, the hard phase content should be less than 50%, after Kulu [Kulu02a]. In the case of a mixed direction of applied force, the structures of double dispersion type are profitable, and therefore, in the erosion with mixed wear mode, double cemented coatings are suggested [Kulu02a]. Generally, “the optimal” composite reinforcement content relating to material wear resistance depends on the wear conditions.

In this study, the tool-steel-based WC-Co hardmetal composites are examples of materials with a double dispersion type of microstructure. The principle of these materials is described in a patent “Method for making tool steel with high thermal fatigue resistance” in 1994 by Runkle [Runkle94a]. The composites of tool steels and WC cermets or WC ceramics fall into the intermediate region in the hardness and toughness properties of the components in the composite.

1.4 Abrasive wear models and maps

In the case of the composites, the effect of the microstructure on material wear behaviour is important. The volume fraction, shape, size and distribution of the reinforcement, as well as the spacing between the reinforcement particles or mean free path, have considerable importance. The type and art of the matrix/binder combination, interfaces and hard phases affect the material wear resistance, not to mention the internal stress state of the composite. The material response depends on the wear system of concern; abrasive particle size and real contact area, for example, are parameters defining the wear system. It seems to be impossible to find “general microstructure-related law” applicable in all the wear systems, because of large variations in materials and systems.

A survey of macroscopic wear models and equations show the trend of handling wear as a system property in the past, but, more recently, the material characteristics have gained a more important role in the evaluation of the wear of materials. Wear models and predictive equations are summarised by Meng and Ludema [*Meng95a*]: The number of different wear equations is large; over 300 equations for friction and wear can be found. *Empirical equations* were common before 1970. *Contact-mechanics-based* equations were common in the years 1970-1980 and the famous Archard equation was introduced into the books on wear phenomena. After contact-mechanics-based equations, *failure-mechanism-based* theories were developed.

Material properties (hardness and toughness) are classically related to wear. For example, the Archard equation (1953) (also known as the Rabinowicz equation) for adhesive and abrasive wear is an old and widely accepted, referred and modified equation. It combines external applied load and hardness of the material. The total volume removed per unit sliding distance Q is

$$Q = \frac{KF_N}{H}, \quad (1)$$

where F_N is total applied normal load, H is the indentation hardness of the wearing material and K is a constant. In practise, better correlation is found between wear resistance and hardness of the surface (after work hardening) than the hardness of the bulk. Models of the materials with more *brittle behaviour* take the fracture toughness and elastic modulus into consideration. The following model for the abrasive wear is based on the *lateral cracking* [*Hutchings92a*]: volume wear rate per unit sliding distance Q due to all particles involved is

$$Q = \alpha_3 N \frac{(E/H)F^{9/8}}{K_C^{1/2} H^{5/8}}, \quad (2)$$

where α_3 is a material-independent constant, N is the number of particles each carrying load F and E is elastic (Young) modulus. K_C is the fracture toughness of the material. In another approach, volume wear rate per unit sliding distance is

$$Q = \alpha_4 N \frac{F^{5/4}}{K_C^{3/4} H^{1/2}}, \quad (3)$$

where α_4 is a constant.

The relationship between structure and wear resistance has been evaluated by several researchers in the case of composite materials. The knowledge of the properties of the pure phases can be taken into account. For example, according to [ZumGahr87a], wear resistance W_v^{-1} in the pin abrasion test with garnet can be related to the carbide size d , carbide volume fraction v_c and mean free path λ in the matrix as follows. The data obtained for analysis was from white cast irons.

$$W_v^{-1} \propto \frac{d^{3/2} v_c}{\lambda}. \quad (4)$$

Erosive wear, classified as a sub-mode of abrasive wear, involves a stress system of complex nature, large local plastic deformations and high strain rates. This makes erosive wear difficult to study; no universally accepted overall model exists. Bingley et al. [Bingley04a] have examined and compared the erosive wear models (for metals) of Hutchings and Sundararajan in order to test their predictive capabilities. In the Sundararajan model, the erosion rate is dependent on the depth of the plastic zone produced [Sundararajan91a], while the model of Hutchings [Hutchings92a] is developed by solving the equations of motion for a particle impacting a target surface. None of the tested models was completely satisfactory in predicting wear rates [Bingley04a], perhaps because of the limiting factors in the model and the selection of experimental materials and angular erosive particles used.

Models of abrasive wear for two phase or multiphase materials have been developed by using the inverse rule of mixtures or by using the linear rule of mixtures. The parameter influencing the wear resistance is generally the volume fraction of the hard phase. The wear models for composites can be found for abrasives in the literature [Lee02a, Axen94a, Axen95a, Colaco03a, ZumGahr87a]. Recently erosive wear of composites has been characterised and modelled by Veinthal [Veinthal05a].

A model of abrasive wear resistance of multiphase materials by Axen et al. [Axen94a, Axen95a] estimates the upper and lower limits for the wear resistance of the composites using linear and inverse rules of mixtures. Their model defines two modes of abrasive wear, differing in the distribution of the load of the two phases. The two modes, equal wear rate, EW, of the phases and equal pressure of the phases, EP, both start from Archard's equation Eq. (1) and follow with rules of mixtures. According to Axen [Axen94a], EW assumes that the linear wear rates of each phase in a composite, and of the composite as a whole, is/are equal. In EW mode, the reinforcing phase carries the maximum possible fraction of the load. When the reinforcing phase is carrying the minimum part of the possible load, the load is uniformly distributed. This follows to the EP condition, equal pressure on the phases. Concerning wear resistance, the specific wear resistance under EW is

$$W_v^{-1} = \frac{A_p}{A} W_{vp}^{-1} + \frac{A_m}{A} W_{vm}^{-1}, \quad (5)$$

and specific wear resistance under *EP* is

$$W_v^{-1} = \left(\frac{A_p}{A W_{vp}^{-1}} + \frac{A_m}{A W_{vm}^{-1}} \right)^{-1}, \quad (6)$$

where A_p is the area fraction of the particle and A_m is the area fraction of the matrix, i.e. A is the total contact area. The specific wear resistance of the particles is W_{vp}^{-1} and of the matrix is W_{vm}^{-1} . Wear modes EW and EP are plotted in terms of volume loss in *Figure 37* in Section 4.2.1.

Mart Lindqvist [*Lindqvist05a*] has developed cone crusher wear models that can predict the worn geometry of manganese steel liners and crusher performance. His models are based on the Archard equation (1) with modifications. Both sliding and squeezing wear have been taken into account based on the wear mechanism analysis of manganese steel liner. The wear rate per crushing stroke is expressed as in (7).

$$\Delta w = \frac{1}{C_1} \int_0^t p v dt + \frac{P_{\max}}{C_2}, \quad (7)$$

where p is the pressure, v is the sliding velocity, C_1 is the sliding wear coefficient and C_2 is the squeezing wear coefficient. The values found for wear coefficients using quartzite were $C_1=208$ KN/mm² for the sliding wear, and $C_2=274$ kN/mm³ for squeezing wear [*Lindqvist05a*]. While in a cone crusher the sliding wear component was analysed to be minimal, the wear equation is reduced to contain only the squeezing wear component. In addition, shear forces were taken into account in further model modifications. A strong relationship between particle size (and shape) and wear rate in compressive crushing was found in the third modification of the model.

Wear maps can express wear resistance or behaviour of materials. Wear map research was developed originally in order to get a wear classification system for ceramics and to provide a database sufficient for wear models. The challenge and the difficulty is the selection of the parameters presented in the map. They have to be the most important and limited in number. It seems unrealistic that a single universal parameter fits all the wear data presented [*Blau04a, Hsu01a, Lim98a, Williams 99a*].

For MMCs, the wear mapping at elevated temperatures and in corrosive conditions has been done extensively by Stack et al. [*Stack97a, Stack01a*]. In these maps, the external and internal parameters related to wear are combined in a visual form; they may serve well the material selection in the specific industrial applications. Studies on cemented carbides have revealed that the dominant mechanism of erosion (and abrasion) depends on the scale of individual contacts discussed earlier [*Hutchings92a*].

The general criticism of wear models is that they can take into account only a limited number of influencing factors. As there are no universal mechanisms of wear, quantitative models are applicable to restricted systems and materials [Williams99a]. The danger of oversimplifications as well as (interpolation and) extrapolation of the wear data can arise [Blau04a]. The challenge is to find the most important parameters with acceptance of limiting the influencing factors in wear research. For complex structures in complex wear system, this is a demanding task.

1.5 Aim of the study

Abrasive wear is a common wear type in industrial applications. In this work, the wear of metal matrix composites is studied, for example, in demanding rock-crushing wear environments. In crushing applications, the currently used material for wear parts is the well-known Hadfield manganese steel. However, metal matrix composites are considered as potential new materials for these applications. Composite structures have been commonly noticed to improve the wear resistance. The aim of the composite structure is to reach performance that cannot be obtained with homogeneous structure or with single components of the structure.

The experimental materials in the study are powder metallurgical steel-based composite materials reinforced with ceramic or hardmetal particles. Wear in a cone crusher environment is under evaluation with selected martensitic and tool-steel-based composites for mineral industry needs. Wear of austenitic- or duplex-steel-based composites is evaluated in dry sand rubber wheel abrasive and erofuge tests. These stainless- or duplex-steel-based composites are designed for energy industry applications and they were developed during the “Materials for Energy Technology in Finnish, KESTO Technology Programme” of Tekes, The National Technology Agency of Finland.

The purpose of this study is to investigate the correlation between wear behaviour and the material-related parameters of the steel-based metal matrix composites. The material-related parameters are microstructural parameters, such as volume fraction of the reinforcements or hard particles, size distribution of the hard particles and spacing between hard particles. The aim is to define and evaluate the important parameters that have a significant influence on the material wear rate, and also the quantitative laws between wear rates and internal parameters, if possible. These parameters are evaluated by varying the matrix material of the composite and by varying the reinforcements in the fixed-matrix material. The external wear conditions were kept fixed in order to define the effects of the material-related parameters on wear rates. The internal parameters are supposed to be extremely important for the composite material wear performance. One of the most important parameters is expected to be the volume fraction of the hard phase.

Furthermore, comparisons between cone crusher wear data obtained with granite stone and other available wear data (split Hopkinson pressure bar test and surface fatigue wear test) have been made in order to find out whether these laboratory tests could “estimate” the material ranking order in the cone crusher wear test.

2 EXPERIMENTAL MATERIALS AND METHODS

2.1 Materials

The metal matrix composites, MMCs, studied here are powder metallurgical, P/M, materials. The materials tested in laboratory abrasive and erosive wear testers (SET1) were austenitic and duplex steel-based composite materials reinforced with Al_2O_3 or Cr_3C_2 ceramics. The composites tested in the laboratory-scale cone crusher (rock crushing) were divided into two sets (SET2 and SET3). In SET2, the steel matrices varied, but the composites were mainly reinforced with recycled WC/Co hardmetal. In SET3, the steel matrix used was tool steel, containing vanadium carbides to increase wear resistance. Reinforcements were WC and TiC ceramics and WC/Co hardmetals. The nomenclature of steel-based composites with WC/Co hardmetal reinforcements is established as composites with double dispersion, differing from the composites of a simple structure.

The production of P/M materials was carried out by hot isostatic pressing, HIP, consolidation. Different powders have been mixed together using dry mixing or wet mixing. In wet mixing, easily evaporating liquid additive is used to ease the particle mixing. After mixing, the powder is filled in capsules, which are evacuated and closed by welding. The capsule is consolidated at high pressure and temperature by the hot isostatic pressing (HIPing) technique. The typical HIP cycle for steel-based composite materials is carried out at 1150 °C, at a pressure of 100 MPa and for a holding time of three hours. The structure of the material and the thickness of the diffusion layer can be affected by HIP cycle selection. The HIPed product will normally offer distinctive advantages in terms of finer grain size and homogeneous microstructure with less segregation and no porosity as compared to conventional casting technology. On the other hand, HIPed products can be easily tailored by microstructure, i.e., by manufacturing evenly distributed double dispersions, or tailored by macrostructure as gradient or multi-metal constructions. HIPing and heat treatment are carefully designed by the manufacturer in order to achieve the optimum internal structure. Composite heat treatments are shown in *Table 5*. The composite materials are described in more detail in Tables 6, 7 and 8.

Table 5 Heat treatments of materials in SET1, SET2 and SET3 in the studied wear experiments.

Materials	Annealing	Quench	Temper
Tool-steel-based composites	Hold 1080 °C 1 h	N gas quenching	Double tempering 2 h 570 °C air cooling
9980-steel-based composites	Hold 1010 °C 2 h	Air cooling	Hold 3 h 580 °C air cooling
2218-steel-based	Hold 900 °C 2 h	Air cooling	Hold 3 h 580 °C air cooling
Manganese-steel-based	Hold 1040 °C 2 h	Air cooling	
MM15 composite	Hold 1080 °C 2 h	Water quench	
AISI 316L-based-composites	Hold 1040 °C 1 h	Air cooling	
Duplex 27-based-composite	Nominal 1050-1100 °C/ 1 hour/25 mm	Water quench	
APM 9935-based-composite	1075 °C 0,5 h (Al_2O_3) 1180 °C 0,5 h (Cr_3C_2)	Water quench	

2.1.1 Tested metal matrix composite sets

Three different sets of materials were selected for this work. Materials in SET1 are austenitic- or duplex-steel-based P/M composites. The only conventional material in this SET1 was the commercial reference material 253MA. It is an austenitic high-temperature steel delivered as a cold-rolled bar. Composite matrix materials were AISI 316L austenitic stainless steel, super-duplex stainless steel Duplok 27 (ferrite and austenite content was not measured, it is usually around 50%:50%) and heat-resistant stainless steel APM 9935 (the chemical compositions are given in *Table 9*). The reinforcements were angular Al_2O_3 and Cr_3C_2 particles. In composite structures, the Al_2O_3 reinforcements kept their original angular shapes and no visible reaction layers between reinforced particles and matrix material were present in optical micrographs. Between Al_2O_3 and austenitic matrix no interfacial reactions have been observed by TEM investigations in earlier studies [*Pagounis98a*]. However, in earlier studies, Cr_3C_2 has been reported to change during HIPing, probably to Cr_{23}C_6 and Cr_7C_3 phases [*Heinonen00a*]. The distribution of the Al_2O_3 reinforcements was homogeneous, but some networking was observed in the case of Cr_3C_2 . Symbols and compositions of the SET1 composites are given in *Table 6*.

Table 6 Symbols and compositions of the materials in SET1.

Symbols	Matrix material	Matrix Vol.%	Reinforcement material	Reinforcement Size (μm)	Reinforcement Vol.%
316L	AISI 316L	100	-	-	-
316LA	AISI 316L	65	Al_2O_3	105-149	35
D27	Duplok 27	100	-	-	-
D27C3F	Duplok 27	70	Cr_3C_2	10-45	30
253MA	253 MA	100	-	-	-
APM	APM 9935	100	-	-	-
APM2A	APM 9935	80	Al_2O_3	105-149	20
APM4A	APM 9935	60	Al_2O_3	105-149	40
APMC1F	APM 9935	90	Cr_3C_2	10-45	10
APMC2F	APM 9935	80	Cr_3C_2	10-45	20
APMC3F	APM 9935	70	Cr_3C_2	10-45	30
APMC1C	APM 9935	90	Cr_3C_2	45-106	10
APMC2C	APM 9935	80	Cr_3C_2	45-106	20
APMC3C	APM 9935	70	Cr_3C_2	45-106	30
APMC4C ¹	APM 9935	60	Cr_3C_2	45-106	40

¹HIPing cycle was shorter, 1h instead of 3h.

In SET2, tool steels (WR4, WR6 and WR7), martensitic steels (Rallo 9980 and 2218) and manganese steel (Hadac) were used as matrices. Their nominal composition is presented in *Table 9*. Recycled tungsten carbide/cobalt hardmetal was used as a particulate reinforcement. Normally the matrix is softer, and reinforcements harder materials in these testing sets. However, in the composite MM15 manganese steel was the reinforcement, which is a softer component as compared to the matrix material, high vanadium tool steel. All the WC/Co reinforced metal matrix composites in SET2 were double dispersion type. This set was designed to evaluate the role of the matrix in the composite structure, while the reinforcing particles were kept fixed. The composites in SET2 for the cone crusher test are introduced in *Table 7*.

In SET3, the matrix metal was a high-vanadium tool steel and the role of the reinforcement was the focus of interest. Different reinforcements were used: tungsten carbide cast particles (WCS), recycled and crushed WC/Co hardmetal, WC/Co dense-coated (WC particle with cobalt) reinforcements and TiC particles. Symbols of the

composites in testing program SET3 are presented in *Table 8*. The nominal chemical compositions of all the matrix steels in SET1, SET2 and SET3 are presented in *Table 9*. The interfaces between tool steel and WC/Co particles has been studied by Lou et al. [*Lou02a*] [*Lou03a*] and the material microstructures in SET2 and SET3 has been studied in the present study and by Ala-Kleme [*Ala-Kleme04a*]. Generally, the shapes of the reinforcements vary from the flat and long to the more round or square, depending on their prior shape and quality. Some defects, fractures or clustering of the reinforcements have been observed in the prepared samples of the same materials as actual cone parts. The prior powder particle boundaries were visible in many of the tool steels with recycled hardmetal, as well as in other steel-based composites. Besides the size, the shape (from angular to more round) and the structure (from hardmetal to completely monolithic) of particle reinforcements varied. A closer description of these materials will be given in Section 2.1.2.

Table 7 Symbols and compositions of the materials in the cone crusher tests, SET2. SET2 was designed for testing the role of the matrix.

Symbols	Matrix	Matrix Wt.%	Reinforcement	Reinforcement Wt.%	Reinforcement Size (µm)	HV matrix Nominal
WR6WC	WR6 ^A	75	WC/Co ^C (10%)	25	200-400	695
WR4WC	WR4 ^A	75	WC/Co ^C (10%)	25	200-400	575
9980aWC	9980 ^B	75	WC/Co ^C (10%)	25	200-400	320
9980bWC	9980 ^B	65	WC/Co ^C (10%)	35	200-400	320
2218WC	2218 ^B	75	WC/Co ^C (10%)	25	200-400	170
HadacWC	Hadac ^B	75	WC/Co ^C (10%)	25	200-400	Work harden
MM15	WR7 ^A	65	Hadac ^B	35	63-177	790
WR6	WR6 ^A	100	-	-	-	695

^ARalloy® WR6 and WR4 by Metso Powdermet Oy,

^BRalloy® 9980, 2218 and

Hadac 120 by Metso Powdermet Oy,

^CRecycled hardmetal by Tikomet Oy .

Table 8 Symbols and composition of the materials in SET3, designed for testing the role of the particle and particulate reinforcements.

Symbol	Matrix	Matrix Vol.%	Reinforcement	Reinforcement type after manufacturer	Reinforcement Vol.%	Reinforcement Size (µm)
30WCSf	WR6 ^A	70	WC ^D	WCS cast	30	45-90
20WCSf	WR6 ^A	80	WC ^D	WCS cast	20	45-90
30WCSc	WR6 ^A	70	WC ^D	WCS cast	30	250-425
20WCSc	WR6 ^A	80	WC ^D	WCS cast	20	250-425
30WCF	WR6 ^A	70	WC/Co ^C (10%)	recycled	30	100-200
30522dcf	WR6 ^A	70	WC/Co ^D	dense coated	30	45-90
30522dcc	WR6 ^A	70	WC/Co ^D	dense coated	30	200-300
30TiCf	WR6 ^A	70	TiC ^D		30	75-250

^ARalloy® WR6 by Metso Powdermet Oy,

^CRecycled hardmetal by Tikomet Oy,

^DCeramics by H.C. Starck GmbH.

Table 9 Chemical contents of the matrices presented as nominal compositions given by manufacturer.

Symbol	C Wt.%	Cr Wt.%	V Wt.%	Mo Wt.%	Mn Wt.%	Ni Wt.%	Co Wt.%	Si Wt.%	Fe Wt.%	Other Wt.%
WR4 ^A	1,8	5,25	9,0	1,3	<0,5			0,9	Bal	
WR6 ^A	2,90	5,25	11,5	1,3	<1,0			<1,0	Bal	
WR7 ^A	3,40	5,00	14,50	1,3					Bal	
9980 ^B	0,03	15,3	0,15	0,9	0,75	5,3	0,1	0,45	Bal	W 0,1; Cu 0,40
2218 ^B	0,1	2,3		1,0		0,7			Bal	
Hadac 120 ^B	1,1-1,3	2,0-3,0	0,4-0,5	<2,0	10,0- 12,0	<1,0		<1,0	Bal	P <0,050; S 0,040; Cu <0,20
316L	0,02	17,2		2,8	1,3	13,8	0,2	0,7	Bal	Cu 0,3
Duplok 27 ^C	0,02	26,1		3,3	1,1	6,6	0,1	0,4	Bal	
APM 9935 ^C	0,09	21,19		0,19	0,61	11,1	0,15	1,73	Bal	Cu, Al, Ti, W, N
253 MA ^D	0,09	20,78		0,20	0,6	10,96		1,7		N, Ce

^ARalloy® WR6, WR4, WR7 by Metso Powdermet Oy,

^BRalloy® 9980, 2218 and Hadac 120 by Metso Powdermet Oy,

^C by Metso Powdermet Oy,

^D by Avesta Sheffield, now Outokumpu Stainless

2.1.2 Characteristics of selected metal matrix composite materials

One purpose of the study is to evaluate the role of the reinforcement particles on material wear behaviour. Composites in SET1 have only a few varying internal parameters. Most of the matrices are austenitic, however with different compositions. Few volume fractions of the specific reinforcement type and size are studied in these matrices. Additionally, two types of reinforcements and three differently sized fractions are used. As a contrast to SET1, materials in SET3 have several varying parameters, i.e., reinforcement type, shape, structure, size and volume fraction. Four composites – 30WCSf, 20WCSf, 30WCSsc, 20WCSsc – have WC particle reinforcements with cast structure. Other WC-based reinforcements have more or less composite structure. Recycled WC/Co hardmetal powder is used as reinforcement in most of the composites (SET2 and 3). Recycled (WC/Co with nominal 10% Co) hardmetal powder was produced through a zinc process, where recycled hardmetal scrap is pulverized, by the company Tikomet Oy of the Tikka Group [Tikomet06a]. The recycled hardmetal appeared to have a porous or lamellae, as well as a normal, hardmetal structure, *Figure 11 and 12*. Other WC/Co powders are also used, where WC particle is densely coated with cobalt. This grade is having a rounder shape in the final structure; however, porosity in the carbides is observed. Titanium carbide reinforcement with 30 vol.% was used in one composite, 30TiCf. The shape of the most ceramic reinforcement particles is irregular, but mostly angular. The main microstructural parameters related to the structural variation of the composites in SET1 are given in *Table 10*. The nominal reinforcement size, d , is used, i.e., the particle diameters were in the range 105-149 μm in the case of aluminium oxide, 10-45 μm and 45-106 μm in the case of chromium carbide, respectively. Spacing, sp , between reinforced particles is calculated based on the assumption of evenly distributed reinforcements taking into account the volume fraction and size of the reinforcements.

Table 10 The microstructural parameters of the composite materials, SET1.

Composite material	Reinforcement Size min (μm)	Reinforcement Size max (μm)	Spacing between reinforcements min (μm)	Spacing between reinforcements max (μm)
316LA	105	149	52	74
D27C3F	10	45	6	28
APM2A	105	149	103	146
APM4A	105	149	42	60
APMC1F	10	45	18	81
APMC2F	10	45	10	44
APMC3F	10	45	6	28
APMC1C	45	106	81	191
APMC2C	45	106	44	104
APMC3C	45	106	28	65
APMC4C	45	106	18	42

Some carbide characteristics of the tool steel-based matrix material and reinforcements are depicted in *Tables 11* and *12* for composites in SET2 and SET3. In the case of SET2, the fraction of the reinforcements was given in weight percents by the manufacturer. The area fractions of the reinforcement particles and the true carbide sizes were evaluated through image analysis techniques. Material characterisation was carried out from materials made in the same production batch as the actual wear-testing components. The microstructure was expected to be similar in all samples in the batch. The optical and scanning electron microscope, SEM, pictures from the samples were analysed by the image analysing program *UTHSCSA Image Tool [UTHSCSA04a]*. The image analysing was performed by manual and automatic operations of the program. The threshold operation of the pictures was made manually. (The Threshold command is used to create a binary image from a grey scale image. [*UTHSCSA04a*]) In case of automatic operations, i.e., object analysis, the pictures were always checked visually so that the analysing tool made the right choices in the case of matrix and hard particle areas in defining area fraction of the objects. The area fractions of the different phases are considered here to represent the volume fractions of the carbides. However, there is an error in the area fraction analysis related to the true volume fraction of the material. The procedures, accuracy and error sources in the image analysis are discussed elsewhere, in Section 4.1.2.

The microstructure of the testing mantle, in the case of material WR6WC, was compared with the analysed material samples using the image analysing program. The average WC/Co content of mantle WR6WC is 18% in area. Since the average WC content of the WC/Co is 90%, the estimated WC content in the composite is near 16% in area. The same WC content was found for the material samples from the same batch too. The VC carbide area fraction in WR6 is approximately 18 to 20% according to the image analysis. The value of 18,2% is in a good agreement with of the VC content found in the literature in the case of a similar type of P/M materials with the same nominal composition [*Dixon04a*]. The size of the VC carbides is a few microns in the HIPed products.

In SET3, the volume fraction of the reinforcements was given by the manufacturer, therefore the nominal volume fractions were used in characterising the composites, *Table 12*. The effect of particle or particulate reinforcements on wear rate was evaluated for SET3 (the matrix was WR6 tool steel in all materials). In SET3 besides

the volume fraction of the reinforcements, *Table 12*, other characteristics of reinforcements varied too. The reinforcement particle sizes, theoretical spacing between reinforcements (depending on the volume fraction and sizes of evenly distributed reinforcements) and the true hard-particle sizes of the particulate reinforcements are presented in *Table 13*.

Table 11 Volume fractions, hard particle sizes and visual characters of reinforcements in SET2.

Materials	VC carbides Vol.%	WC Vol.%	Total Vol.%	VC Size (μm)	WC Size (μm)	Reinforcement Size (μm)	Cobalt	Reinforcement shape Visual
WR6WC	15,0	15,9	30,9	1 to few	$3 \pm 0,5$	200-400	In WC	Porous, angular
WR4WC	12,2	14,0	26,2	1 to few	$3 \pm 0,5$	200-400	In WC	Porous, angular
9980aWC	-	11,1	11,1	1 to few	$3 \pm 0,5$	200-400	In WC	Porous, angular
9980bWC	-	15,2	15,2	1 to few	$3 \pm 0,5$	200-400	In WC	Porous, angular
2218WC	-	13,2	13,2	1 to few	$3 \pm 0,5$	200-400	In WC	Porous, angular
HadacWC	-	13,7	13,7	-	$3 \pm 0,5$	200-400	In WC	Porous, angular
WR6	18,2	0	18,2	1 to few	-	-	-	-
MM15	14,8	0	14,8	1 to few	-	-	-	-

Table 12 Volume fractions, and visual characters of reinforcements in SET3.

Materials	VC carbides Vol. % Nominal	WC Vol. % Nominal	Total carbide Vol. % Nominal	Cobalt	Reinforcement Shape Visual
30WCSf	12,74	30	42,74	No	Solid, angular
20WCSf	14,56	20	34,56	No	Solid, angular
30WCSc	12,74	30	42,74	No	Solid, angular
20WCSc	14,56	20	34,56	No	Solid, angular
30WCf	12,74	27	39,74	In WC	Porous, angular
30522dcf	12,74	26,4	39,14	Around WC	Porous, round
30522dcc	12,74	26,4	39,14	Around WC	Extremely porous, round
30TiCf	12,74	TiC 30	42,74	No WC	Solid, angular

Table 13 WR6-based composites, numerical values for the characteristics of the composite structure.

Material	Reinforcement Size min (μm)	Reinforcement Size max (μm)	Spacing between reinforcements min (μm)	Spacing between reinforcements max (μm)	True carbide Size min (μm)	True carbide Size max (μm)
WR6WC	200	400	217,7	435,3	1	7*
30WCSf	45	90	27,8	55,6	45	90
20WCSf	45	90	44,2	88,3	45	90
30WCSc	250	425	154,4	262,5	250	425
20WCSc	250	425	245,3	417,0	250	425
30WCf	100	200	61,8	123,5	1	7
30522dcf	45	90	27,8	55,6	~5*	~20-25*
30522dcc	200	300	123,5	185,3	~5*	~20-25*
30TiCf	75	250	46,3	154,4	75	250

*Estimated visually

Based on the image analysis, the particle reinforcements are sometimes unevenly distributed. Especially the shape of recycled WC/Co particles was irregular, *Figure 10*. In this optical micrograph, the boundaries between round prior powder particles are visible.

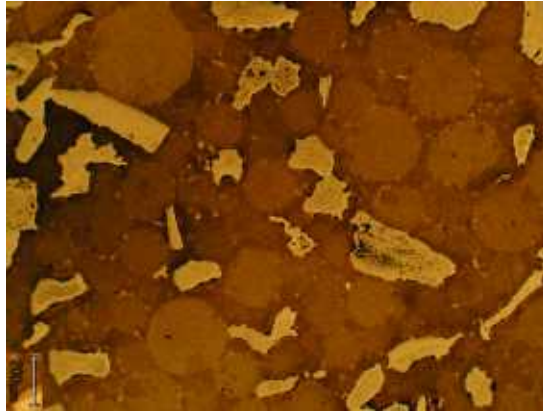
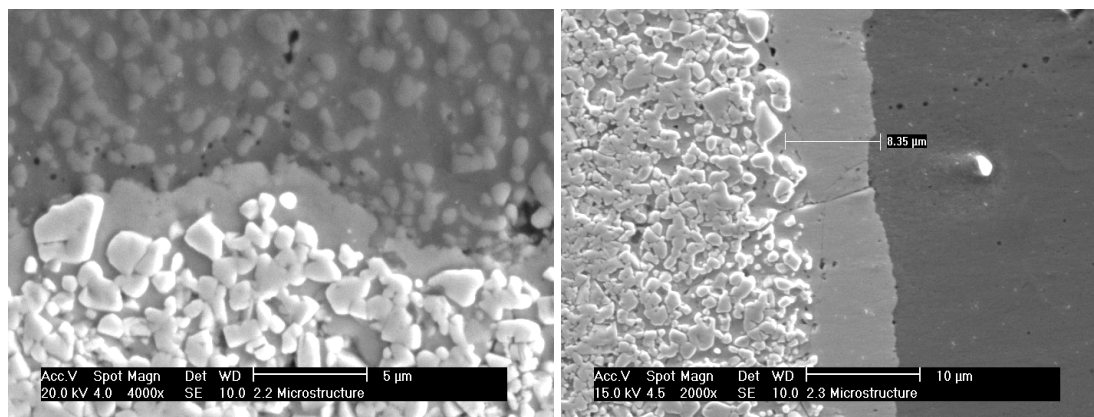


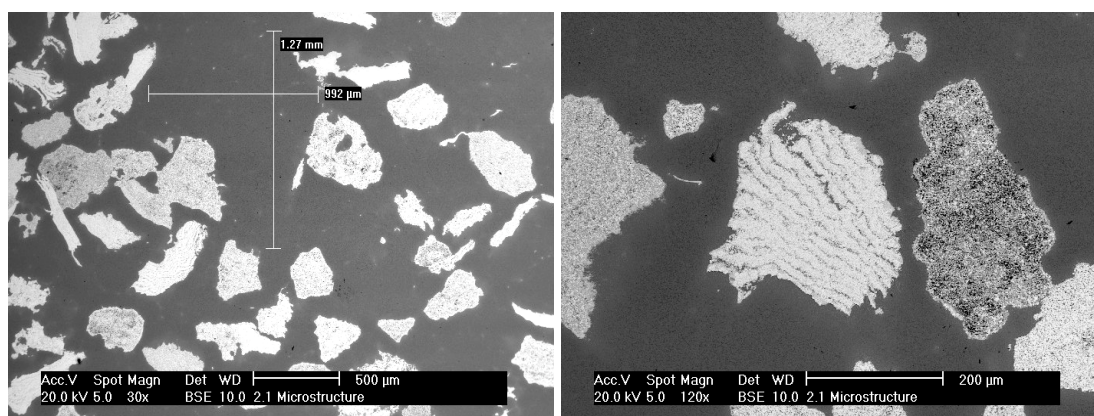
Figure 10 Optical microscope picture of tool-steel-WR4 (dark)-based composite with recycled WC/Co (light) reinforcements. The round prior powder particle boundaries are clearly seen in the image. In the left side 200 μm line segment.

In *Figures 11a* and *b* recycled WC/Co reinforcement particle in tool steel WR6 and in martensitic 9980 steel matrix can be seen. Round and evenly distributed vanadium carbides of a few micrometers in size are seen in the tool steel matrix (dark) *Figure 11a*. The actual WC particles (lightest areas) of the reinforcements are seen in the cobalt binder. The prior powder boundaries, (seen in the *Figure 10*), appear as oxide necklaces in the SEM pictures, as in *Figure 11.b* on the right-hand side of the dark 9980 matrix area. This means that powder particle surfaces have been oxidised prior to the HIP consolidation, which actually is not the wanted situation. Also, porosity of reinforcement was observed in materials with hardmetal or carbide reinforcements in these test materials. The wearing parts are large in area, and macroscopically the reinforcement distribution of the materials is considered homogeneous in the scale of wear-inducing particles (stones), which were, in the present case, 10 to 20 mm in size. The interfacial reaction zones between particulate reinforcements (light area) and the matrix (dark area) can be observed in both pictures. In *Figure 11b*, the reaction zone between matrix and reinforcement is over 5 μm of thickness. The interfacial reaction zones were relatively thin between tool steel and recycled WC/Co, as in *Figure 11a*.

The distribution and variations in structure of the reinforcement particles in the tool steel matrix is seen in *Figures 12a* and *b*.



a) b)
 Figure 11 SEM-micrographs of the steel based composites: a) Recycled WC/Co reinforcement in WR6 tool steel and b) Recycled WC/Co reinforcement in 9980 martensitic steel composite. The differences in the thickness of the interfacial reaction zone can be seen. Note the different magnification in the black text bar.



a) b)
 Figure 12 SEM-micrographs of the tool-steel based composites: a) Recycled WC/Co reinforcements in tool steel, WR6WC. The light areas are recycled WC/Co and dark the matrix, b) same material with higher magnification. The variations in the reinforcement particle structure (light areas) can be seen. The recycled hardmetal appeared to have a porous or lamellae, as well as a normal, hardmetal structure, as seen in figure b.

Reinforced tungsten carbide particle coated with cobalt in tool steel matrix is presented in *Figure 13*. The prior shape of this type of carbide particles was rounder than that in recycled WC/Co. However, this carbide grade seemed to be extremely porous. In these composites, there is a relatively large vanadium carbide-free zone (over 20 micrometers in thickness) around the reinforcement particles, represented as the lighter area in *Figure 13*.

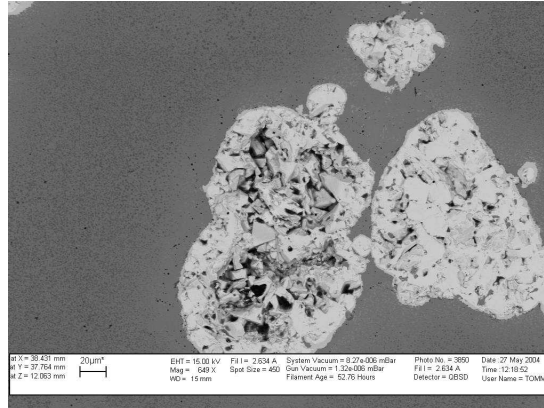


Figure 13 SEM-micrograph of the composite with tool steel matrix and WC particles dense coated with cobalt.

Cast WC and TiC reinforcements in SET3 were pore-free and uniform by the structure differing from the dispersion-type WC/Co carbides. In *Figure 14 a*, tungsten carbide is partly present (light area), and the solidification structure is seen faintly inside the carbide, as well as thick interfacial reaction layers around the carbide. After mechanical grinding and polishing, cracked carbides can be seen on the surface. When looked at closely, cracks seem to start near the boundary between interface layer and matrix. The cracks continue in both directions, both into carbide and into matrix. However, cracks are shorter in the matrix. Composite 30TiCf was reinforced with angular titanium carbides, in the *Figure 14 b*. In the picture, it can be seen that material is removed from the carbide surfaces in a brittle manner during mechanical grinding and polishing.

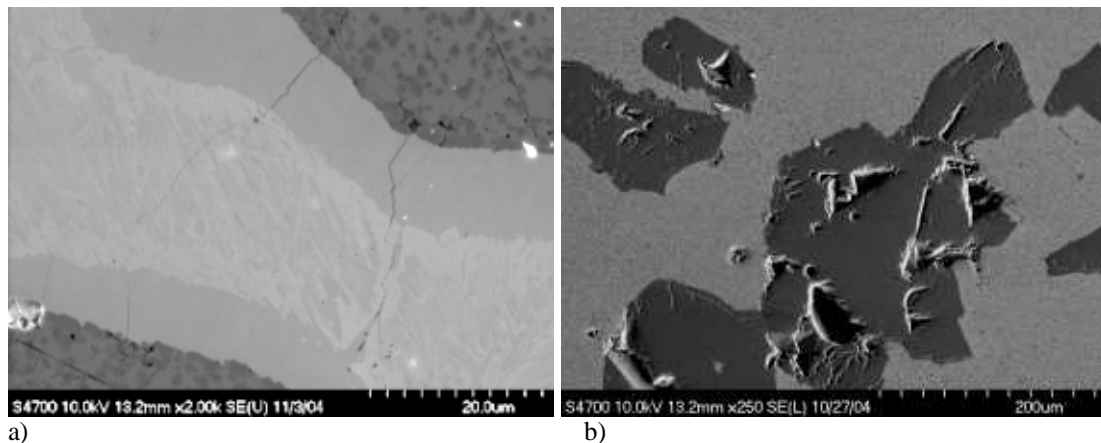


Figure 14 SEM-micrograph of composites in SET3 a) cast WC particle (light area) with some cracks on the ground and mechanically polished surface and b) titanium carbide reinforcements (dark areas). Some material is removed in grinding from the TiC. Matrix is high-vanadium tool steel in both cases.

The distribution of the reinforcements was visually homogenous in the large scale, although locally uneven distributions could be found in the samples. Larger

reinforcement particles of 250-425 μm in size are not connected with each other in the composite structure, *Figure 15*. From the manufacturing point of view, the relationship between reinforcement powder particle size and matrix powder particle size is important. Clustering of hard particles or networking of the whole carbide structure can appear if the matrix powder particle size is large compared to reinforcement particle size.

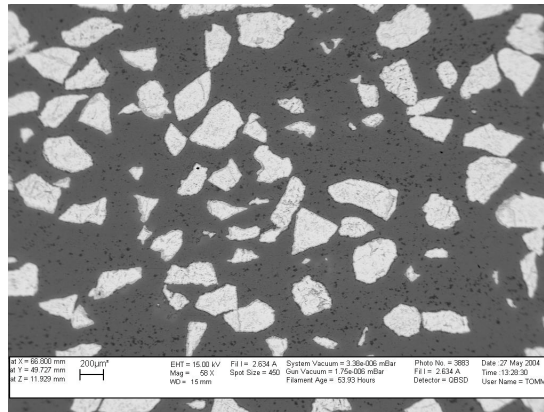


Figure 15 SEM-micrographs of the relative large 250-425 μm cast WC reinforcement particles in tool steel matrix of the composite 30WCSc. Reinforcements are not connected to each other.

2.2 Experimental methods

2.2.1 Dry sand rubber wheel test and erofuge test

Abrasive wear tests were carried out for selected materials in SET1 at Helsinki University of Technology with a dry sand rubber wheel, DSRW, tester. Tests were carried out basically according to ASTM G65-91 standard [ASTMG65-91]. The testing parameters were the following: force 130 N, rotation speed 266 rpm without load, sand flow 138 g/min, test duration about 10 min and wheel diameter 180 mm. Quartz sand used was of irregular shape (99,5% SiO₂, 0,23% Al₂O₃ and 0,04% Fe₂O₃) and having a particle size distribution between 100 and 600 µm. Sand is not in accordance with standard practice ASTM G65-91. The sample sizes were (25*55*15) mm³. The results are presented as weight loss (g), volume loss (mm³) and wear rates (mg/g), i.e. (the weight loss of the test specimen)/(abrasive sand used).

Erosive wear tests were carried out for composites in SET1 at Tampere University of Technology. An erosive wear tester based on a centrifugal accelerator [GOST23.201-78] described in [Kleis05a] and similar to that used by, for example, Kúbarsepp et al. [Kúbarsepp01a], was employed. Erosive particles were fed into the centre of the rotor, then particles were accelerated through the rotor channels, and finally the erosive particles hit the specimens at a certain angle. Impacting particles were quartz sand (SiO₂) of 100-600 µm particle diameter and irregular particle shape. The impact angles used were 30° and 60° and the velocity of the particles was 40 m/s. Fifteen samples (15x25x4) mm³ (surfaces ground with 1200 grit emery paper) could be exposed to erosion at each run. Most of the materials were tested repetitively four times at a specific angle. Results are calculated from the measured mass loss (mg) by dividing it with the mass of erosive particles supposed to impact one specimen (i.e., amount of the sand used (30 kg) multiplied by relative amount of used sand hitting one test sample ($8,5^\circ/360^\circ = 0,023611$, one sample covers 8,5° of the periphery of the circle)).

2.2.2 Cone crusher test

The small-scale Nordberg laboratory cone crusher, called B90, is used in order to obtain information on the wear rates of the mantle. The stones are crushed in compression in the cavity between the concave and mantle. Principle of the cone crusher was presented in the *Figure 4* in Section 1.2. The loss of material in the liners (concave and mantle) affects the product (rock) quality and the crusher efficiency. The codes of testing practise with B90 have been developed at Metso Minerals Oy and tests were carried out in the Metso Mineral's testing laboratory in Tampere by the testing technician. The cone crusher is presented in *Figure 16 a* and *b*. True dimensions of the B90 are: length 765 mm, width 765 mm, height 720 mm, and the total weight of the equipment is 260 kg. The tested samples, mantles, were 130/240 mm in diameter with height of 85 mm.



a) b)
Figure 16 a) The forklift truck is filling the feeder of B90 cone crusher, b) open B90 equipment, and the upper part of the mantle is seen in the figure.

The stones used in the cone crusher wear tests were mica-gneiss for SET2 and granite for both material sets, SET2 and SET3. The stone properties for Finland Sorila granite and Finland Lakalaiiva mica-gneiss are presented elsewhere [Ruuskanen06a]. Both stones are multi-minerals by composition. According to Metso Minerals and [Ruuskanen06a], the UCS¹ of the used Sorila granite is 193,9 MPa and UCS of Lakalaiiva mica-gneiss is 63,7 MPa, Young's modulus for Sorila is 70,9 GPa, and for Lakalaiiva it is 72,4 GPa. The abrasive was dried for every test and tests were not conducted when raining. The granite rocks used as abrasive material (feed) in the tests are shown in Figure 17.



Figure 17 Rock used as abrasive material in the tests is slightly red granite.

The operating parameters of B90 are fixed according to the standardised testing procedure by Metso Minerals and controlled in order to confirm the test repeatability and reliability. The close side setting, CSS, was 5 mm, stroke 4,0 mm and abrasive material (feed) size was 10-20 mm in every test. Both stones, granite and mica-gneiss, were sieved out into the standardised size fraction and dried before the wear tests. The

¹ Ultimate Compressive Strength

power consumption kWh , flow rate (capacity) ton/h (taken 8 times during the test) and abrasive consumption kg were reported; the feed material and end product were checked by sieve analysis. About 2500 to 4500 kg abrasives were used for each test material; the wear rates were measured for three to six times per material. In a few cases, only two measurements were carried out for SET3 materials if an acceptably small variation existed between the two results. With the composite WR6WC, altogether twelve measurements were taken, in order to evaluate the test repeatability and reliability. With this material the coefficient of variation was 8%. Variation caused by B90 test configurations has been estimated to be $\pm 8\%$ also by Metso Minerals.

The wear rate measurements were made from the mantles, one of which is shown in *Figure 18*. Results are calculated as mass loss (g) of the tested wear part divided by the mass of abrasive particles (kg) flown through the cavity.



Figure 18 Laboratory cone crusher wear part, mantle and measuring stick of 20 cm are shown in the picture.

2.2.3 Other experimental methods

After the wear tests, dimensional measurements of the mantle wear geometry and surface roughness measurements of the worn surfaces were carried out at Metso Minerals laboratory by technicians. The surface roughness of the SET2 materials after wear tests was measured with Mitutoyo SJ.201 equipment. Wear surfaces were studied visually with a stereo microscope and scanning electron microscopes. SEM equipments used were LEO SEM 1450 with INCA EDS, Philips SEM XL30 with EDAX EDS and Hitachi FE-SEM S-4700 with INCA EDS.

The wear mechanisms of the materials in the laboratory cone crusher were evaluated by surface replicas. This was done because the real wear parts were retained for further wear tests. The replicas of the mantle wear surfaces were made by Repliset3, which is a replicating system by Struers. The resolution of replicas is 0,1 micrometer according to the manufacturer.

Hardness test (Rockwell) equipment was Albert Gnehm 160. Hardness measurements were carried out on test material samples.

3 RESULTS

3.1 Abrasive and erosive wear of steel-based composites

3.1.1 Abrasive wear rates

Abrasive rubber wheel test results of the austenitic, duplex and heat-resistant steel-based composite materials reinforced with Al_2O_3 and Cr_3C_2 ceramics are shown in *Table 14* and *Figure 19*. The results are average values, AVEs, of two tests. The average coefficient of variation, COV, was 9,3%. In order to meet ASTM specification, the COV must not exceed 7% [*ASTMG65-91*][*Hawk99a*]. Symbols and compositions of the composites of SET1 materials have been given earlier in *Table 6* in Chapter 2.1.1. However, some of the SET1 materials were left out of DSRW test.

Table 14 Rubber wheel test results of the austenitic and duplex steel-based composites. The letter A or C are abbreviations referring to Al_2O_3 or Cr_3C_2 reinforcements, respectively; the number indicates volume fraction of reinforcement (x 10) and the last letter F or C stands for fine and coarse particle size of the reinforcements of the tested materials.

Material	Weight loss (g)	STDEV (g)	Density (g/cm ³)	Volume loss (mm ³)	Wear rate (mg/g)
APM	1,357	0,098	7,71	176	1,030
D27	1,222	0,286	7,8	157	0,927
D27C3F	0,136	-	7,464	18	0,103
APMA2	0,727	0,009	6,962	104	0,551
APMC1C	0,815	0,063	7,607	107	0,618
APMC3C	0,349	0,022	7,401	47	0,264
APMC1F	0,584	0,017	7,607	77	0,443
APMC2F	0,347	0,034	7,504	46	0,263
APMC3F	0,227	0,035	7,401	31	0,172

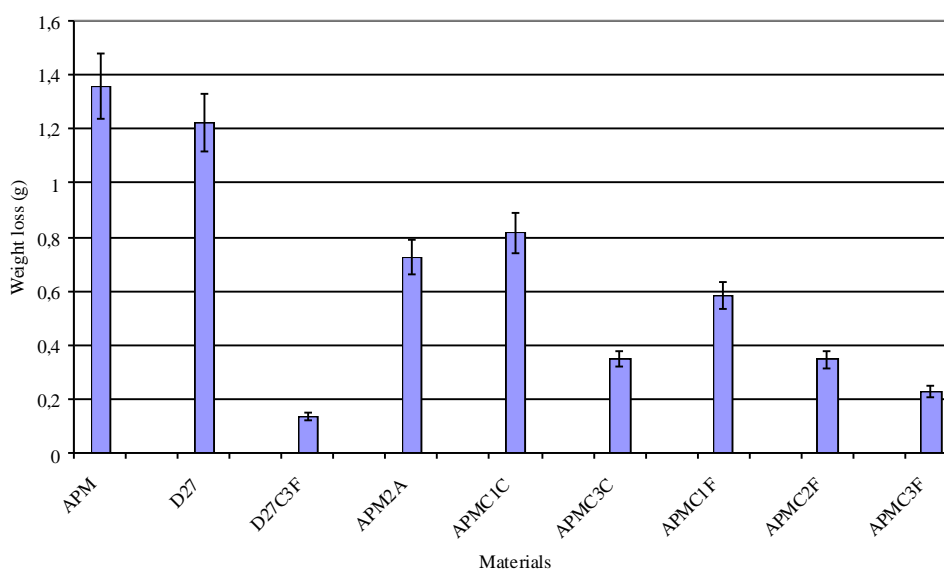


Figure 19 Weight losses of the materials in the rubber wheel abrasion tests. The first two columns on the left are plain matrix materials. The error bar according to the average coefficient of variation, COV, was 9,3% in the test.

3.1.2 Erosive wear rates

The wear rates of the erofuge test change in the present case after the first measurement of test specimens, which is seen in cumulative weight loss plotting, shown in *Figure 20*. Reliability of the data and error sources are discussed in Section 4.1.

Erosive wear test results are given in *Table 15* and *Figure 21*. Symbols and compositions of the composites were specified earlier in *Table 6* in Section 2.1.1. The erosive wear tests were carried out in 1999 and 2001. In the supposed steady-state region, wear rates were gained at a 30 degree impact angle. The coefficient of variation, COV, was 6,4%, while, at a 60-degree impact angle, the average COV was 5,5%. The results of erosion tests carried out in 1999 at a 60° impact angle using in total 30 kgs of abrasive in the wear test are also presented in Liu's doctoral thesis [*Liu03a*] on eight materials: 253MA, APM, APMA2, APMC1F, APMC3F, APMC1C, APMC2C and APMC3C. Wear tests were carried out during and after the TEKES project (Erosion and erosion-corrosion resistant powder metallurgical materials for the application of energy technology ERCOMAT). The author worked in the project and the part of the erofuge tests were also done by author.

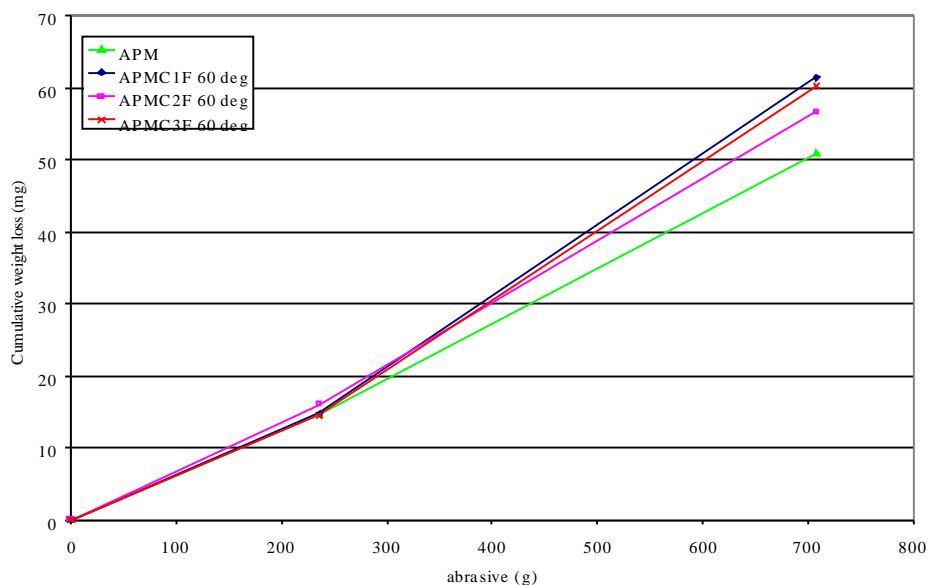


Figure 20 Some cumulative weight losses in erofuge tests, erosive particle impact angle 60 degrees, velocity 40 m/s.

Table 15 Erosive wear rates obtained in erofuge test, when 30 kg per test abrasive was used and particle velocity was 40 m/s. The letters A and C are abbreviations referring to Al_2O_3 or Cr_3C_2 reinforcements. Respectively, the number indicates volume fraction of reinforcement (x 10) and the last letter F or C stands for fine and coarse particle size of the reinforcements of the tested materials.

Material	30° impact	30° impact	30° impact	60° impact	60° impact	60° impact
	angle	angle	angle	angle	angle	angle
	AVE	2001	1999	AVE	2001	1999
	(mg/g)	(mg/g)	(mg/g)	(mg/g)	(mg/g)	(mg/g)
253MA	0,075	0,075	-	0,088	0,081	0,094
APM	0,075	0,071	0,078	0,079	0,072	0,087
APMA2	0,081	0,084	0,078	0,087	0,085	0,088
APMA4	0,088	0,088	-	0,102	0,102	-
APMC1F	0,076	0,074	0,077	0,088	0,087	0,090
APMC2F	0,084	0,084	-	0,080	0,080	-
APMC3F	0,066	0,062	0,070	0,090	0,085	0,095
APMC1C	0,078	0,078	0,078	0,081	0,076	0,086
APMC2C	0,078	0,083	0,074	0,085	0,081	0,089
APMC3C	0,059	0,053	0,065	0,088	0,088	0,088
APMC4C	0,108	0,108	-	0,126	0,126	-
316L	0,072	0,072	-	0,064	0,064	-
316LA	0,071	0,071	-	0,095	0,095	-
D27	0,071	0,071	-	0,071	0,071	-
D27C3F	0,064	0,064	-	0,098	0,098	-

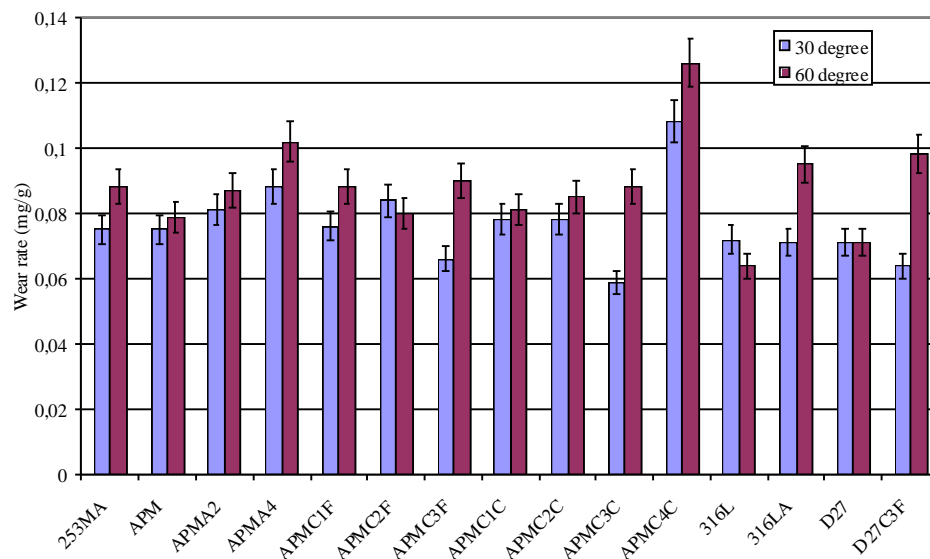


Figure 21 Erosive wear rates obtained in erofuge tests of the SET1 materials. Impact angles 30-and 60-degrees, particle velocity 40 m/s.

3.1.3 Hardness values

Rockwell hardness values, HRC, of the SET1 materials tested in rubber wheel equipment, are presented in *Figure 22*. The HRC values could not be measured for APM matrix material and APMA2 composite, because of the softness of the materials. The proper hardness value in these cases is HRB: the HRB hardness of AMP matrix was 90,4 HRB and that of the APM2A composite was 96,4 HRB. Increasing reinforcement volume fraction increases the hardness values. The average COV was 2,6% in hardness measurements.

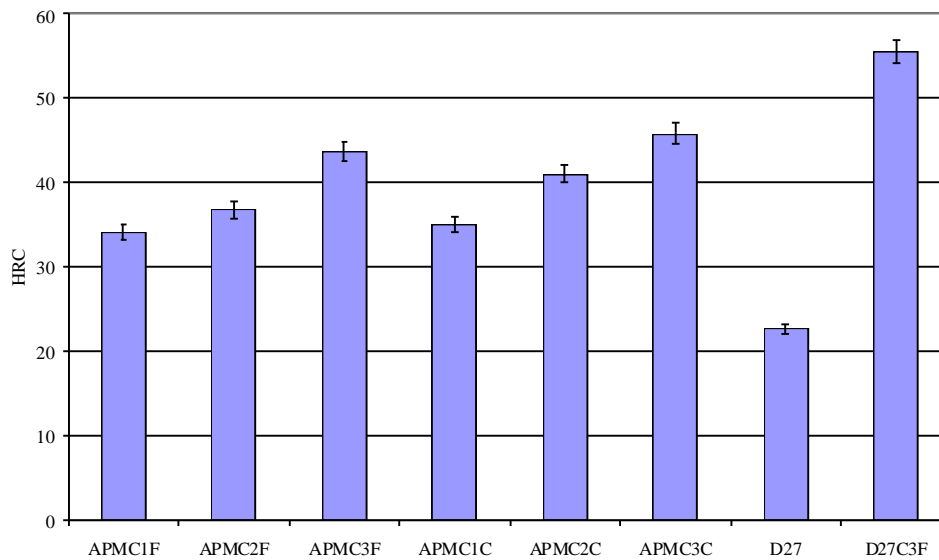


Figure 22 HRC hardness for the SET1 materials. Matrix material APM and composite APM2A were too soft for this type of hardness measurement.

3.1.4 Worn surfaces after erosive wear laboratory tests

The following SEM images show typical wear surfaces after erosive wear tests. The eroded surface of austenitic-steel-based composite containing aluminium oxide, composite APM4A, eroded with 60-degree impact angle is presented in *Figure 23* with two magnifications. Respectively, duplex-steel-based composite with chromium carbides, composite D27C, is presented in *Figure 24* with two magnifications. The sizes of the hard phase particles varied in both cases. The ceramic particles showed brittle behaviour, while all the matrices seemed to be deformed. Erosive wear of steel-based composites at 60-degree impact angle has been evaluated earlier by Liu [Liu03a]; the matrices were deformed and oxides and carbides seemed to be prone to cracking. This is also observed in the following *Figure 23*.

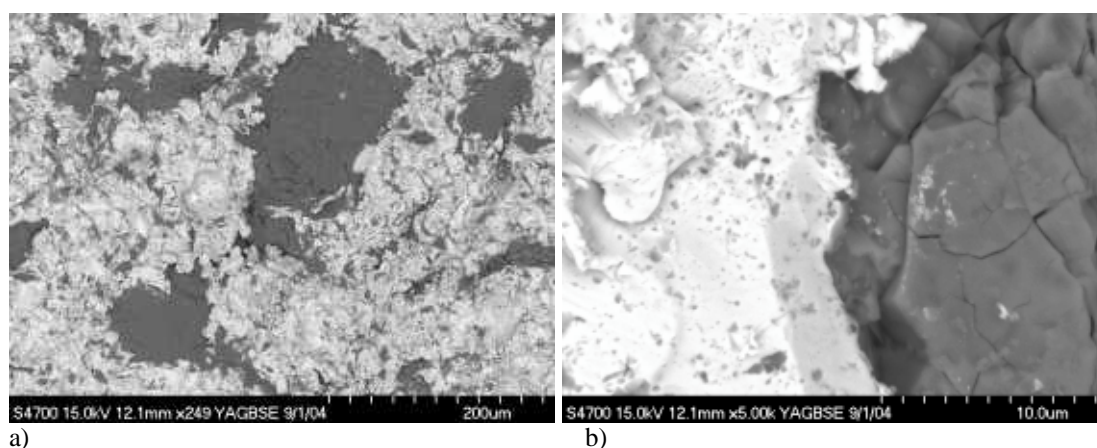


Figure 23 a) and b): examples of worn surfaces of the austenitic-steel-based composites containing aluminium oxide, composite APMA4. The aluminium oxide is light element and shown as dark the matrix is white. Erosive wear test at a 60-degree impact angle with particle velocity of 40 m/s. SEM BSE images, two magnifications.

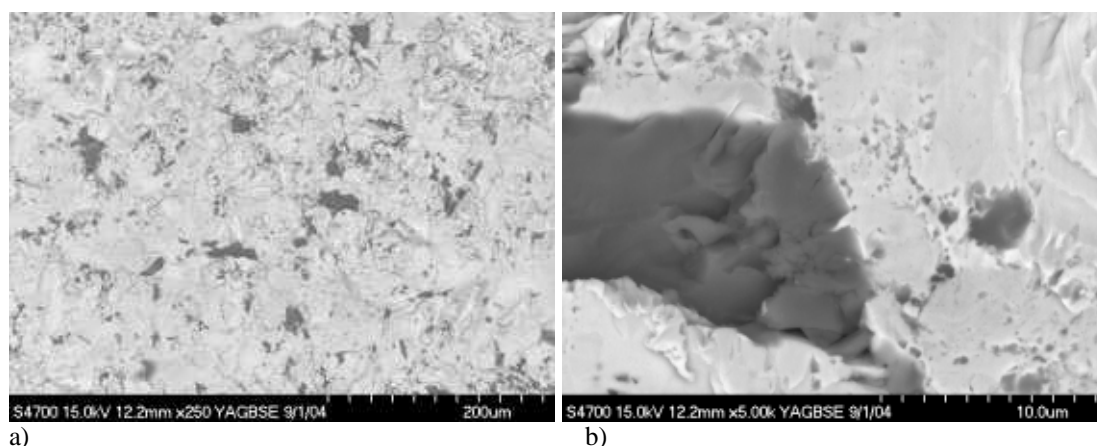


Figure 24 a) and b): examples of the worn surface of the duplex-steel-based composite with chromium carbides, composite D27C, eroded at a 60-degree impact angle and 40 m/s particle velocity. SEM BSE images, two magnifications.

Comparisons of the wear surfaces after erosion tests at impact angles of 30 degrees and 60 degrees of AISI 316 stainless-steel-based composite material with Al_2O_3 reinforcement are shown in *Figures 25 and 26*. Eroding particle velocity was 40 m/s. It seems that at a 30-degree impact angle, more apparent sliding scars are present in the matrix surface than at a 60-degree impact angle. At both angles, reinforcement Al_2O_3 seems to behave in a brittle manner, e.g. *Figure 23b*. At a 60-degree impact angle, the matrix area of the composites seems to have more ploughing and displacement type of wear scars.

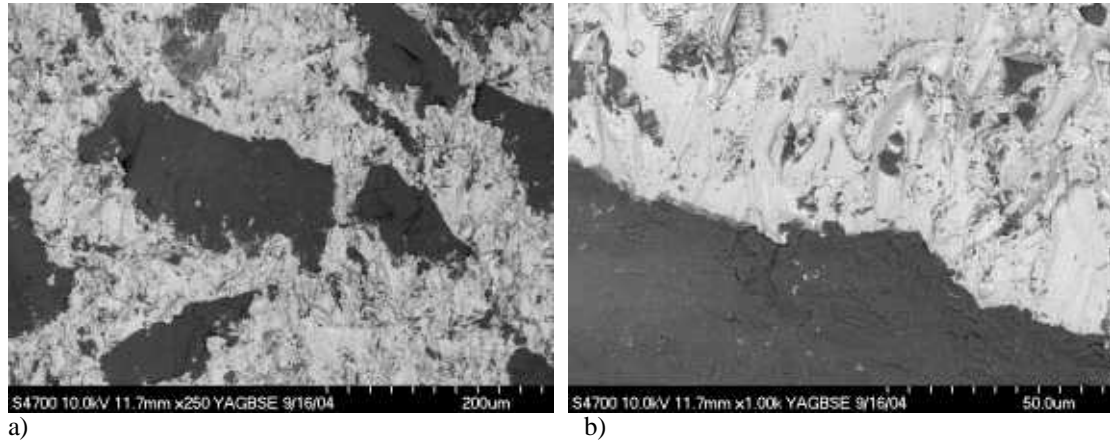


Figure 25 a) and b): worn surfaces of the composite AISI 316L with Al_2O_3 tested in erofuge tests at a 30-degree impact angle with the particle velocity of 40 m/s. SEM BSE images, two magnifications.

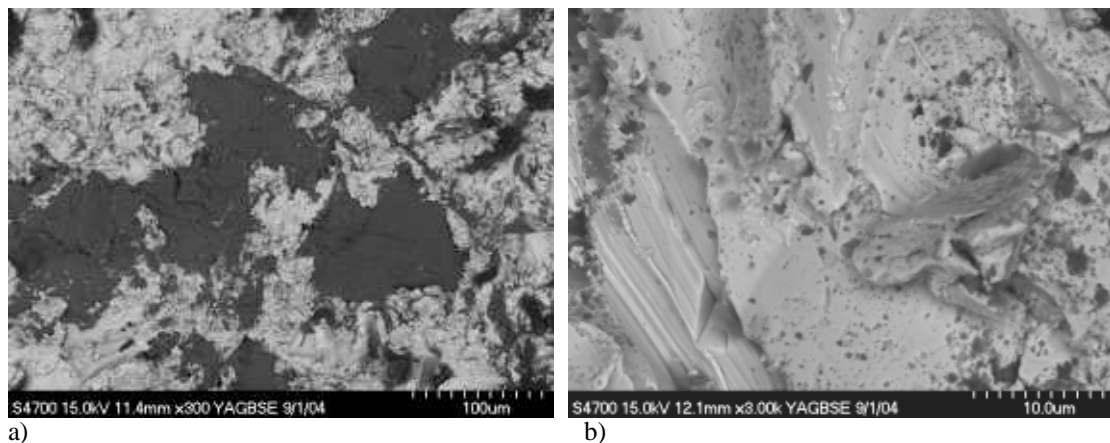


Figure 26 a) and b): worn surfaces of the composite AISI 316L with Al_2O_3 tested in erofuge test at a 60-degree impact angle with the particle velocity of 40 m/s. SEM BSE images, two magnifications.

3.2 Laboratory-scale cone crusher wear tests

3.2.1 Wear of the composites with different matrices

The SET2 materials can be divided into three groups: tool-steel-based composites (WR6WC and WR4WC) martensitic-steel-based composites (9980aWC, 9980bWC, 2218WC) and composites with manganese steel (HadacWC, MM15). The measured wear rates of the materials of SET2 are obtained with two stone types, i.e., mica-gneiss and granite; these are presented in *Table 16*. The same results are presented in graphical form in *Figure 27*. Average COV in SET2 was 11,7%.

Some test results are omitted in *Table 16* because the test parameters did not remain stable. These tests were 9980aWC and HadacWC tested with mica-gneiss stone and 2218WC tested with granite stone. Additionally, the results marked with ()* were clearly not steady-state wear rates, i.e., the first wear result (and also the second) of the set of six tests were very different from the others. The cumulative wear losses of selected materials of SET2 are presented in *Figure 28*.

Table 16 The wear rates obtained in cone crusher wear test with mica-gneiss and granite stone on the steady-state region of wear, SET2.

Symbol	Wear rate average (g/ton) Mica-gneiss	Wear rate (Mica-gneiss) STDEV	Wear rate average (g/ton) Granite	Wear rate (Granite) STDEV
WR6WC	1,5	0,1	2,0	0,2
WR4WC	3,8	0,3	5,6	0,2
9980aWC	-	-	(18,2)* 16,2	(5,9)* 1,6
9980bWC	7,8	0,4	(19,2)* 16,9	(4,7)* 1,6
2218WC	9,0	1,0	-	-
HadacWC	-	-	(11,6)* 9,6	(3,2)* 1,1
MM15	2,2	0,2	3,3	0,5
WR6	3,1	0,4	4,7	0,2

*Initial state of wear is included.

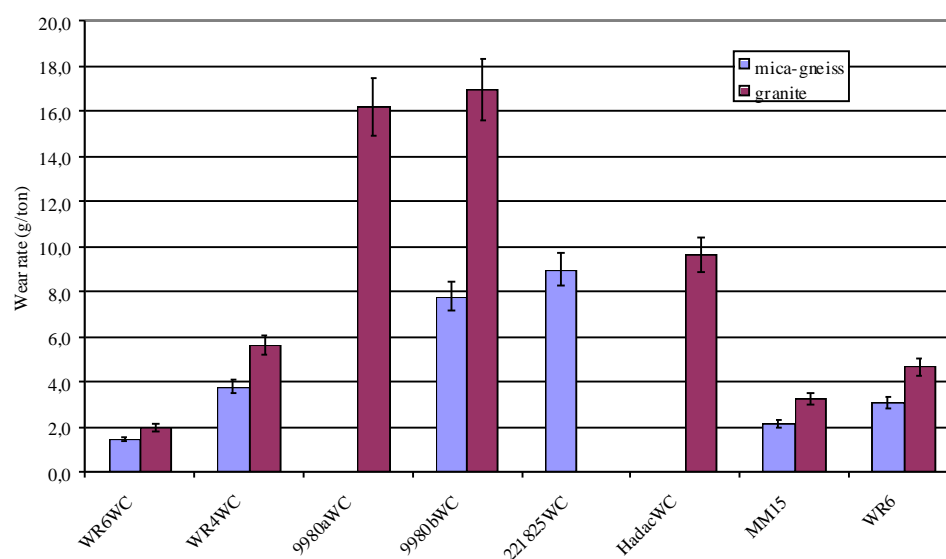


Figure 27 Wear rates of materials in the cone crusher wear tests of SET2 materials using mica-gneiss and granite stone wear media. The error bar is according to the average coefficient of variation, COV. It was 11,7 % in the test.

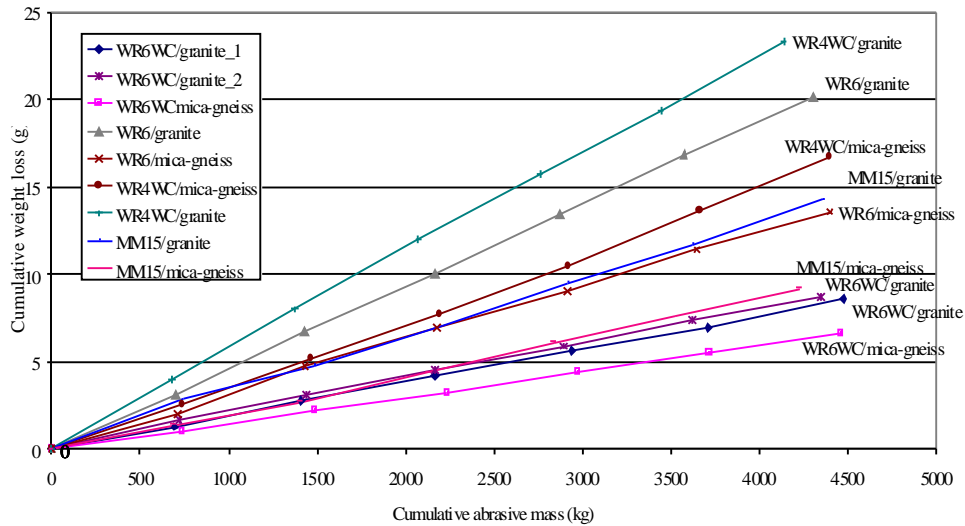


Figure 28 Cumulative weight losses as a function of the amount of used abrasive, obtained in cone crusher wear tests of selected materials of SET2. The granite 1 and 2 tests are two identical testing rounds.

In SET2, the total carbide content of the composites differs and the reinforcements consist of two types of carbides, VC and WC. The VC and the WC carbide contents of different materials are presented in *Figure 29*. The volume fractions of the carbides are presented in *Table 11* in Section 2.1.2.

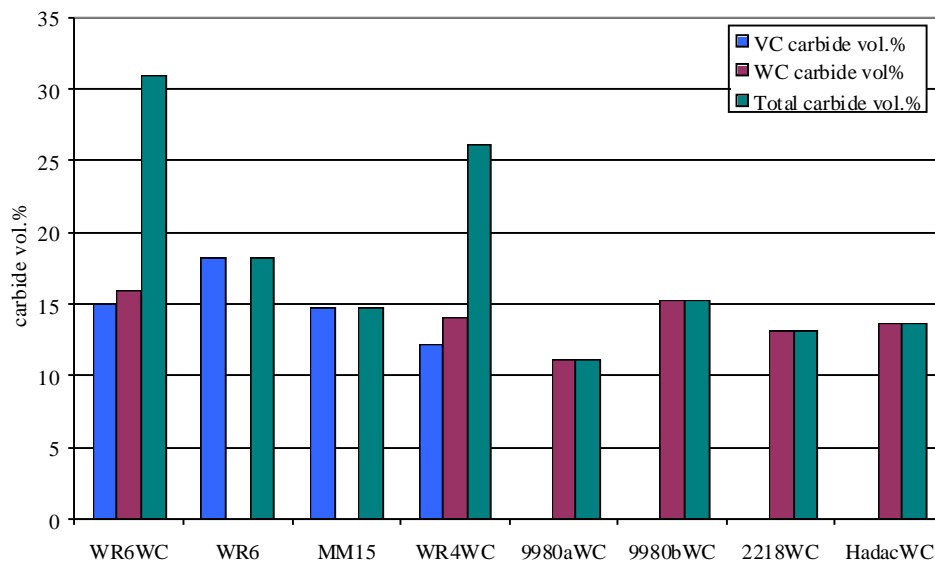


Figure 29 Total carbide content of the materials in SET2 and the content of the separate tungsten and vanadium carbides in steel matrices. The measurements are done with image analysis program.

3.2.2 Wear of the composites with different particle reinforcements

The materials in SET3 were designed on the basis of knowledge obtained from the results of SET2. Considerably hard tool steel WR6 was selected for the matrix of all these composites. Particle reinforcements of different kinds were included in the testing program. Reinforcements *differed by the structure* (solid reinforcement particles and hardmetal reinforcements with dispersed small hard particles in the metallic binder), or *by the hard phase* (WC, TiC). Average COV in the wear test results of SET3 was 14,9. This is higher than in SET2, but the wear rates were also considerably lower.

Table 17 SET3 wear rates in cone crusher wear test with granite stone.

Symbol	Wear rate average (g/ton)	
	Granite	STDEV
30WCSf	3,6	1,3
20WCSf	5,5	0,8
30WCSc	4,2	0,4
20WCSc	2,4	0,2
30WCf	2,8	0,5
30522df	3,6	0,4
30522dcc	3,6	0,7
30TiCf	3,6	0,4

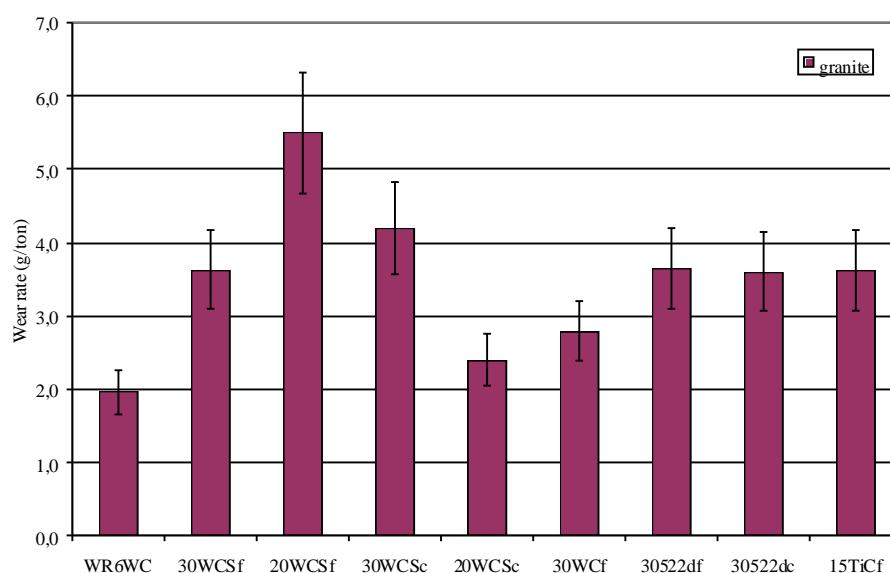


Figure 30 Wear rate results of tool-steel WR6-based composites (SET3) with particle reinforcements, in cone crusher tests with granite stone.

3.2.3 Wear surfaces after laboratory cone crusher tests

Wear surfaces were evaluated by SEM and stereomicroscope using surface replicas. The mantle wear parts were also evaluated visually and by stereomicroscope. The surfaces were relatively large, so only a small area of each material could be evaluated in SEM. Under stereomicroscopy, no differences in the wear surfaces were noticed at different parts of the laboratory crusher mantle (from top to bottom). The geometrical dimensions of the mantles were not changed during the wearing time in this study, but it is observed that liners can wear differently at different parts [Lindqvist03b]. This is expected to happen in larger scale crushers, and therefore the laboratory-scale crusher does not present the "real" full-scale case completely.

The materials in SET2 had a larger variation in the absolute wear rates than the materials in SET3. In SET2, the lowest surface roughness (and wear rate) after wear tests was associated with WR6WC, WR6 and MM15 materials; Ra (μ) values of worn surfaces were near 4 with all these materials (WR6 3,08...4,77 μ , MM15 2,74...4,23 μ , WR6WC 2,98...4,71 μ). Other materials have rougher surfaces in SET2, with Ra (μ) values of near 6 after wear test (WR4WC 4,06...6,61 μ , 9980aWC 4,56...6,67 μ , 9980bWC 4,46...7,53 μ , 221825WC 4,58...6,32, Hadac25WC 4,38...6,13). Under stereomicroscopy, the macro-scale roughness of the surfaces and the rock indentation scars are clearly seen on most of the materials in both sets. Both "upraised hard particle hills" as well as "valleys" were seen in the surfaces of composites.

Different matrices of the materials in SET2 tolerate wear differently. The number of sliding scars seems to be smaller in composites with the tool-steel matrices, as compared to those with martensitic-steel or manganese-steel matrix. However, it is expected that in every material sliding scars can be found when the magnification is high enough, although they may not be observed in the replicas. The direction of the scars existing in the upper part (of the mantle) tends to be around 45° from the horizontal on both directions as observed in *Figure 31 a*. This behaviour is observed in several materials. The direction of scars may reveal the typical feed particle movement in the cavity. The width of the scars varies considerably, and can be around 100 μ m *Figure 31 b*.

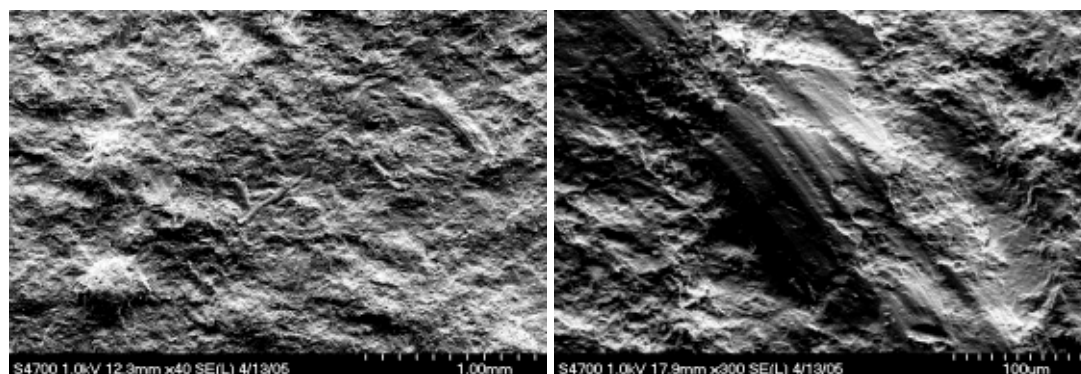


Figure 31 SEM micrographs of the wear surface replica of the WR6-based composite after cone crusher wear test with granite stone. Sliding scars in the matrix surface. Two magnifications.

Wear surfaces of the WR6-based materials after cone crusher wear tests with granite and mica-gneiss wear media resemble each other. Only few sliding scars were observed in the replica samples and the surface was relative smooth as compared to other test materials. It seems that reinforcement particles are “upraised”, i.e., the wear rate of the matrix material is higher and reinforcement wear rate lower. This was confirmed visually by stereomicroscopic study of the real wear parts. Typical SEM micrographs of the replicas of the WR6-based composites of SETS 2 and 3 are shown in *Figures 32 and 33*. The composite structure is seen in these figures; valleys (in true surface hills) are the marks of the less worn reinforcements. In *Figure 33*, the rougher surface of the coarse carbide reinforced composite 30WCSc is compared to the finer composite structure in 30522dcf.

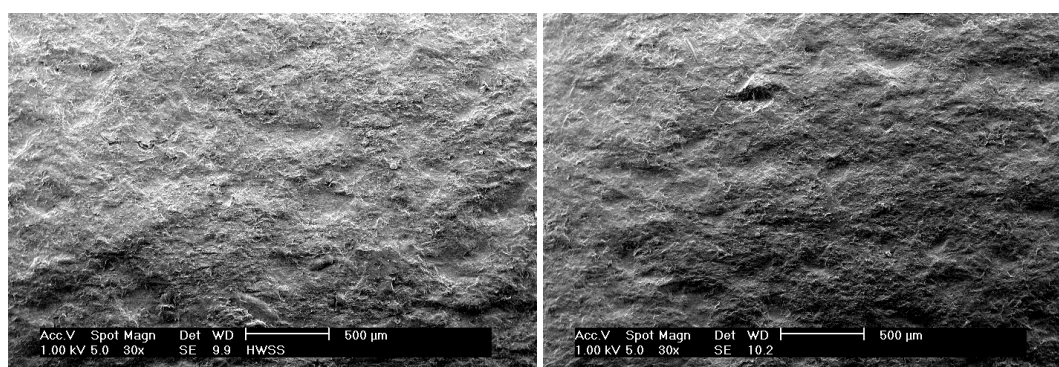


Figure 32 SEM micrographs of the wear surface replica of WR6WC a) after crushing granite stone b) after crushing mica-gneiss stone.

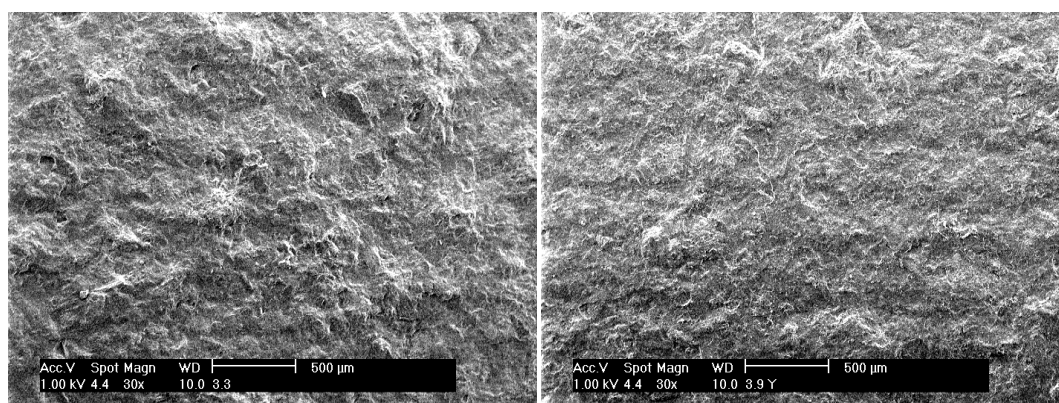


Figure 33 SEM micrographs of the WR6-based composites with a) solid reinforcements in 30WCSc and b) smaller (45-90 µm) dense coated reinforcements in 30522dcf after crushing granite stone.

It seems that the WR4-based composite has the same type of wear behaviour as the WR6-based composites: the reinforcement particles are “upraised” from the matrix material, and the wear rate of the matrix material is faster. In *Figure 34*, the sliding scars of the abrasive particles in the WR4-based composite are shown, and, in *Figure 35*, typical examples of the wear surfaces of the martensitic steel-based and manganese steel-based composites are seen.

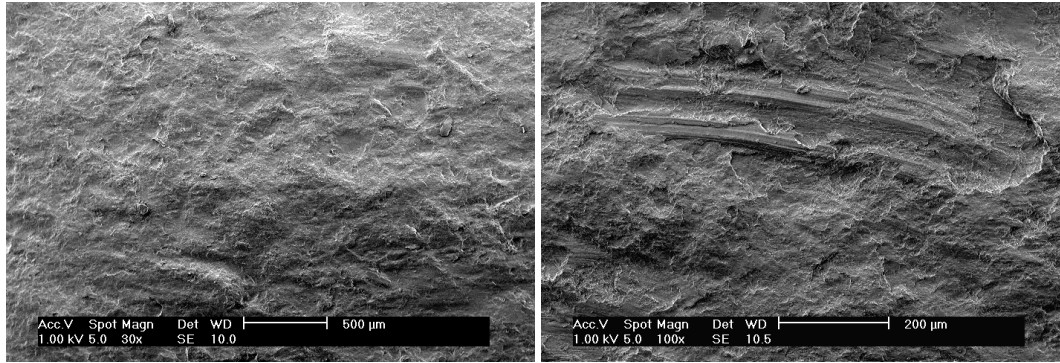


Figure 34 SEM micrographs of the wear surface replicas of WR4-based composite a) after crushing granite stone and b) after crushing mica-gneiss stone. Two magnifications.

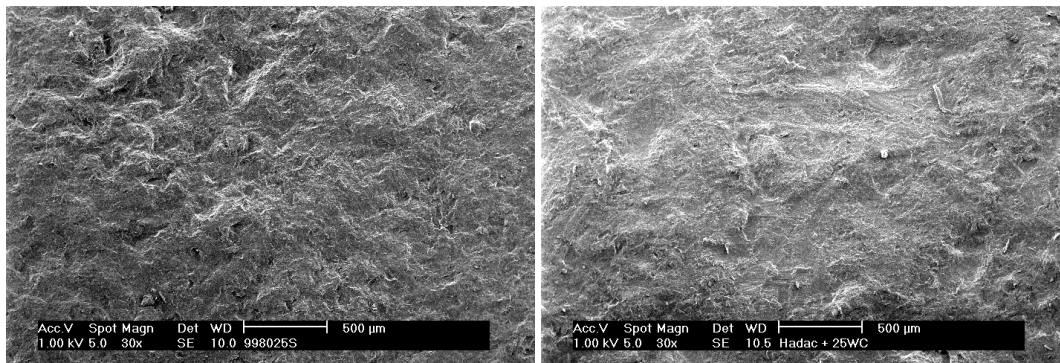


Figure 35 SEM micrographs of typical surface replicas of composites with a) martensitic steel matrix, b) manganese steel-based composite, WC/Co reinforcements, after crushing granite stone.

4 DISCUSSION

The wear performance of the materials is highly dependent on the structure of the material/composite and on the wear environment. The present chapter discusses the relations between wear rate and material structure in the studied wear environments. The role of hardness is also considered and the wear rates in the simulative cone crusher wear experiment are compared to other test results. At the end of the chapter comparisons between cone crusher wear tests data and other available wear data, the split Hopkinson pressure bar test data and surface fatigue test data, are made.

4.1 *The reliability of data*

4.1.1 The reliability of the wear experiments

Dry sand rubber wheel abrasive wear

It can be argued that the dry sand rubber wheel abrasive wear experiments, performed according to ASTM G65-91, actually do not present any real wear situation. However, DSRW is a standard wear test and it is widely used to measure the abrasive wear resistance in order to rank the materials, but not for determining the absolute wear rates of the materials [Hawk99a]. Another critical point about this test is that the area of the contact changes as the test proceeds and this makes the comparison between specimens impossible [Hawk99a]. Abrasive stone is one reason for the scatter in rubber wheel test results between different laboratories. The test results of the same material can be very different with different stone. In the present study, differing from the standard procedure, the abrasive used is a rock from Nilsjä in Finland.

According to [Hawk99a], the experiment reproducibility is at best when the volume losses of the specimens are between 20 to 100 mm³. In the present experiments, a large variation from 18 to 176 mm³ of volume losses was observed. Average coefficient of variation, COV, is 9,3%, which is relatively high. High average values of COV, from 7,15% to 10,96%, were also found elsewhere [Osara01a] with the steel-based composite materials of a type similar to that in the present study. In order to meet the ASTM specification, the COV must not exceed 7% [Hawk99a]. In the case of the present composite materials, the local uneven distribution of the reinforcements in the different test specimens can increase the scatter of wear test results, as the testing area of the sample is small and the local variation of the relative coarse reinforcement particles is present. This applies to all wear experiments on composite materials where specimen sizes are relatively small and the variation in the composite structure is caused by an unsuccessful process of mixing the starting material powders.

However, rubber wheel wear test is a well-known and relative simple experiment. It has therefore taken its place in a good and profitable ranking test of materials.

Erofuge erosive wear

In erofuge experiments, the ordinary way of presenting the wear results is the mass (mg) or volume losses (mm³) divided by the weight of abrasive used (in g or kg) [Hussainova01b][Söderberg81a]. However, the operating parameters (stone-related

parameters, impact angles, and velocities) can vary considerably in different studies. This makes comparison of the different wear research results found in the literature difficult, especially when small changes in operation parameters cause high changes in erosive wear rates of materials. The advantage of the erofuge test is that several specimens, including a standard reference specimen, can be tested under the same conditions and at same time, therefore giving results that are truly comparable to each other. The detailed description of the testing device is given by Kleis in [Kleis05a].

The role of the composite structure is important in the erosion phenomenon [Kosel92a]. The local uneven distribution of the reinforcement particles may cause scatter between the test specimens. The COV values of the erosive wear rates reported in this study were from 5,5% to 6,4%, which is considered as acceptable. Other more crucial points in defining the reliability of the wear test results are as follows:

- It was observed in this study that the abrasives will stick to the deformed metallic matrices, also reported earlier by Liu [Liu03].
- The composites with higher volume fraction of reinforcements usually have more reinforcement-related defects, which will be discussed in the next Section, 4.1.2: The scatter and defects of the composite structure.

Wear in laboratory cone crusher

The nature of the laboratory cone crusher, called here B90, wear test is completely different as compared to prior laboratory dry sand rubber wheel or erofuge tests. In this simulative wear test, the degree of realism is supposed to be higher than in any pure one-wear-mode laboratory test, concerning the material wear performance estimation in the actual cone crusher application. The B90 experiment simulates the real wear environment in many ways. The movement of the stone particles and the crusher geometry are assumed to be similar to those of the real scale equipment. However, it also lacks several aspects included in real full-scale crusher facilities. The B90 is much smaller than actual cone crushers. This means that, at least the size distribution of the mineral particles and the forces present differ from the real application. As compared to many other laboratory wear tests, the exact single particle real movement is not known in the B90 equipment. The amount of the sliding wear compared to the wear controlled by rock particle indentations is also not known in this experiment.

In the present laboratory cone crusher wear experiments the external parameters were fixed and the performance of the wearing material was the main interest. Mica-gneiss stone (used with SET2) and granite stone (used with SET2 and SET3) were the only “varying” external parameters. Granite and mica-gneiss are natural stones, and therefore multi-minerals with inevitably some variation in structure. The granite, from the nearby city Tampere, Finland, was selected for the experiments based on the advice of rock specialists. This was because it has a relatively homogeneous quality as compared with many other stones. The deposit in the ground is large and therefore the availability of the rock was good for tests. The granite stone is considered as a very abrasive stone. Mica-gneiss stone was used only in the SET2 wear experiments; and it is softer than granite. The idea of using so-called medium abrasive stone was to evaluate how much effect the different stones have on wear rates and the ranking order of the materials.

In these tests, the “natural” variation of the operation parameters (stone, weather etc.) has to be accepted. The shape of the stone particles was irregular, which results in variations in the true contact areas of the stone particles (and wear volumes of the liners), even with similar nominal particle sizes of abrasive stone. The stone particle sizes were fixed by a screening process. All the tests that failed in the stabilisation of the external testing parameters were eliminated. The reasons for this rejection were, for example:

- unfinished wear part surfaces or the wrong surface geometry,
- false operating parameters, for example, close side setting, and
- initial state of wear (steady state of wear not achieved).

An important advantage of the B90 cone crusher laboratory experiment as compared to many other laboratory tests is that the wearing surface is large as compared to the scale of the unevenly distributed reinforcements of the composites. The local scatter and unevenly distributed reinforcements of the composite materials will not affect the results, as they can in the case of small specimens and testing areas. However, the whole mantle as wear specimen increases the expenses of the experiments. Also, the time needed for the experiments (starting from metal powder compaction of the test material and finishing when the experiments were completed) was considerably long. This type of simulative wear test is very valuable in every sense; however, the time spent to obtain the few tested values often results in the use of simpler laboratory tests with simple test specimens. For example, small plates can be used instead of HIPed cone crusher wear parts.

The average coefficient of variation, COV, of the wear test results was 11,7% in SET2 and 14,9% in SET3; however, with some materials, the COV was about 2% and, at the highest, over 40% with low-wear-rate materials. When the wear rate is low, the “normal” scatter of this cone crusher wear test will be high as compared to the absolute wear rates of the tested materials. As a result of this testing, the configuration (set of external parameters) will not be adequate if the wear rates decrease further due to the size of the measurement error compared to the test result. The laboratory cone crusher wear experiment was originally designed for the standard material, manganese steel, which has generally higher wear rates in these tests than the best of the tested HIPed P/M tool steels. Comparing the laboratory-scale simulative wear test with the impact jaw crusher wear test, scatter up to 20% or more has been found in some cases in these circumstances [*Hawk99a*].

The wear rate results are expressed in the form of (g/ton) material weight loss per used abrasive in the wear test. The most of the materials studied in this work were materials with tungsten carbide reinforcements. However, as compared to the lighter non-tungsten materials MM15, WR6 and materials with titanium, the *volume* loss of these “light” materials will be higher and a shift in wear rates will occur in these cases, if presented in term of volume losses instead of weight losses. However, the results representing true measuring values are what is wanted, because the volume loss already is a calculated value in the case of these composites. The density is a measured value, which means that, if presenting the results in volumes, there would be error sources of two tests (wear test and density test) in the wear-rate values. Another source of the result sifting and the source of scatter is the wear of the concave. It was made of wear-resistant material, but still, through the progress of

time, the wear of the concave will have an effect on the “setting parameters” and indirectly on the wear of the mantle. The wear of the concave will increase the cavity volume in the crusher slightly; however, in these experiments, this point is considered to influence the overall scatter of the experiments.

4.1.2 The scatter and defects of the composite structure

In reality, there is scatter in the reinforcement sizes, shapes, distribution and matrix powder particle sizes in this study, *Figure 36*. (However, the homogeneity is dependent on the observation area.) The particle sizes and shapes of the raw powders and the mixing process of the powders affect the final distribution of the reinforcements. Local inhomogeneous areas in the composite structure have to be accepted to an extent defined by the manufacturing process and raw materials. Clusters and networks of reinforcements may also occur to some extent. In *Figure 36 a* and *b*, coarse aluminium oxide reinforcements and fine chromium carbide reinforcements in the steel matrices of the SET1 composites can be seen in the same magnification.

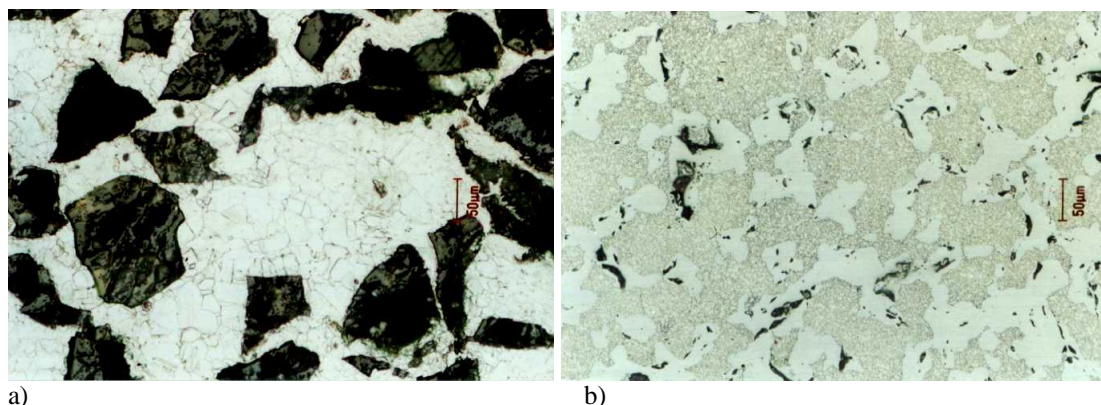


Figure 36 The size scale, uneven shape and networking of the reinforcements are seen a) in AISI 316L austenitic stainless steel with relative coarse Al_2O_3 reinforcements and b) in duplex stainless steel Duplok 27 with fine Cr_3C_2 reinforcements. Optical microscope pictures, with the same magnification.

Design of the composites is a challenge because several phases show different physical properties, such as the thermal expansion coefficient, solubility of alloying elements etc. In the HIPing process, the compatibility of the powders in production, control of the diffusion zones and the formation of the secondary phases, as well as formation of internal stresses etc., are aspects to be considered. Dilemmas in the material production can arise. For example, austenitic- and duplex-steel-based composites in SET1 in this study need a rapid cooling rate after heat treatment, in order to avoid unwanted secondary phases. On the other hand, generally rapid temperature changes or deformation can cause internal stresses. The quality of the raw materials is also directly reflected in the final material structures. Defects observed in the composite structures during the current are:

- oxide necklaces in the prior powder particle boundaries, caused by oxidised powder prior to consolidation,

- porosity in the metallic matrix or in recycled hardmetal reinforcements,
- porosity or cracks in interfaces between matrix and reinforcements and
- relatively large, visible interfacial reaction layers.

One critical point in the present wear tests was the MMC sample preparation. As the material contained ductile and brittle phases, the sample surface might have been deformed or defects/cracks might have been formed during the sample preparation. Especially in the laboratory tests, DSRW and erofuge test, the sample preparation was made up with special care in order to avoid the deformation or defect formation (spark machining, manual grinding). The cone surfaces in the cone crusher wear test were machined conventionally. As machining is a “rough” surface treatment, it was important to continue the wear tests as long as the steady-state wear rate was obtained in the cone crusher tests.

Data from composite microstructures collected from images of material surfaces, as well as the nominal values of materials, were used. Automatic and manual functions of the image analysing program were combined. The critical point in these analyses seems to be threshold operation, the definition of the borderline between black and white in order to further analyse the size and area fraction of the hard phases or the impact scars. In this study, the area fractions have been considered to estimate volume fractions, thought to result in only a small error as compared to overall scatter. Considerably large pixel numbers have been used to visualise the boundaries more accurately and to get more-accurate measures. Considering the scatter and "non-ideal" character of the composite structure, the collected numerical characteristics of the structure can be considered as trend-setting average values. The image analysing results were in this study observed to largely depend on the manual operations in the threshold phase, after many trials of the image analysis of the microstructure. Therefore, values given by manufacturer were considered as reliable as image analysis results of the present composites.

4.2 Abrasive and erosive wear performance of steel-based composites

4.2.1 Dependence of abrasive wear on reinforcement-related parameters

Volume fraction of the hard phase is a widely recognised microstructural parameter of the composites. The dependence of the wear rate on the volume fraction of the hard phase is discussed in the case of the materials presented in *Table 6* (Section 2.1.1). The dry sand rubber wheel (DSRW) abrasive wear rates under discussion are presented in *Table 14* (Section 3.1.1). The volume losses in DSRW tests are presented in *Figure 37* as a function of the nominal oxide/carbide volume fraction. It is shown that the abrasion resistance of the studied matrix materials (APM and Duploc) is improved when either the Cr_3C_2 or Al_2O_3 content of the composites is increased. The wear rate is decreased by over 80%, when the reinforcement volume percent increases from 0 to 30. The austenitic and duplex steel matrices are relatively soft and not particularly wear resistant. When comparing the relative wear resistance of the matrices and composites (*Table 14*), the plain duplex steel and duplex steel with 30 vol.% fine Cr_3C_2 reinforcements have a slightly lower volume loss compared to plain APM or APM with 30 vol.% fine Cr_3C_2 , respectively.

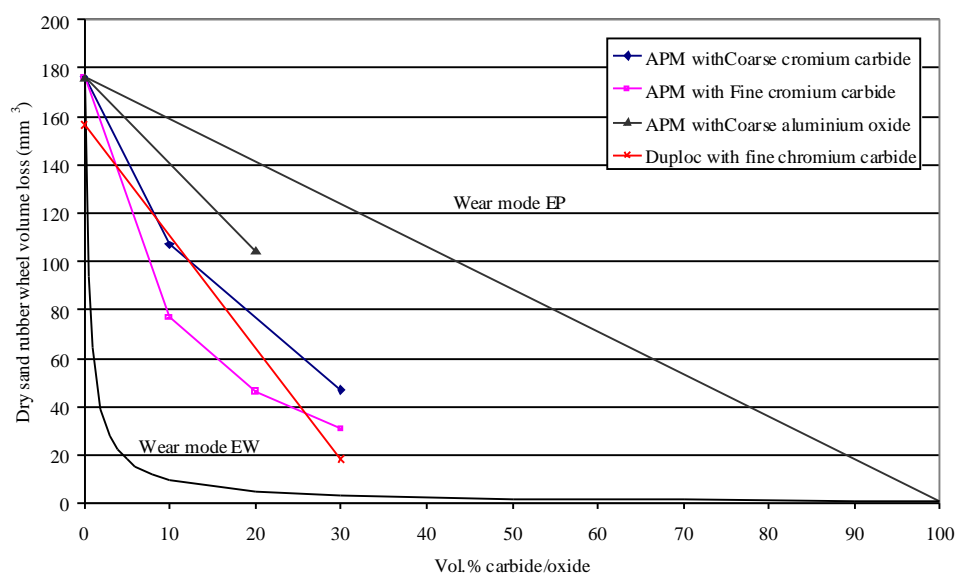


Figure 37 Volume loss of the composites in DSRW test. Loss of material due to wear is presented as a function of reinforcement volume percent. Composites with two matrix materials APM and Duploc have been plotted here. The linear trend line (EP wear mode) shows the upper limit of the wear. The lower limit of wear is shown by EW wear mode according to [Axen94a]. Both EP and EW are calculated theoretically by setting the carbide volume loss as 1 mm^3 and then calculating linear (EP) and inverse (EW) rules of mixture for the APM-matrix-based composites.

The reinforcements (*Figure 37*) seem to have a clear effect on the wear resistance of composites with chromium carbides, and aluminium oxides. The increase of the hard phase volume fraction has also been reported to decrease the wear rate (in rubber wheel tests) in earlier studies, i.e., with P/M-iron-based composites with ceramic

reinforcements [Pagounis98a]. When studying the magnitude of the reinforcement effect, the model of abrasive wear resistance of multiphase materials of Axen et al. [Axen 94a], explained in Section 1.4, can be utilised. The basic idea of the Equations (5) and (6) have been implemented in *Figure 37*. Two modes, equal wear rate, EW, of the phases and equal pressures of the phases, EP, both start from Archard's equation (Eq. (1) in Section 1.4) and continue with rules of mixtures. The linear trend line shows the upper limit of the wear, according to the EP (equal pressure) wear mode, while the lower limit of wear is shown by the EW (equal wear rate) wear mode. As the bulk carbide or oxide wear is considered to be extremely low, both EP and EW are calculated theoretically by setting the carbide volume loss as 1 mm^3 and then calculating the volume losses from linear (EP) and inverse (EW) rules of mixture for the APM matrix composites. It should be noticed that, in Equations (5) and (6), the wear phenomenon is presented as wear resistance and in *Figure 37* as volume loss. The volume losses of the all four tested composites seems to be considerably decreased when compared to plain matrix material; this is the case especially with composite reinforced with finer chromium carbides. This means that composites seem to follow either a near EW or mixed mode wear (*Figure 37*). Equal wear rate of phases, EW, means that both phases are worn down parallel; this mode corresponds to the ideal state and a composite is taking full advantage of its reinforcements [Axen94a]. Axen et al. have verified the model with several materials. The SiC-particle-reinforced aluminium was worn in EP mode under conditions that promote large abrasive grooves (high loads and coarse abrasives), while under milder condition the composites were worn under the mixed mode (in pin-on-drum two-body abrasion tests). Rubber- and bakelite-matrix-based composites followed EW mode lines.

Because of the considerable beneficial influence of the reinforcement particles on the wear rate, it can be concluded that bonding between matrix and reinforcement particles is strong enough under the present wear conditions to prevent reinforcement to fall out too easily from the matrix. The “coarse” reinforcements are upraised on the wear surfaces, which means that the matrix material has at least a slightly higher wear rate than the reinforcement particles. In the case of “fine” reinforcements in composites, the abrasive sand will not have so much space to penetrate between the reinforcement particles.

The question of the influence of other microstructural parameters of the composites, such as the size of the reinforcement particles and spacing between the particles on the abrasive wear rate is then addressed. The effect of the size of the reinforcements on wear rates in DSRW within SET1 materials (materials *Table 6*, Section 2.1.1 and sizes *Table 10*, Section 2.1.2, wear results *Table 14*, Section 3.1.1) is shown in *Figure 38*. It can be seen in *Figure 38* that size of the reinforcements also has a considerably strong effect on the volume losses. In the case of chromium carbides in the austenitic matrix, fine chromium carbides perform better at the same volume fractions than coarse carbides. (Trend lines for each volume fractions (tested values 10/100, 20/100 and 30/100) are added to *Figure 38*.) The wear rate decreases by about 30 percent with the finer carbide reinforced composites as compared to coarse carbides of the same type.

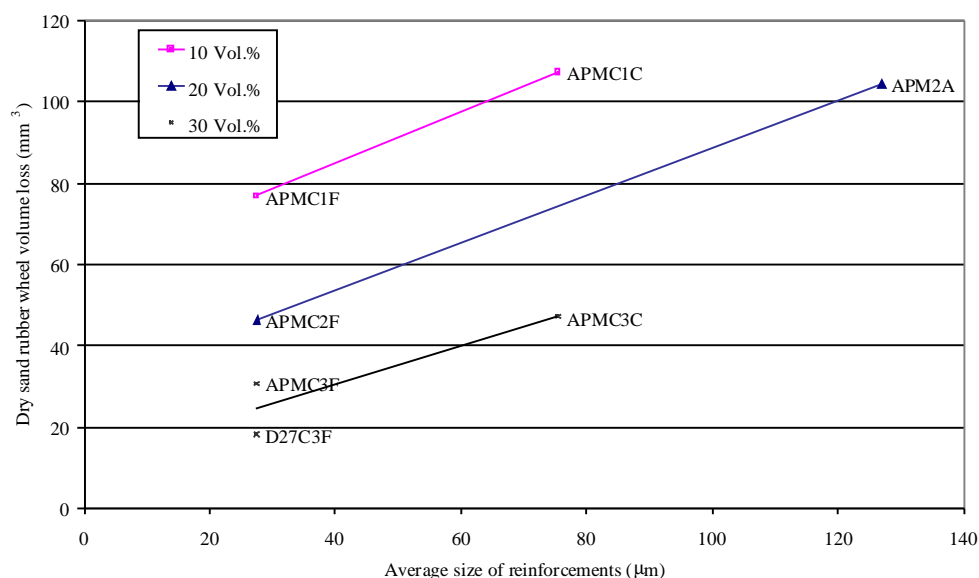


Figure 38 The volume losses vs. the average size of reinforcements of the tested composite materials in the dry sand rubber wheel tests. It can be noted that with the same volume fractions (tested values 10/100, 20/100 and 30/100), the composites with smaller reinforcement sizes have lower wear rates. Bulk matrix wear rates are not on the scale of the figure (APM volume loss was 176 mm³, D27 volume loss was 157 mm³).

When concerning the influence of the spacing between the reinforcement particles on volume losses in DSRW within SET1 materials in *Figure 39*, the trend of smaller spacing with a smaller volume loss can be seen. (Materials are presented in *Table 6*, Section 2.1.1 and spacings in *Table 10*, Section 2.1.2 and wear results in *Table 14*, Section 3.1.1.) The spacing between particles is smaller with finer carbide sizes as well as with higher volume fractions of reinforcements (and therefore the overall hardness is also higher in these composites, see results in *Figure 22* in Section 3.1.2). It is noteworthy that spacing between reinforcement particles is not an independent internal parameter, as the spacing depends both on the volume fraction of the reinforcements and on the size of the reinforcements. The spacing between particles has an important role from the physical point of view: it determines the free paths for grooving the matrix by abrasive particles. In the present case, the abrasive particles were angular and with the size from 100 to 600 µm; however, sharp grooving edges of the abrasive particles are much smaller.

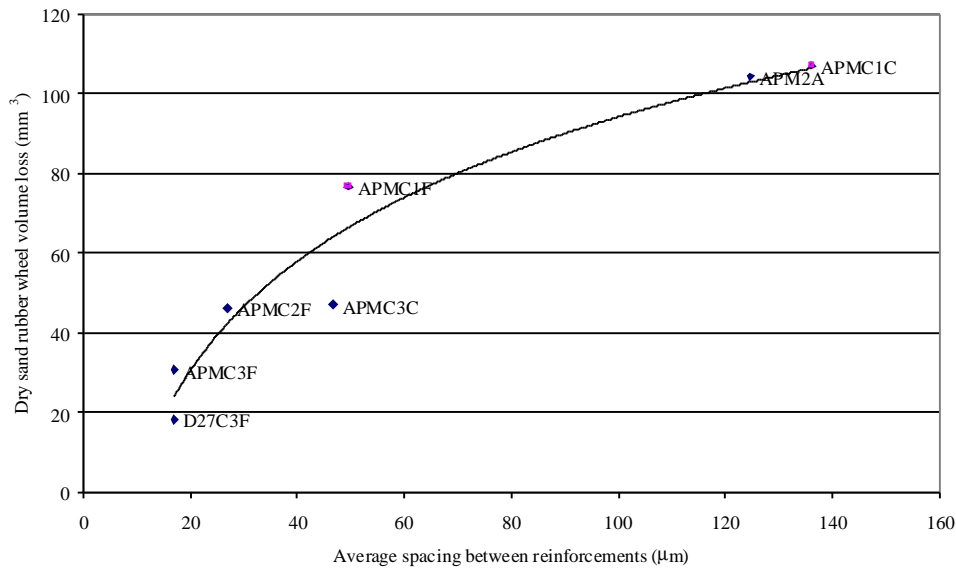


Figure 39 The volume loss vs. the average spacing between reinforcements of the tested composite materials as measured in dry sand rubber wheel abrasion test. Higher volume fractions of reinforcements and their smaller size decrease the spacing between reinforcements.

In the pin abrasion test with garnet, it has been found that the wear rate is related to carbide size, volume fraction and the mean free path by Equation (4), presented earlier [ZumGahr87a]. With the present results from SET1, such relationship cannot be found. However, as shown in *Figure 40*, the correlation can be found between wear rate and the ratio of two internal parameters, reinforcement volume percent and spacing between reinforcements ($wear\ rate \propto spacing/volume\ percent$). This can be rationalised as follows. The coarse reinforcement sizes (Al_2O_3 105-149 μm and Cr_3C_2 45-106 μm) are relatively close to abrasive particle sizes (100-600 μm). In the composites with coarse reinforcements, the reinforcing particles also have the highest spacing *Table 10* in Section 2.1.2. This means that in abrasive wear situations, the material is more heterogeneous, i.e., finer abrasive stone particles will fit between the coarse reinforcement particles and may groove the matrix material. Besides the volume percent of the hard particles, the spacing between particles seems to be more crucial than the size of the particles. The observations of the wear surfaces also support this idea. On the wear surfaces of composites, hard reinforcements are upraised on the surfaces and the matrix around the particles has been worn out. This implies that the more homogeneous the composite is, the more wear resistant it is, i.e., the smallest spacing gives the best wear resistance. Consequently, the logarithmic fitting in *Figure 40* may not be “real”, i.e., the reason for the sharp change in the slope may be the “boundary” between a heterogeneously behaving composite and a homogeneously behaving composite in this specific wear environment.

In wear, the contact area of the abrasive particle defines the homogeneity of the material, as discussed earlier in Section 1.2. The importance of the relative sizes of the particle contact zone and the hard phase regions in the abrasive wear of a composite material has been pointed out by Hutchings [Hutchings92a]. Only when the abrasive particle type is fixed and the particle size is constant can the internal material

parameters be evaluated separately as in the present case. The spacing between particles is commonly characterised by the mean free path. It is used, e.g. for the characterisation of hardmetals. Concerning polymer composites, the distribution of the reinforcing phase, represented by the mean free path, is noticed as an additional factor for describing the abrasive wear resistance besides the volume fraction of the reinforcing phase [ZumGahr87a].

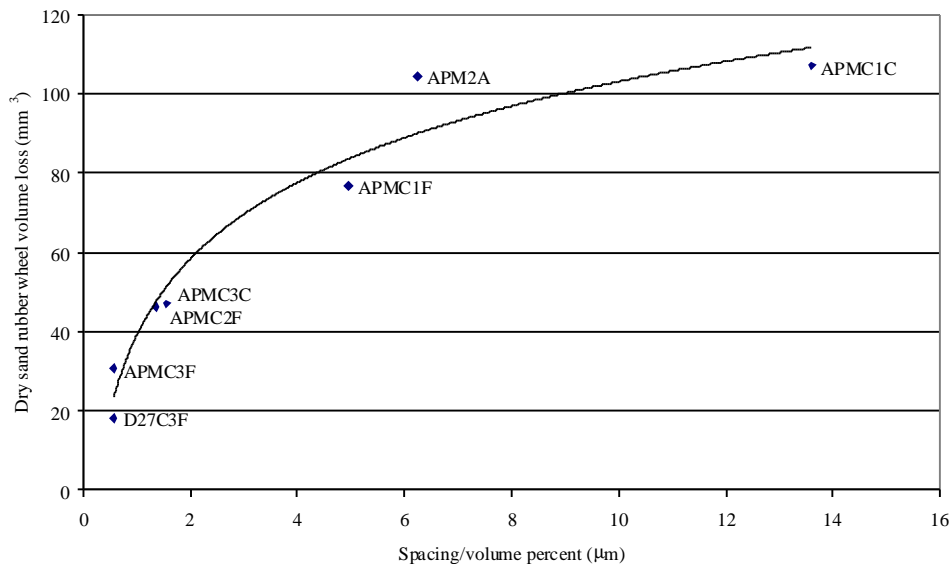


Figure 40 The volume losses vs. the ratio of the internal microstructural parameters (the spacing and volume fraction) as measured in DSRW test.

Hardness is one of the most recognised parameters in the wear of metallic materials. The DSRW volume losses have been presented as a function of inverse HRC hardness values of the composites, in *Figure 41*, (wear results in *Table 14* in Section 3.1.1, hardness results in *Figure 22*, in Section 3.1.3). The HRC value of the plain matrix material D27 is shown, but the HRC value for the APM matrix is not, because it could not be measured reliably due to the softness of the material. Composites with the same volume fraction of hard particles have higher values of hardness (*Figure 22*, in Section 3.1.3), when the hard particle size is decreased. In the tested cases, the best performing particle size range is 10 to 45 µm, with volume fraction 30%. Finer structures with homogeneously dispersed carbides are also generally considered as wear-resistant materials in abrasive wear. Such materials are, for example, tool steels, white cast irons or hardmetals. They also have significantly higher HRC values, as compared to the stainless steel matrix in the present composites.

Hardness is one of the central parameters in the widely referred Archard equation for wear, Eq. (1). In the present case, increasing composite hardness correlates also well with decreasing abrasive volume loss, as can be seen in *Figure 41*. The relationship between hardness (H) and wear rate is in our case found to be $W_v \approx \alpha \cdot H^{-1} + \beta$,

where α 5550 (mm^3) and β is -81 (mm^3) by using Microsoft Excel to fit the equation constants. This relationship predicts zero wear at the hardness of ~ 67 HRC.

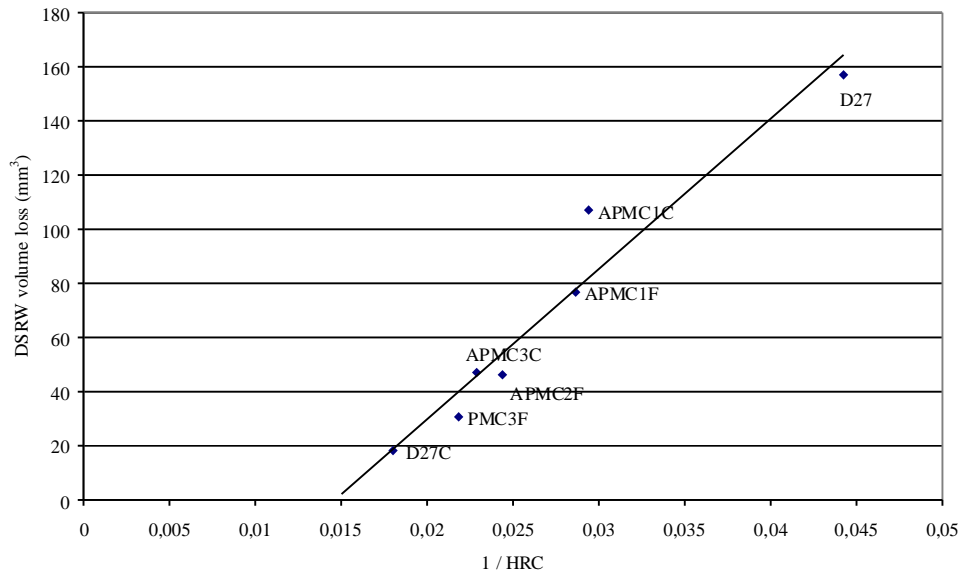


Figure 41 Volume losses vs. composite hardness in dry sand rubber wheel tests. Hardness value of APM-matrix material could not be measured in HRC units due to the softness of the material.

The materials seem to follow the modified Archard wear equation, i.e., the wear resistance is increased with the hardness (and volume fraction of the hard particles). The material wear also fits between the upper and lower limits defined by Axen et al. [Axen94a]. Besides the volume fraction of the hard particles, the spacing between hard particles seems to be more crucial than the size of the hard particles. Spacing between particles implies that the more homogeneous the composite is in relation to the wear environment, the more wear resistant it is, i.e., the smallest spacing between hard particles gives the best results. When the abrasive particle type is fixed and the size is constant, only then can internal material parameters be correlated separately with wear as in the present case. Otherwise, the internal and external wear-related parameters should be combined.

4.2.2 Dependence of erosive wear rate on reinforcement-related parameters

In erosive wear, the influence of the reinforcements on wear rates is very different as compared to rubber wheel abrasive wear. The effect of the reinforcement is highly influenced by the wear environment, especially by the impact angle of the erosive particle flow. In the present study, the wear behaviour of materials was evaluated at two impact angles, i.e., angles of 30 and 60 degrees ($v=40\text{m/s}$, erodent quartz sand with particle size in the range of 100-600 μm) *Table 15* (Section 3.1.2).

At a 30-degree impact angle, more sliding scars are present in the matrix surface than at 60-degree impact angles. These differences are shown in *Figures 25, 26* in the case of AISI 316/ Al_2O_3 composite. The matrix areas are highly deformed at both impact angles and aluminium oxide particles have shown brittle behaviour in both cases. In these composites, the surface is “living” with the wear processes. Reinforcement particles are crushed and removed to some extent, and the erodent particles are attached and embedded in the soft and ductile matrix. The eroded surfaces at a 60-degree impact angle, studied by Liu, contained embedded particles over the entire surface [*Liu03a*]. It was also discovered that the major wear mechanisms of matrix were ploughing and type-I cutting, *Figure 2*. Furthermore, “the topographic features indicate that the erosion losses of the composites were controlled mainly by the damage patterns of the ceramic reinforcements” [*Liu03a*]. The breakage of the ceramics in a purely brittle manner and the weakness of the particle bonding were observed in the case of Al_2O_3 . In composites with Cr_3C_2 reinforcement, plastic deformation was observed and, according to Liu [*Liu03a*], this played a role in the course of the material removal.

The influence of the reinforcement volume fraction on erosive wear rate can be seen in *Figures 42, 43* and *44* at tested impact angles. In the whole set, the increase of the wear rate at a 60-degree impact angle can be seen at the higher volume fractions, *Figures 43* and *44*. At a 30-degree impact angle, the relationship between volume fraction of the reinforcement and wear rate is weak and non-linear in SET1 materials, *Figure 42*. Erosive wear rates were more or less at the same level regardless of whether plain matrix material or a composite was tested. When studying the influence of the chromium carbide volume fraction on the wear rate, it seems that wear rate decreases at 30-degree impact angles, *Figure 42*. In the case of a composite with 40 vol.% coarse Cr_3C_2 and Al_2O_3 , the wear rate is increased in comparison to composites with lower reinforcement content. As a conclusion, it could be said that no real improvement of wear resistance caused by the reinforcement addition was observed. This is in agreement with [*Kose192a*], where it is noticed that erosive wear resistance of the relative coarse composite structure rarely increases “due to the synergistic increase of erosion rate of hard, brittle phase by its presence as a dispersed phase in a relative soft matrix.”

In many materials, wear rates at both angles were close to each other and, when taking into account the scatter of results (discussed in Section 4.1.1), the differences between impact angles are not so evident. In *Figures 42* and *43*, a slight increase of the wear rate (30 vol.% composites) at a 60-degree impact angle has been noticed, compared to a 30-degree impact angle. This behaviour can also be seen in *Figure 44*. Veinthal [*Veinthal05a*] has studied the erosion performance of steel-based composites with TiC, WC and NbC reinforcements. In all composites, the erosion rate increased with

the erodent impact angle from 30- to 90-degree ($v=50$ m/s and erodent quartz sand with particle size in the range of 100 to 300 μm). With lower erodent velocity (20 m/s), the differences between impact angles of 30- and 60-degrees were not significant, but they increased between 60- to 90-degree impact angles. The general trend [Finnie95a, Kleis05a] is that the brittle materials have a higher erosion rate at higher impact angles as compared to ductile materials. This trend also applies here as the composites with higher hard-particle content are more brittle on average. The evaluation of the impact angle effect becomes more complicated theoretically in composites consisting of several materials, both inherently ductile and brittle.

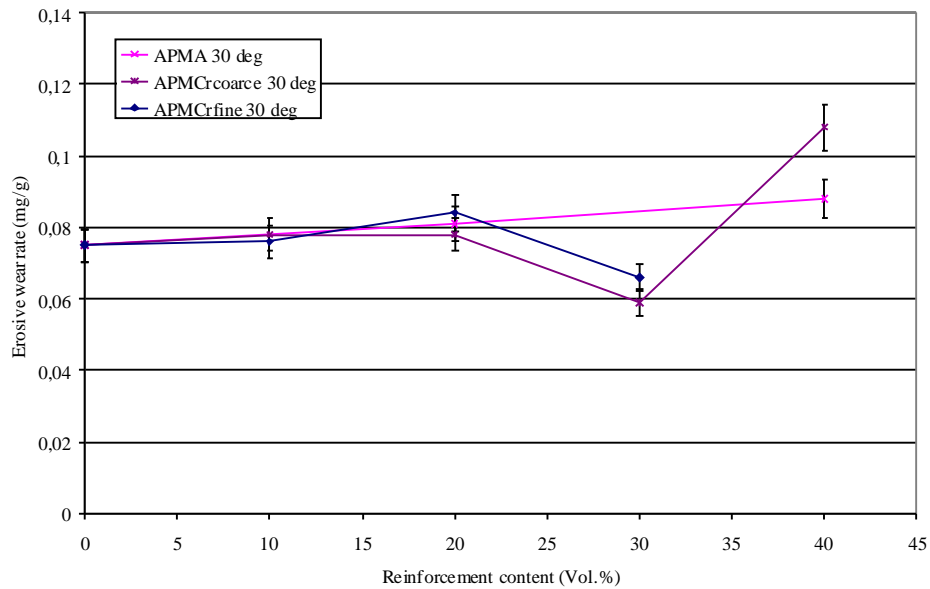


Figure 42 Erosive wear rate vs. volume percent of reinforcements at 30-degree impact angle with APM-steel-based composites ($v=40$ m/s). Composite APMCr is with Cr_3C_2 tested with 10, 20, 30 vol.%, and composite APMA is with Al_2O_3 tested with 20 and 40 vol.%.

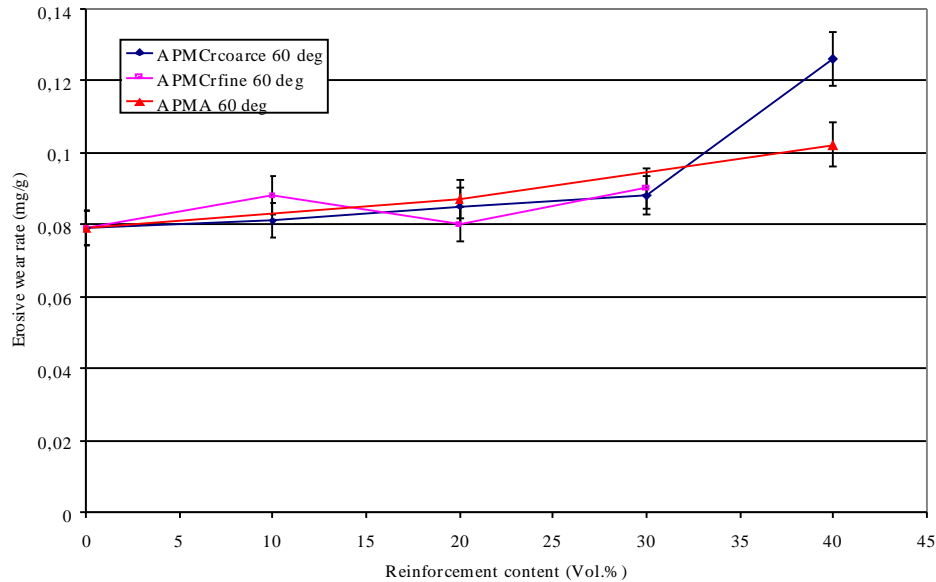


Figure 43 Erosive wear rates vs. volume percent of reinforcements at 60-degree impact angle with APM-steel-based composites ($v=40$ m/s). Composite APMCr is with Cr_3C_2 tested with 10, 20, 30 vol.%, and composite APMA is with Al_2O_3 tested with 20 and 40 vol.%.

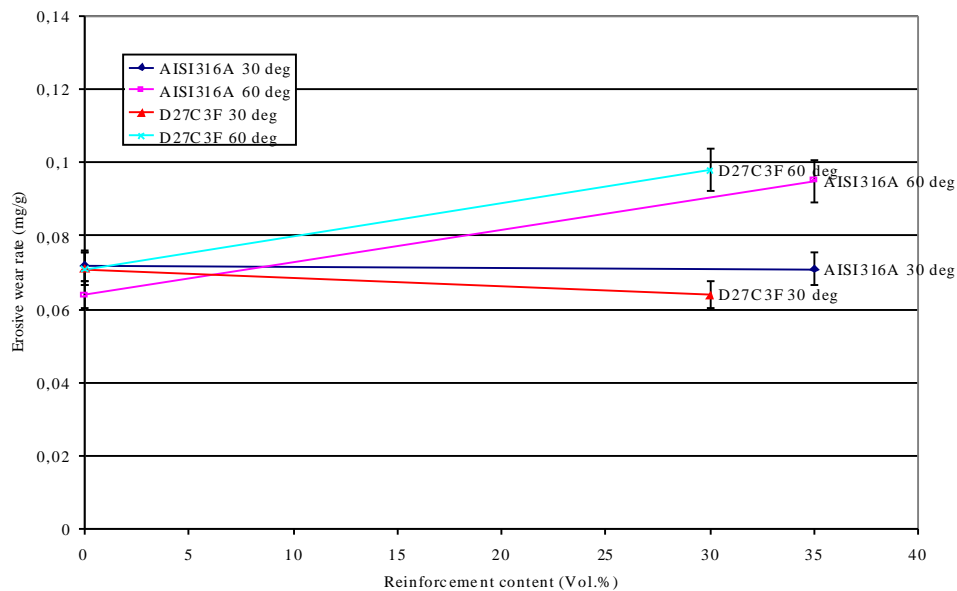


Figure 44 Erosive wear rates at 30-degree impact angle and 60-degree impact angle of austenitic- and duplex-steel-based composites ($v=40$ m/s).

In erosive wear, comparisons between different studies support the view that the influence of the reinforcement/hard particle volume fraction is highly dependent on the wear conditions. The “scale of individual contacts” [Hutchings92a] has a major effect on the erosion behaviour of the metal matrix composites. In wear, the contact area of the abrasive particle in relation to the scale of the microstructure defines the homogeneity of the material. As discussed earlier in Section 1.2, a large contact area compared to the scale of the material microstructure defines material as homogeneous and vice versa, a small contact area of the abrasive particles as compared to the scale

of the material microstructure leads to heterogeneous wear behaviour of the material. When studying *Figures 23, 25 and 26* representing composites with coarser reinforcements, the scale of wear marks seems to be much smaller than the scale of the structure, while in *Figure 24* the wear marks tend to be of equal size with the scale of the structure. In the following, the effects of the particle size and the spacing of the reinforcement particles in SET1 are evaluated in order to find out whether any general trends exist. When considering the effect of the size of the reinforcement particles, *Figure 45*, the average reinforcement size does not seem to have any significant effect on the erosive wear rates if all the composites are collected in the same presentation. The reason for this is that, when presenting the wear rates of all composites as the function of the reinforcement size, the composites with specific reinforcement size have different volume fractions of hard phase, and therefore are plotted as horizontal lines. Separating the specific volume fractions with their own tested impact angles and connecting them with lines, we will discover that the composites containing higher volume fractions of hard particles have a slightly decreased wear rate with an increase in hard particle size. The exception to this are composites with 20 vol.% hard phase at both impact angles and 10 vol.% composites at a 30-degree impact angle.

When studying the effect of reinforcement spacing, the biggest differences between wear rates of the studied composites existed at the smallest spacing values (*Figure 46*). Larger spacing improved wear resistance of the composites with the highest volume fractions of hard phase at both impact angles. With the smallest volume fractions, no significant differences in wear rates were observed.

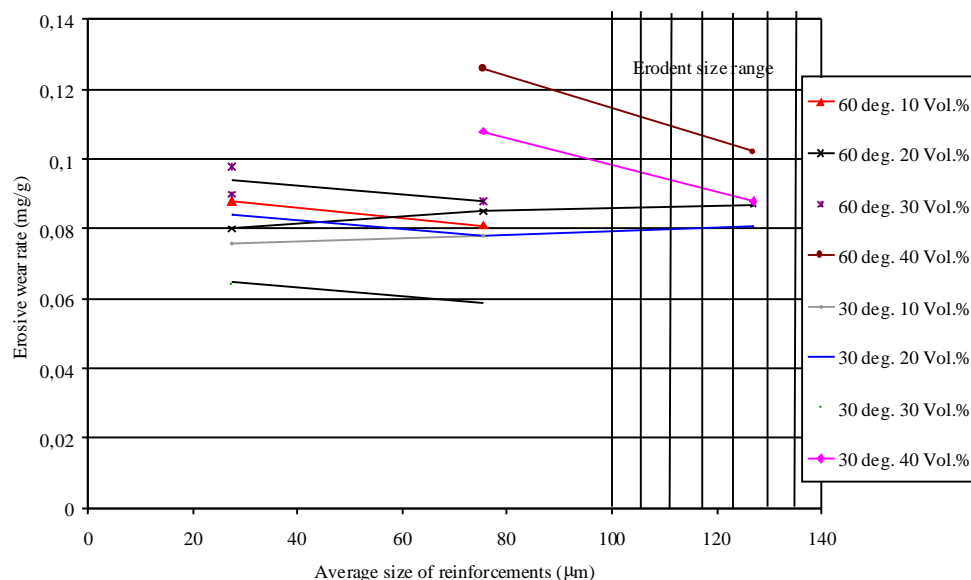


Figure 45 Erosive wear rate vs. the average size of the reinforcements at 30-degree and 60-degree impact angles of SET1 composites.

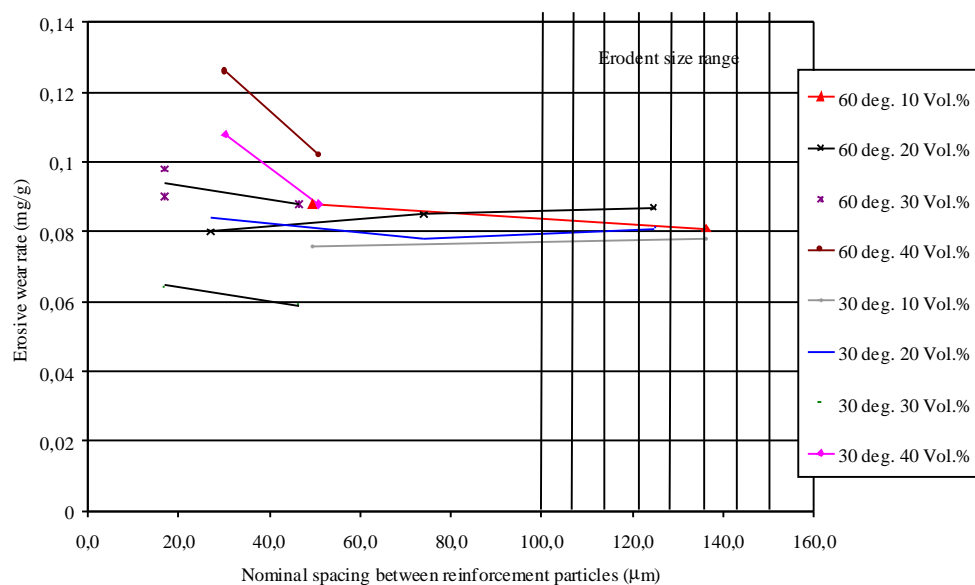


Figure 46 Erosive wear rate vs. average spacing between reinforcement particles of tested SET1 materials at 30-degree and 60-degree impact angles.

As conclusion on the effects of the reinforcement size and spacing on the erosive wear resistance at a fixed volume fraction, the wear resistance is noticed to improve with increase of average reinforcement size. While the particle spacing depends on the volume fraction and size of the hard particles, larger reinforcement particle size results in larger spacing between reinforcement particles at the fixed volume fraction. Hence, an improvement of the wear resistance was also observed with the increase of the nominal spacing in case of composites with the higher volume fraction of the hard phase. The increase of the hard particle spacing has been noticed to increase fracture toughness of the composite according to [Berns03a] and thus lower the bending strength. On the other hand, large hard particles will crack easily as illustrated earlier in Figure 8. In material selection for erosion conditions, toughness is considered an important parameter, since fracturing determines the wear resistance, especially at normal and high (>60) impact angles. At lower impact angles, the hardness of the eroding material will play a more important role [Kleis05a]. At a 30-degree impact angle, slight improvement of the wear resistance with the increase of the hard particle content (Fig. 42) was noticed up to 30 vol.% of the hard phase also in this study.

4.3 Dependence of cone crusher wear rate on internal material parameters of composite materials

In a cone crusher wear environment, several wear micromechanisms of wear has been found to be present simultaneously, e.g. Lindqvist [Lindqvist03a] has detected squeezing and sliding. Different wear marks were found also in this study, in *Figures 31 and 34*. In the case of pure sliding, cutting and ploughing of soft metallic matrix are dominant, while ceramic reinforcements are only ground. In the case of pure compression/indentation, microcracking of ceramic reinforcement is the crucial phenomenon, while the matrix will be plastically deformed. The resistance to the fatigue, i.e., the repeated wearing actions, may also be important material property. Relationships between wearing motion and wear mechanisms are affected by reinforcement-related parameters and matrix material. This network of the relationships is unique to the wear environment and materials. The importance of internal microstructural parameters in composite wear has been noticed, e.g., by Berns et al. [Berns95a][Berns98b][Berns98c][Berns97a][Berns03a].

In this chapter, the role of the matrix material and the different reinforcements of the present composite materials (SET2 and SET3) in the wear rate development are discussed based on the laboratory cone crusher tests. The role of the interfaces between the matrix and the reinforcements in wear rate development is not evaluated here. In the successful production of the composites, the interface between matrix and reinforcements should not be the weakest link in wear: bonding should be strong and ductile enough to hinder the pull-out of the reinforcements too early in wear situations.

In general, after the experience and attempts to analyse the tested materials, it can be stated that the trends concerning the interaction between microstructure parameters and wear can only be found within similar types of materials. When trying to compare highly different materials having different wear mechanisms, too many variables are involved to enable any sound conclusions.

4.3.1 Dependence of wear rate on the material carbide type and content

One of the widely used parameters in determining the influence of the microstructure on the wear behaviour is the volume fraction of the hard phase. In SET2, the trend of decreasing wear rate with increasing hard particle content can be seen in *Figure 47* with both the stone types, i.e., mica-gneiss and granite (wear rates in *Table 16* and hard particle content in *Figure 29* in Section 3.2.1). Reinforcement contents were originally determined and produced in weight % in this set and an image analysis was carried out for the conversion of the reinforcement content into area %, which is presented here as vol.%. For the total carbide content, both VC carbides (dispersed evenly in the matrix) and reinforced WC/Co (hardmetals, where carbides are in clusters) were counted together. The average hard particle content values are trend setting, as the standard deviation value of the hard particle content were relative high. This is seen by analysing the numerical values from the images discussed earlier. However, the following aspects can be brought into discussion:

- Matrix VC content seems to affect beneficially the composite wear rate. In *Figure 47*, the materials WR6, MM15, WR4WC and WR6WC contain VC and have the lowest wear rates as compared to other tested steels. With softer matrices, the sliding is observed on the wear surfaces. Vanadium carbides are increasing the macrohardness of the matrix materials and harder matrices are capable of resisting indentation and groove formation.
- It also seems that 35 wt.% addition of softer manganese steel into the matrix with high VC content shows good performance, i.e., material MM15 (in *Figure 47*). The matrix material WR7 has the highest VC content of all the tested materials, while the manganese steel as a soft material brings to the composite the increased toughness. The wear rate is much lower than that of other materials with the same volume fraction of hard phase.
- Most of the composites were WC/Co-reinforced (with the exception of MM15), but their wear rates seem to vary widely, although WC/Co contents in different materials vary only between 10 and 15 vol.% according to image analysis. This implies also that matrix dominates the wear-rate level of the composites and the matrix VC content seems to have a greater effect on the wear rate than WC content in SET2.

For SET2 materials, the wear rate and the volume fraction of the hard phase seems to obey the power-law relationship, $y = \alpha x^\beta$ (*Figure 47*). By analysing further five SET2 materials exposed to two stone types, *Figure 48*, it can be noted that, when weighted the WC volume percent with 0.36 and the vanadium carbides with 1, a linear correlation between wear rate and the volume percent of the carbides is obtained. The types and volume percents of different carbides in SET2 are presented in *Figure 29* in Section 3.2.1. By this modification, a linear fit between the wear rate and the adjusted carbide volume percent has the best R^2 value, 1, in the tested range. It is obvious that the dependence between wear rate and adjusted volume percent cannot actually be extrapolated very far; however, this type of numerical exercise reveals the minor effect of WC/Co reinforcement on the wear rate as compared to the VC carbide effect in the tested range. In order to estimate the effect of the different carbides (VC and WC) on wear rate, the correlation between wear rate and volume fraction of each individual carbide type is assumed to be linear in the following discussion. Actually, it is not always linear, as Axen et al. [Axen94a, Axen95a] have pointed out. The dependence between wear rate and carbide or reinforcement volume fraction is expected to follow an equation of the type $W_v \propto \lambda / (d^{\beta/2} v_c)$ according to equation (4) [ZumGahr87a] presented in Section 1.4.

The basic characteristics of the composites combining WC and VC are the following: vanadium carbide particles are evenly distributed in the matrix material and therefore increase the overall matrix HRC hardness, while WC particles are clustered, having a more localised effect on wear. However, the reason for the small effect of WC/CO on the wear rate may be the easy pull-out of the reinforcements in wear, in spite of the fact that it was not observed from wear-surface replicas. In conclusion, the role of the wear-resistance level of the matrix is more crucial than the role of the reinforcements in the formation of wear rates in SET2. In other words, the total hard particle/carbide content of composites is more important than reinforcement content when concerning wear performance of materials. Materials in SET2 have been tested using two kinds of rocks, granite and mica-gneiss. The effects of the stones are discussed in Section 4.3.3.

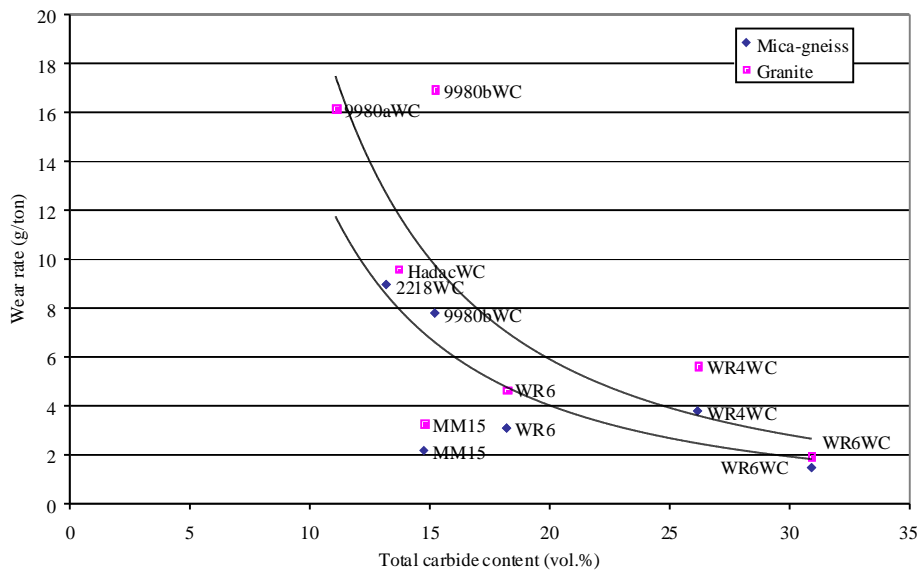


Figure 47 The wear rate in cone crusher B90 test vs. total carbide content in the materials of SET2. Crushed stones were granite and mica-gneiss. Composite MM15 is not included in the trend lines of the plot.

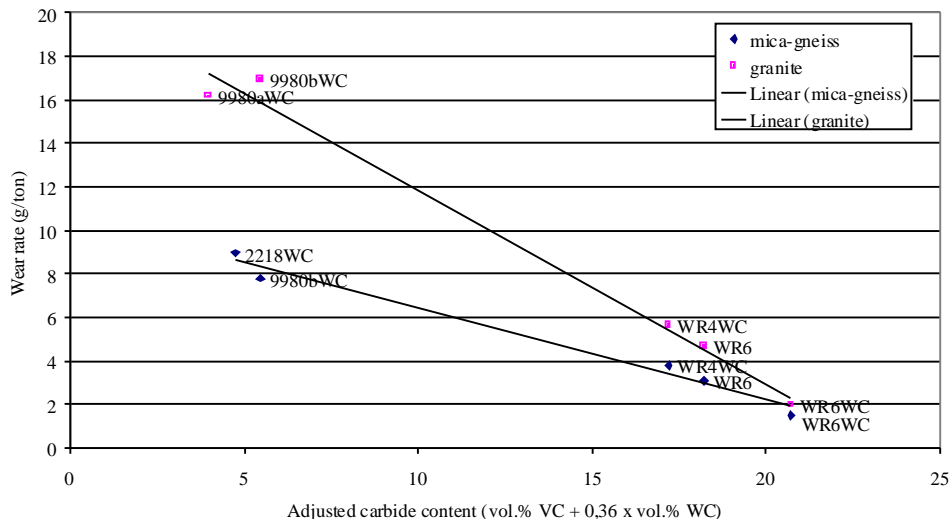


Figure 48 The influence of adjusted carbide volume percent on wear rate in cone crusher B90 wear test. The volume percent of VC carbides is multiplied by 1, while the volume percent of WC is multiplied by 0,36. The linear trend lines are best fitting to the experimental data. Stones were granite and mica-gneiss. The materials in the plot are the same as in Figure 47 without the composite MM15.

The dependence of the wear rate on carbide content in the SET3 materials differs considerably from materials in SET2. In SET3, the matrix material of the composite was tool steel. In WR6-based materials, the differences in wear rates are expected to reveal the effects of different reinforcements. In most of the cases, the addition of reinforcements was found to increase the wear resistance as compared to plain WR6 matrix, *Figure 49*. However, larger differences in wear rates were obtained with the variation of the matrices in SET2.

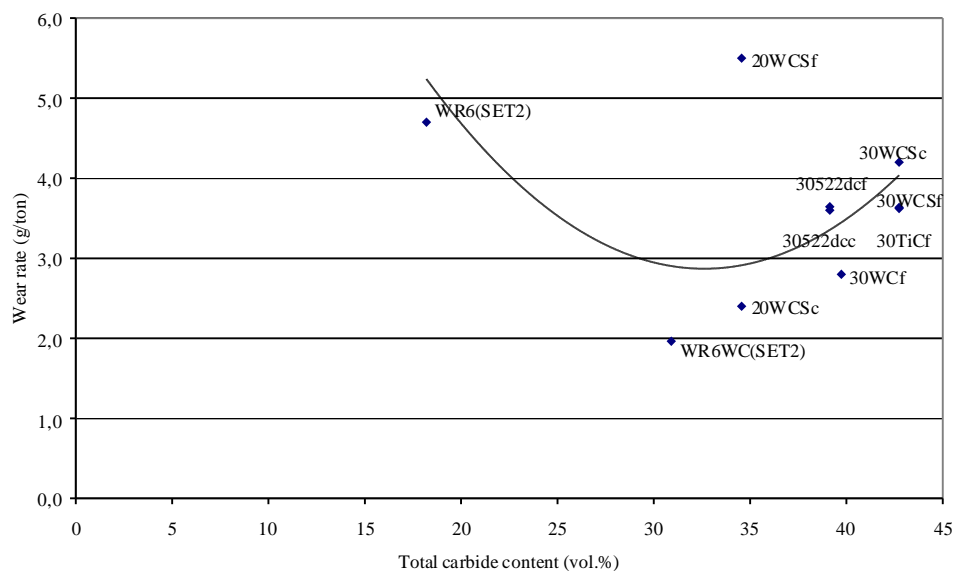


Figure 49 The wear rate in B90 cone crusher laboratory wear test vs. total carbide content of the WR6-based materials against granite stone. In tool-steel-based composites, the reinforcement types varied in a fixed matrix.

In tool steel (WR6)-based composites, the wear rates actually seem to increase with increasing total carbide content, although there is considerable scatter in the results (*Figure 49*) and the hard reinforcements have varying characteristics. This behaviour is the opposite of that observed in SET2. In WR6-based composites, different types of carbides, solid and double dispersion, were used with varying shapes and sizes. There seems to be a minimum wear rate within this set of materials; however, composite with fine cast carbides, 20WCSf, does not fit the trend. Results with higher volume fractions generally were around 4 g/ton, independent on whether the reinforcement types were fine or coarse, dense coated or cast type. However, the reason for the behaviour may be the reinforcement type rather than the volume fraction. Therefore, the discussion of the SET3 results will be based on the behaviour of the particular reinforcement types (*Figure 51*).

Results from SET2 and SET3 are plotted together in terms of wear rates versus total carbide content in order to find the scale of the wearing rates in both sets, *Figure 50*. It can be noticed that the selection of the matrix materials causes high differences in wear rates (SET2 materials), while the different reinforcements caused considerably small variation in wear rates (SET3 WR6-based materials). This means that the role of the total carbide content and wear resistance level of the matrix is more crucial than the role of the reinforcements in the formation of wear rates in cone crusher-type laboratory wear test, as discussed on the basis of *Figure 48*.

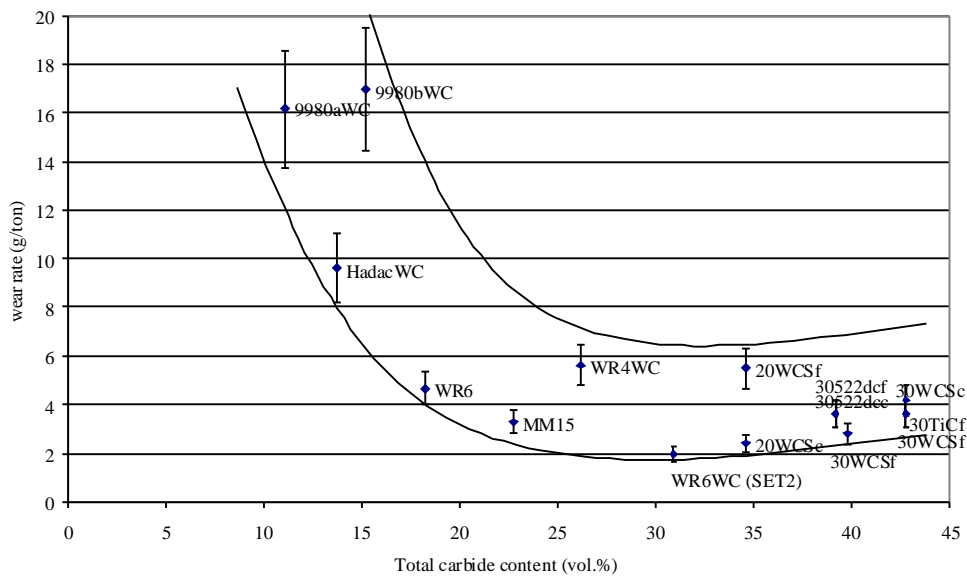


Figure 50 Wear rates of all tested materials as a function of total carbide content in the cone crusher B90 wear test. Wear media is granite stone.

Borderlines for minimum and maximum values of the wear rate have been sketched on *Figure 50*, based on SET2 and SET3 results. The presence of “wear minimum” as a function of volume fraction is somewhat questionable, because the reinforcement characteristics are varying and the volume fraction is only one varying parameter among others, e.g., the types of reinforcements. The range of volume fractions is limited and the scatter of results within the range is noticeable. Theoretically, the presence of minimum is possible with the composites, when the relative quantities of the active wear mechanisms change. The presence of minimum in the plot of wear rate as a function of carbide content in composites has been observed in other wear environments, for example, in some cases in sliding contacts and in erosion [ZumGahr87a][Stack97a].

The wear rates of the individual materials in SET3 are presented in *Figure 51* as a function of nominal reinforcement volume fraction. Here each composite type is shown by its own line: composites with cast WC fine (45-95) particles, cast WC coarse (250-425) particles, recycled WC/Co fine (100-200) particles and recycled WC/Co coarse (200-400) particles. These reinforcements have differences in sizes, shapes and clustering. The particles may contribute to different wear micromechanisms during the stone contact on the surface. Based on *Figure 51*, it can be stated at smaller volume fractions coarse particles, both recycled hardmetal reinforcement and cast WC carbide, seem to perform better than finer particles of the same reinforcements. Wear resistance of the composites with finer reinforcements is increasing with the increase of hard particle content in the tested range. On the other hand, the wear rate increases in coarse solid cast WC reinforced composite with an increase of WC content from 20 to 30 vol.%. However, a limited number of different volume fractions was tested. For further studies, it would be very interesting to find out the behaviour of the larger range of volume fraction, at least up to 40 vol.% WC contents on each reinforcement type.

The replica observations did not reveal any systematic reinforcement particle drops or pull-outs due to the wear; commonly, reinforcement particles were upraised on the cone-wearing surface, hindering the wear rates as compared to pure matrix material, e.g. *Figure 32*. As the width of the grooves was relatively large, this resulted in that the large reinforcements were more effective, on the basis of their larger potentiality to hinder the grooving. When comparing WC/Co and cast WC, hardmetal is tougher than pure ceramic, i.e., the possibility of cracking is higher with cast WC particles.

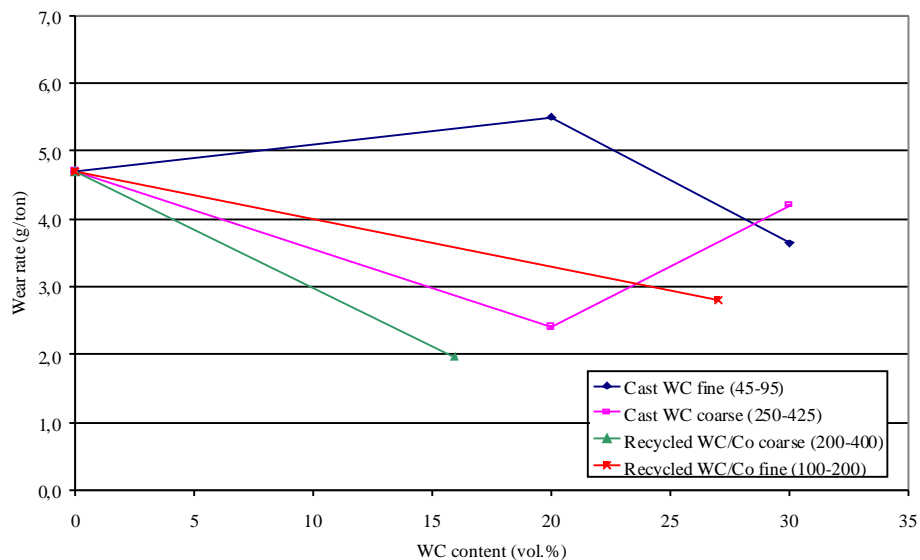


Figure 51 Wear rate in cone crusher B90 wear test as a function of tungsten carbide content of the composites in SET3. Granite stone as a wear medium.

Based on the analysis of the experiments, it is shown clearly that each individual composite has to be evaluated separately. Different types of reinforcement have different effects on composite wear rate as a function of reinforcement volume fraction.

4.3.2 Dependence of wear rate on the sizes of the reinforcement particles and hard particles

In this section, the effects of reinforcement particle and true hard particle sizes (inside reinforcements) on the wear resistance are discussed in case of the WR6-based composites.

The wear rates of the SET3 materials are shown as a function of average size of the carbides of the reinforcement particles and the average size of the reinforcement particles, *Figures 52 and 53*. Characteristics and sizes of the present reinforcement particles are presented in *Tables 12-13* in Section 2.1.1; they are also investigated elsewhere [*Sipilehto04a*]. Although these microstructural values show considerable scatter, i.e., structures are locally inhomogeneous and clustering of the carbides exists, the reinforcements are characterised by the true carbide sizes (e.g., in hardmetals). Wear rate versus true carbide size is presented in *Figure 52*; among the materials in SET3, the composites with intermediate sizes of the carbides were the worst with respect to wear. However, volume fraction of the carbides has a strong effect on the wear rate; the study of composites with different volume fractions may therefore disguise the possible trends caused by the true carbide size. When considering the materials with 30 vol.% (in material symbols value 30 in the plot), there may be a shallow gradient for increasing wear rate with true carbide size.

The relationship between wear rate and average reinforcement particle size is presented in *Figure 53*. The reinforcement size is considered to be the average size of the reinforcement particles, i.e., solid carbide size or hardmetal size (carbide cluster). After drawing in the figure the minimum and maximum wear rate borderlines, it seems that generally larger reinforcements perform better than the smallest ones. In pure abrasive wear, the size of the reinforcement particles should be equal to the sizes of the grooves. For example, material that behaves well for grinding rollers contains round-shaped hard particles with no contact between hard particles, and the size of the hard reinforcements is relative large, around 150 μm in diameter [*Theisen 04a*].

Comparison of the wear results with the results given in the literature is difficult, since similar tests have not been carried out for these types of composites. However, some general trends have been observed for good wear resistance in multi-mode wear systems or in wear systems where a combination of hardness and toughness properties is needed [*Theisen01a, 04a*] [*Berns98a, 98b, 98c, 00a*]. Relative large reinforcement particle sizes are favourable, since on rough abrasion metal matrix composites with 50 to 100 μm reinforcement size have shown good performance [*Berns95a*]. However, small true particle sizes are also beneficial, as it is known that the increase in hard particle size will decrease bending strength, R_m . [*Berns98b*]. Also, an increase in spacing will increase fracture toughness, K_{Ic} , as outlined earlier in the introduction (Section 1.3) [*Berns98b*], which leads to double dispersion structures. The actual crack initiation has been investigated earlier [*Broekmann96a*] with MMCs. The failure mechanism under external loads as identified, as hard phase cleavage, but crack initiation in the matrix was not observed by Broekmann et al. It seems that large solid reinforcement particles should be avoided in such wear systems where fracture of reinforcements occurs and this can lead to rapid decrease of wear resistance.

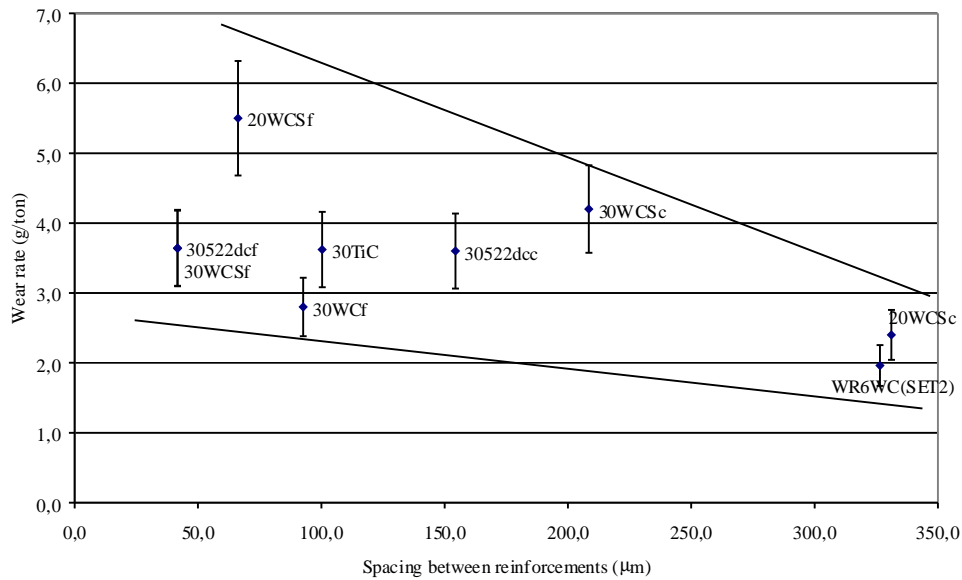


Figure 54 Wear rate vs. average spacing between reinforcements in WR6-based composites tested in cone crusher B90 wear tests.

The wear rate (in the pin abrasion test with garnet) is related to carbide size and mean free path according to Equation (4) in Section 1.4 [ZumGahr87a]. In this study, a relationship similar to the inverse function $W_v \propto \lambda/(d^{3/2} v_c)$ is plotted in Figure 55, based on the materials of SET3. Even though the horizontal axis is in logarithmic scale and the materials in the plot have a large scatter, the general trend can nevertheless be seen.

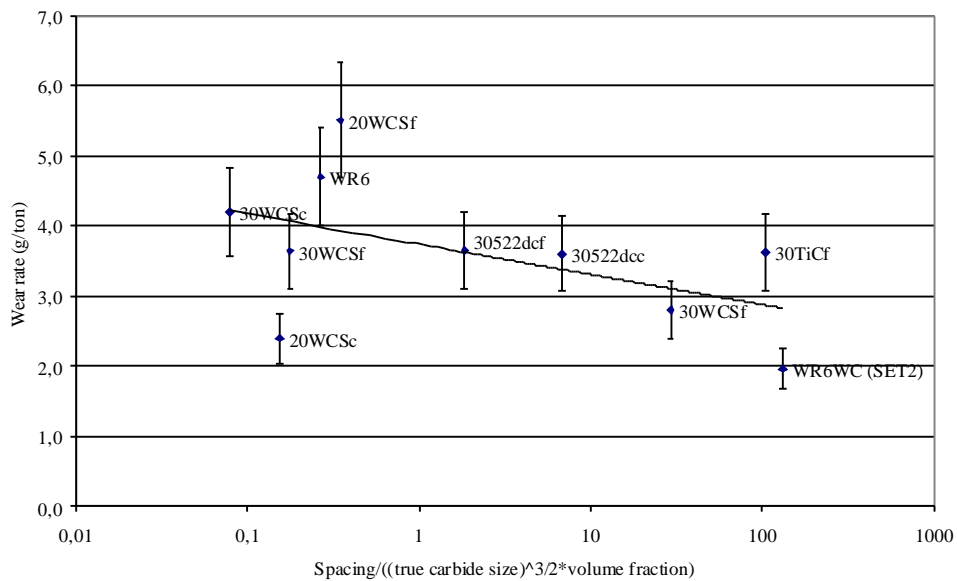


Figure 55 The relationship between wear rate and microstructural parameters ($\lambda/(d^{3/2} v_c)$) according to the Zum Gahr [ZumGahr87a] relationship. Note the logarithmic scale is on the horizontal axis. Data is measured in cone crusher laboratory experiments on SET3 materials.

Based on the analysis, the following general conclusions of the influencing parameters in abrasive wear can be made. The reinforcement-related parameters, which affect the wear behaviour in the present case, *seemed to be primary total carbide content in SET2 materials and the type of the reinforcement in SET3*. The tested material sets have many internal variables and a limited number of tests was made on a single variable. The total volume fraction of the carbides is the most important parameter in SET2 and the type of the reinforcement in SET3. The reinforcement type seems to be a considerably strong factor, *Figure 51*, as it overshadows many internal parameters such as size and spacing of the particles. Therefore, the actual optimum combination of internal parameters for a single composite structure could not be determined based on these tests. However, the trend-setting mapping of the internal parameters has technical importance and can be discussed as a guideline for further studies.

4.3.3 Dependence of the wear rate on the hardness of SET2 composites

A comparison between wear rates of selected materials in SET2 and available composite inverse hardness values is given in *Figure 56*. Hardness values are presented elsewhere [*Ala-Kleme04a*]. The manganese containing composites are excluded from the plot. Generally the wear rate seems to decrease with increasing hardness values. The hardness of different phases is not measured, but the estimated average hardness values of the matrix materials are collected in *Table 7*; it seems that the wear rate of the composites also depends on the hardness of the matrix materials. This is to be expected since the composite hardness level is also influenced by the matrix material hardness. The wear rate of the composite WR6WC (SET2) is lower than that of the plain matrix WR6. However, the hardness of the plain matrix WR6 is slightly higher than the hardness of the respective composite WR6WC [*Ala-Kleme04a*]. Still the properties of the matrix can be different in composites as compared to plain matrix material because, for instance, the porosity of the composite can influence the macrohardness values.

The relationship between wear rate and hardness (*Figure 56*), it differs again from the Archard equation (1). True Archard equation type relationship, $W_v \approx \alpha \cdot H^{-1}$, does not describe well the obtained data. However, as in the case of dry sand rubber wheel abrasion test (Section 4.2.1), the data corresponds well to a modified Archard equation, $W_v \approx \alpha \cdot H^{-1} + \beta$, for both wearing agent stones. In the best fit for granite, α is 2088 (mm³) and β is -33 (mm³), while for mica-gneiss, α is 1116 (mm³) and β is -17 (mm³). Here again, the fits to both data sets predict zero wear at about 53-57 HRC, as in the earlier dry sand rubber wheel test on SET1. The materials in both sets (SET1 and SET2) are considerably different; nevertheless, both are MMC materials. The plain constant of the modified Archard equation vary in both sets, but, as has been noted by Roberts [*Roberts06a*], wear rates can vary by a factor of about 100000x (pin-on-disk experiment), when friction coefficient varies by a factor of 2x, maximum 5x.

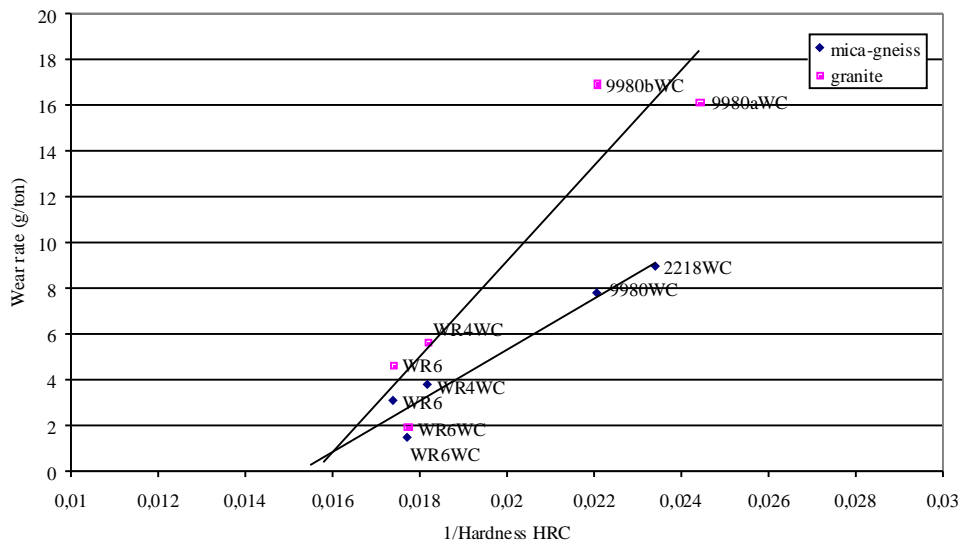


Figure 56 The wear rate in cone crusher B90 wear test vs. inverse composite hardness in SET2. Manganese steel containing composite is not included. HRC data from [Ala-Kleme04a].

The wear surfaces of the materials in SET2 revealed sliding scars, e.g. *Figure 31 and 34*. In many cases these were small. This indicates that the wear mechanisms are more or less related to plastic deformation in matrix material. In the composites reinforced with large cast WC particles, the wear surfaces have marks of sharp/angular shapes, which refer to brittle behaviour of the carbides. On the other hand, the wear mechanism of composites reinforced with double dispersion type carbides seems to result in a smoother wear surface (e.g. in WC/Co reinforced composites) than what is found in the materials reinforced with cast carbides.

Materials in SET2 have been tested using two kinds of stones, granite and mica-gneiss. The ranking order between materials did not change with the granite or mica-gneiss. Mica-gneiss stone resulted in, on average, 60 to 70% lower wear rates as compared to the granite stone. An increase in composite wear rate with increasing hardness of the abrasive is observed; this is also commonly reported in the literature, e.g., [Hutchings92a]. The hardness-to-hardness ratio, H_s/H_a , or vice versa, H_a/H_s , (s = surface and a = abrasive) is recognised as important in abrasive and erosive wear. In the current tests, the hardness of the abrasives was 5-7 on Mohs scale, mica-gneiss being softer, and granite harder. When the observed H_a/H_s ratio is $> \sim 1.2$ the mode is called hard abrasion, and vice versa, when the ratio is $< \sim 1.2$ soft abrasion. The composite WC reinforcement is harder than the abrasive stones and therefore the H_a/H_s is below 1, this means soft abrasion mode concerning the wear of reinforcement particles.

4.4 Correlation between cone crusher wear test data and modified split Hopkinson pressure bar test and surface fatigue wear test data

Some comparisons between cone crusher wear data obtained with granite stone and other available wear data have been made. The idea of such comparisons is to investigate whether some of the laboratory tests could “estimate” the wear rates in a more complex cone crusher wear environment. Firstly, the cone crusher wear test data were compared with the modified split Hopkinson pressure bar wear data of the SET2 and SET3 materials. Secondly, the cone crusher wear test data were compared with the surface fatigue wear data of the SET2 and SET3 materials.

The single groove tests of the SET2 materials were carried out by Hokka [Hokka04a]; the results and testing configurations are described elsewhere [Hokka04a, Saarinen06a]. The grooves were made using the modified split Hopkinson pressure bar, SHPB, technique modified by Kuokkala and Hokka [Kuokkala04a, Hokka04b], the assembly is seen in *Figure 57*. The scratching element is a wolfram carbide stylus with a 120-degree apex angle and 350 μm tip-end radius. Two different loads were used, 317 N and 464 N. The speed of the grooving element is 3,5 m/s at the beginning, but it decreases to zero during the grooving. The strain rate of material is difficult to estimate, because the material flows forwards, sideways and upwards in the forming groove [Kuokkala04a].

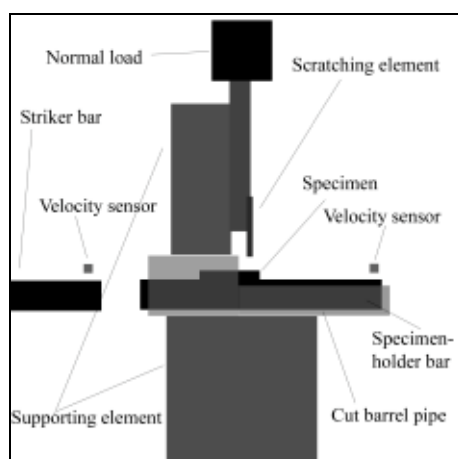


Figure 57 The assembly of the modified split Hopkinson pressure bar single-scratch testing device. [Hokka04a]

When comparing B90 wear results and SHPB groove volumes of the SET2 materials, *Figure 58*, it is observed that the materials with higher groove volumes in SHPB also have higher wear rates in the B90 test. Generally, the SHPB test and B90 tests have a similar ranking order of the materials in SET2. In the case of the 317 N load, a clear linear correlation is seen between these two tests, while in the case of 464 N load, the composite MM15 deviates from the linear trend. In MM15 composite, the matrix vanadium carbide content is highest and this metal-metal composite contains manganese steel. The low values in SHPB scratch tests indicate that no clear scratch is formed and the groove dimensions are close to those of the surface roughness.

Therefore, the higher values in the SHPB results are the most reliable. Sources of scatter for the material and B90 test were discussed earlier.

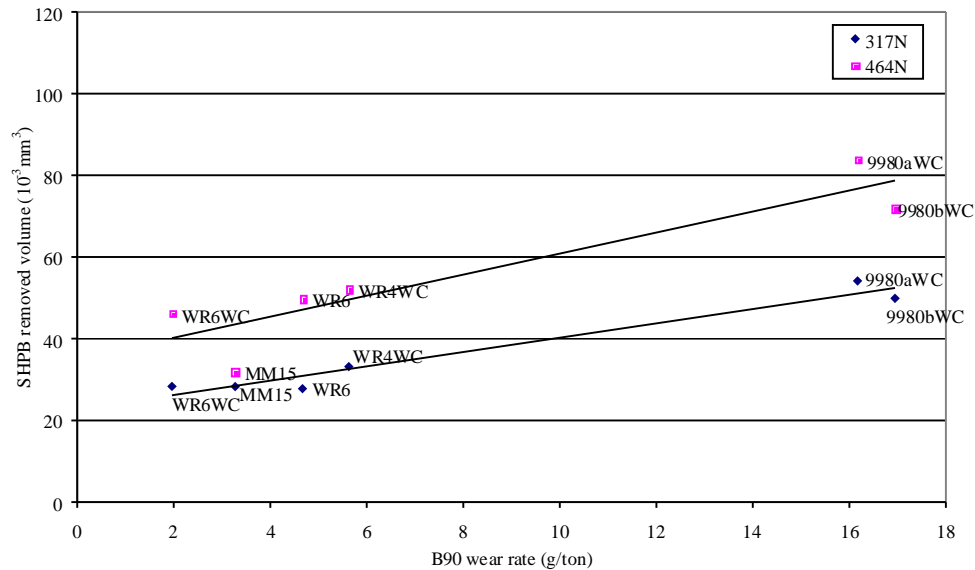


Figure 58 True removed groove volumes produced by the split Hopkinson pressure bar test at two forces (317N and 464 N) vs. wear rates in cone crusher B90 wear test of the SET2 composites (with granite stone as wearing material). The manganese-steel-based composite is not included in the plot. The true measured values are used in the figure and in the fitting; therefore, the cone crusher test wear rates are not transferred to volume losses. SHPB data from [Saarinen06a].

When combining the data from material sets SET2 and SET3, the correlation between groove volume and B90 wear rate will become more scattered and even non-linear, *Figure 59*. The SHPB wear groove volumes follow generally the nominal carbide content of the composites quite linearly, *Figure 60*. In the cone crusher wear tests, this correlation is not linear, *Figure 50*.

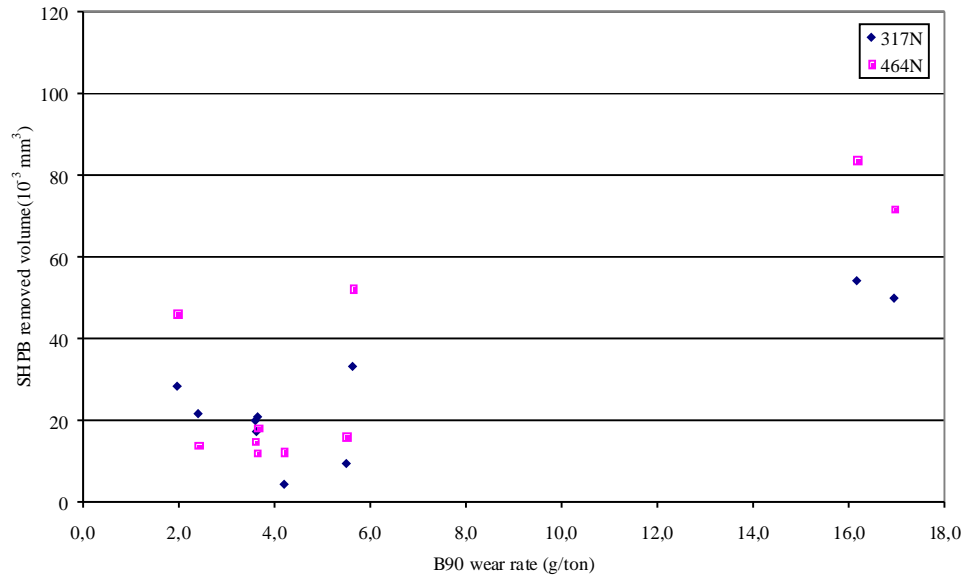


Figure 59 True removed groove volume (10^{-3} mm^3) produced by the Split Hopkinson Pressure Bar test at two forces vs. wear rates in cone crusher B90 wear test (g/ton) for both sets, SET2 and SET3 (no manganese steels included). SHPB data from [Saarinen06a].

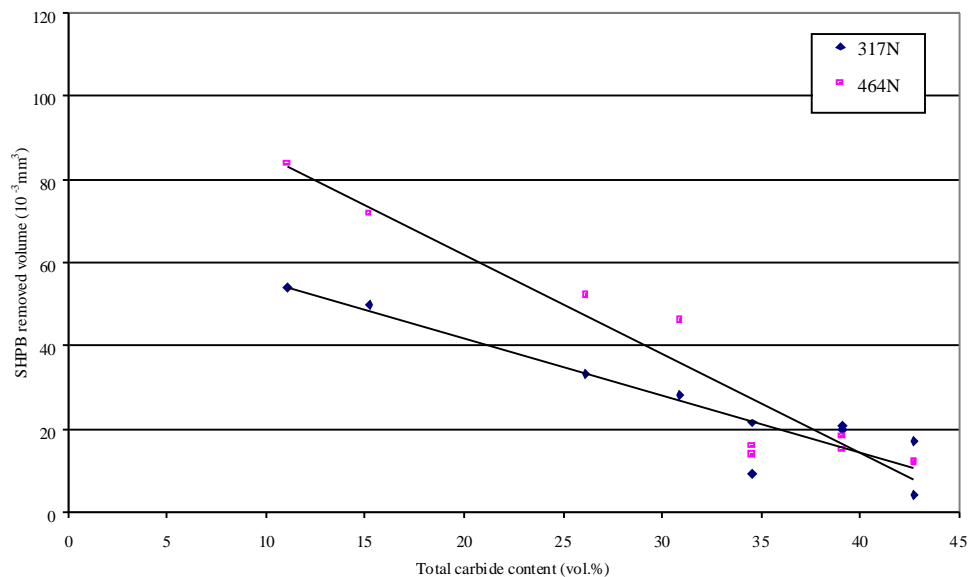


Figure 60 True groove volume (10^{-3} mm^3) produced by the Split Hopkinson Pressure Bar test vs. nominal carbide content (vol.%) of studied composite materials, in material sets SET2 and SET3 (no manganese steels included). SHPB data from [Saarinen06a].

Within the studied materials, the ranking order of the SET2 composites in SHPB experiments is similar to that of the laboratory cone crusher experiments; with SET3 this is not the case. The similar ranking orders within SET2 materials could be explained by the strong influence of matrix material on the penetration. In the case of SET3, where the matrix was fixed and reinforcements varied, the SHPB could not estimate the ranking order, probably for several reasons. The SHPB was a single wear event test as B90 is a simulative wear test including several wear modes. Scratching

represents only one wear mechanism type that occurs in a cone crusher. Also, simulative tests have considerably more statistical than single event tests. The wear volumes were small in tool-steel-based composites and therefore the measuring accuracy was not very good. For improving the accuracy of the results on tool-steel-based composites, the single scratch test has to be modified further.

Surface fatigue wear, SFW, testing configurations and results are described by [Hokka04a, Saarinen06a], a principle of the surface fatigue wear testing machine is seen in Figure 61. The SFW test system consists of a servohydraulic material testing machine with an external computer system used to control the x-y movement of the specimen by motors. The indenter is a 5 mm steel bearing ball. After each indentation, the specimen is moved by a distance of 200 μm to cover an area of 3*3 mm² with a regular rectangular pattern. The number of cycles of 30000, with a normal load of 1500 N was used to produce surface fatigue wear in the studied materials [Hokka04b].

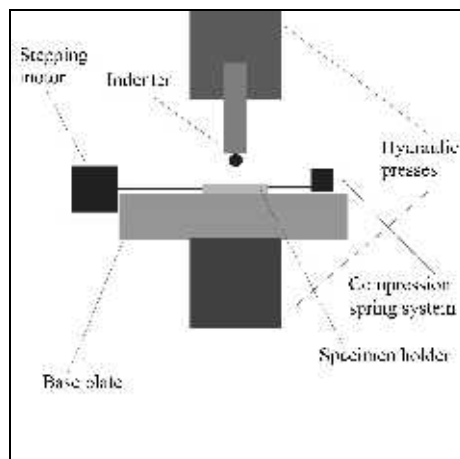


Figure 61 A side view of the surface fatigue wear testing machine. [Hokka04a]

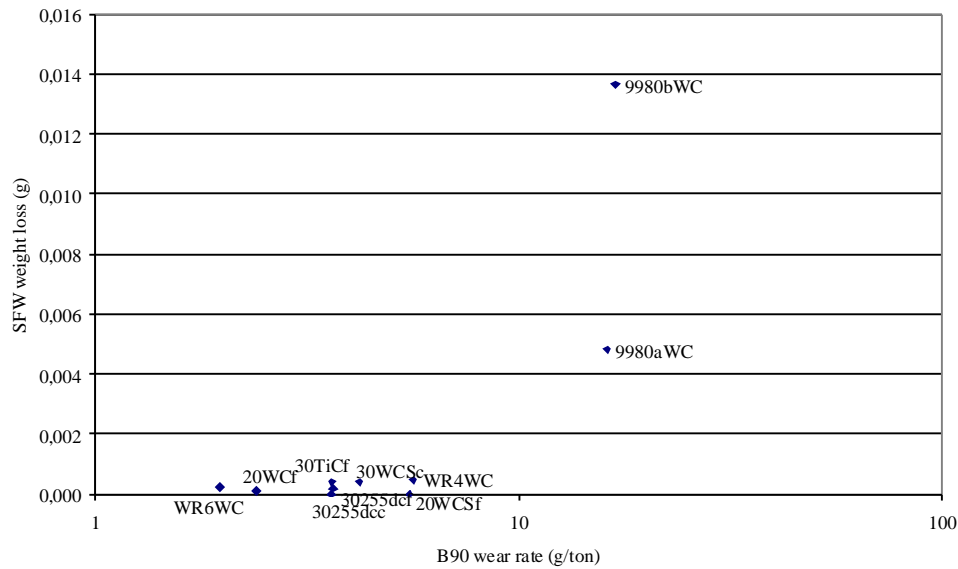


Figure 62 The cone crusher B90 test wear rate (g/ton) vs. surface fatigue weight loss (mg) (no manganese steels included) for both sets of materials, SET2 and SET3. SFW data from [Saarinen06a].

SFW weight losses have been plotted against cone crusher wear rates for both SET2 and SET3 materials, in *Figure 62*. The martensitic-steel-based composites had the highest wear rates and weight losses in both tests. The rest of the materials, i.e., tool-steel-based composites and tool steel, had small weight losses in the SFW test, but large differences in B90 tests. SFW values of SET3 were very low, i.e., there was negligible material removal from the surface on the tested parameters. This means that the testing parameters are not suitable for SET3 composites, resulting in no real material removal differences between composite materials. It seems that, under these circumstances (testing parameters), the SFW test could only estimate the limiting values for the cone crusher wear performance, but it cannot rank the materials otherwise in the same way as the cone crusher laboratory test.

5 SUMMARY AND CONCLUSIONS

The wear behaviour of different types of metal matrix composite material was studied in both abrasive and erosive laboratory tests and in simulative cone crusher test in order to explore the relation between microstructural material characteristics and wear behaviour. Powder metallurgical austenitic-, duplex- and heat-resistant-steel-based composites reinforced with Al_2O_3 or Cr_3C_2 ceramics were evaluated under abrasive and erosive wear conditions. The reinforcements were angular Al_2O_3 with a size fraction of 105-149 μm and Cr_3C_2 particles with size fractions 10-45 and 45-106 μm . Volume fraction varied mainly from 10 to 30%. In laboratory cone crusher experiments, there was a larger variation of the studied composite materials than in abrasive and erosive tests. In cone crusher wear tests the reinforcements of the composites were WC and TiC ceramics and WC/Co hardmetals, the reinforcement volume fractions varied from 11 to 30%, and the size of the reinforcement particles varied from 45 to 425 μm .

The microstructural parameters of the composites have a significant influence on the wear rate and wear resistance of the composites. This influence and its strength vary with the wear conditions, as confirmed on the basis of the results of this study. These parameters influence material properties, such as hardness and toughness, which are commonly connected to the wear performance of the material. The important findings from the studied reinforcement-related parameters were:

- 1) In the cone crusher wear environment, one of the most important parameters influencing the wear resistance was the *total* volume fraction of the hard particles. In the case of multi-phase structures, the total hard particle content of the composites is more important than added reinforcement content alone as far as the wear performance of materials is concerned.
- 2) In the cone crusher wear environment, the type of the hard particles has a very noticeable effect on material wear behaviour. It overshadows the effects of such internal parameters as reinforcement size and spacing between reinforcement particles.
- 3) In all the tested wear environments, the spacing between the hard particles is considered as an informative parameter. Sometimes it is even more informative than the size of the reinforcements. The spacing between reinforcements influences the homogeneity of the material microstructure involved in the wear event, i.e., the scale of the individual contacts at the fixed abrasive size. It also influences composite toughness. The role of the spacing or the reinforcement size in the wear process depends on external wear parameters, such as abrasive particle size.

Comparisons of wear tests:

- 4) Comparison of cone crusher wear data to the data produced by the single scratching test and multiple indentation test shows that the laboratory scale one-mode wear tests can only partly give the answers to wear problems. More realistic functional wear tests are needed for each individual application. The multi-mode wear system in a cone crusher is a complicated case.

Based on the present studies, the following conclusions can be drawn from the individual experiments.

For abrasive wear:

The important internal composite structure-related parameter having an effect on the abrasive wear rate is the volume fraction of hard particles. The abrasive wear rate of tested composite materials decreased with increasing hard particle content in the dry sand rubber wheel tests. The wear rate can be decreased over 80%, with a reinforcement volume percent increase from 0 to 30.

Concerning the average reinforcement particle sizes of composites, composites with smaller reinforcement sizes have lower wear rates as compared to coarse reinforcements. The wear rate decreases by about 30 percent with the finer carbide reinforced composites as compared to coarse carbides of the same type.

The spacing between particles is a more informative internal parameter than the size of the reinforcements. The spacing between the reinforcements is related to the composite homogeneity in the abrasive wear environment more than the other parameters evaluated here. Spacing determines the physical limit for abrasive particles to penetrate between reinforcing particles. Therefore the influence of particle spacing (as well as reinforcement size) on the wear rate is strongly dependent on the abrasive particle size.

The hardness of the composite shows a clear correlation with dry sand rubber wheel volume losses. The wear rate decreases with increasing composite hardness.

For erosive wear (two impact angles 30-degree and 60-degree):

The increase of the volume fraction of the reinforcement particles did not have a marked effect on the wear rates; the erosive wear behaviour depended strongly on the erodent impact angle. At a 60-degree impact angle, the increase of reinforcement volume fraction increased wear rate, about a 50% increase in wear rate was observed with 40 vol.% reinforcement as compared to plain matrix material. On the other hand, at a 30-degree impact angle, a slight improvement in wear resistance with increasing volume fraction was noticed up to 30 vol.% reinforcement addition.

The spacing between reinforcements turned out to be an informative parameter. Larger spacing improved wear resistance of the composites with the highest volume fractions of hard phase at both impact angles. It is known that the increase of the hard particle spacing increases the fracture toughness of the composites. Toughness is also considered as an important parameter, since in erosion fracturing determines the wear resistance, especially at normal and high (>60) impact angles. Composites having apparently higher toughness and larger spacing between reinforcement particles had a better wear resistance in the studied erosive wear conditions than those with smaller spacing.

For laboratory cone crusher wear and internal composite parameters:

The primary parameters, which influenced the wear behaviour of the composites, were the total hard particle content and the type of the hard particles.

The total hard particle content of the composites is more important than the reinforcement particle content. The effect of the increasing total carbide content was significant in decreasing wear rates. The reinforcement content

between the composites could be similar, but the wear rate of the different composites could vary by hundreds of percentage points, depending on the matrix selection. The role of the matrix characteristics and the matrix carbide content, i.e., the total carbide content, was more crucial than that of the reinforcement particles in the formation of wear rates.

The reinforcement type seems to be a noticeably strong factor in material wear behaviour. It overshadows such internal parameters as size and spacing of reinforcement particles. The size of the reinforcement and the spacing between reinforcements have earlier been found to affect the wear rates, e.g., in the present study in DSRW tests. However, in the present testing configuration, no general trends between the size and spacing between reinforcement particles and the wear rate were found.

It is shown clearly that each individual composite has to be evaluated separately, because different types of reinforcement have different effects on composite wear rate as a function of reinforcement volume fraction. In further studies aimed at decreasing the wear rate, the wear performance of composites with a finer size of the true carbides and larger spacing between reinforcements than studied in the present tests should be evaluated on the basis of the trend-setting mapping.

For laboratory cone crusher multi-mode wear system:

The real industrial complicated multi-mode wear systems have to be evaluated by functional wear tests with as realistic surface loading exposures as possible. Neither the single scratching event test nor the multiple indentation test could result completely in a material ranking order similar to that of the cone crusher wear experiment, where both particle sliding and indentation were present.

The single scratching event test, i.e., the split Hopkinson pressure bar (SHPB) test, gives a ranking order similar to that of the cone crusher wear test, when the composite total hard particle content and matrix material are the studied variables. However, when the matrix material was fixed and several types of reinforcements were used with a relatively narrow range of volume fractions, the SHPB test could not estimate the ranking order of the materials in cone crusher B90 wear tests. Generally, sliding and scratching are present in the cone crusher wear process, but the composites with different types of reinforcements resulted in a different wear-rate ranking order in the SHPB and B90 tests.

Under the circumstances, the surface fatigue wear (SFW) test could only estimate the limiting parameter values for good cone crusher wear performance; it could not rank the materials otherwise for the cone crusher laboratory test. The same steel-based composites were ranked as worst behaving both in the SFW test and the B90 test; all of the other materials had relatively low weight losses in the SFW test.

REFERENCES

- [Ala-Kleme04a] S. Ala-Kleme, WC/Co -lujitettujen teräsmatriisikomposiittien kulumis- ja sitkeysominaisuudet, Diplomityö, Espoo, Finland 2004, p. 109. In Finnish.
- [ASTMG65-91] ASTM G65-91, "Standard Test Method for Measuring Abrasion Using the Dry Sand/Rubber Wheel Apparatus," ASTM International.
- [Axen94a] N. Axen and S. Jacobson, A model for the abrasive wear resistance of multiphase materials, *Wear* 174 (1994) pp. 187-199.
- [Axen95a] N. Axen, B. Lundberg, Abrasive wear in intermediate mode of multiphase materials, *Tribology International* Vol. 28, No. 8, pp. 523-529, 1995.
- [Berns95a] Hans Berns, Microstructural properties of wear-resistant alloys, *Wear* 181-183 (1995) pp. 271-279.
- [Berns97a] Hans Berns, Sinesio Franco, Effect of coarse hard particles on high-temperature sliding abrasion of new metal matrix composites, *Wear* 203-204 (1997) 608-614.
- [Berns98a] Hans Berns, Nguyen van Chuong, Hartverbundwerkstoff mit zweistufigem Dispersionsgefüge in Hartlegierungen und Hartverbundwerkstoffe, Befüge, Eigenschaften, Bearbeitung, Anwendung, Hrsg. Hans Berns, Springer-Verlag Berlin Heidelberg 1998. In German.
- [Berns98b] Hans Berns, A. Melander, D. Weichert, N. Asnafi, C. Broeckmann, A. Gross-Weege, A new material for cold forging tools, *Computational Materials Science* 11 (1998) pp. 166-180.
- [Berns98c] Hans Berns, Wear resistant MMC with improved toughness and corrosion resistance, PM World Congress, Oct.1998 Granada.
- [Berns99a] Hans Berns, Stefan Koch, High temperature sliding abrasion of a nickel-base alloy and composite, *Wear* 225-229 (1999) 154-162.
- [Berns99b] Hans Berns, Influence of abrasive particles on wear mechanism and wear resistance in sliding abrasion test at elevated temperatures, *Wear* 233-235 (1999) 424-430.
- [Berns03a] Hans Berns, Comparison of wear resistant MMC and white cast iron, *Wear* 254 (2003) 47-54.

- [Bingley04a] M.S. Bingley, D.J. O'Flynn, Examination and comparison of various erosive wear models, *Wear*, Volume 258, (2005) 511-525.
- [Blau92a] P. J. Blau, Glossary of Terms in ASM Handbook, Vol. 18 Friction, Lubrication and Wear Technology, printed in USA, 1992, 942 p.
- [Blau04a] P.J. Blau, Friction, wear and surface testing in ASM Handbook Vol. 8 Mechanical testing and evaluation, <http://products.asminternational.org/hbk/index.jsp> 6.9.2004
- [Broeckmann96a] C. Broeckmann, A. Pyzalla-Schiek, Microstructural aspects of failure in particle reinforced metal matrix composites, *Computational Materials Science* 5 (1996) pp. 32-44.
- [Colaco03a] R. Colaco, R. Vilar, A model for abrasive wear of metallic matrix particle-reinforced materials, *Wear* 254 (2003) 625-634.
- [Courtney00a] Courtney, T.H., Mechanical Behavior of Materials, 2nd. Ed., McGraw-Hill Companies, Inc., Singapore, 2000, 733 p.
- [Deng01a] Xin Deng, B.R. Patterson, K.K.Chawla, M.C. Koopman, Z. Fang, G. Lockwood, A. Griffo, Mechanical properties of a hybrid cemented carbide composite, *International Journal of Refractory Metals & Hard Materials* 19 (2001) 547-552.
- [Deng02a] Xin Deng, B.R. Patterson, K.K.Chawla, M.C. Koopman, C. Mackin, Z. Fang, G. Lockwood, A. Griffo, Microstructure/hardness relationship in a dual composite, *Journal of Material Science Letters* 21, 2002, 707-709.
- [Dixon04a] R.B. Dixon, W. Stasko, and K.E. Pinnow, Cold-Work Particle Metallurgy Tool Steels in Vol. 7 Powder Metal Technologies and Application, ASM Handbook online, <http://products.asminternational.org/hbk/index.jsp> 3.12.2004
- [Dogan01a] Ö.N. Doğan, J.A. Hawk, J.H. Tylczak, Wear of cast chromium steels with TiC reinforcement, *Wear* 250 (2001) 462-469.
- [Eloranta95a] J. Eloranta, Influence of Crushing Process Variables on the Product Quality of Crushed Rock, PhD Thesis, Tampere University of Technology, Publication 168, Finland 1995, pp. 118.
- [Fang01a] Z. Zak Fang, Anthony Griffo, Brian White, Greg Lockwood, Dan Belnap, Greg Hilmas, Jonathan Bitler, Fracture resistant super hard materials and hardmetals composite with functionally designed microstructure, *International Journal of Refractory Metals and Hard Materials* 19 (2001) 453-459.

- [Finnie95a] Iain Finnie, Some reflection on the past and future of erosion, *Wear* 186-187 (1995) 1-10.
- [GOST23.201-78] GOST 23.201-78, Products wear resistance assurance. Gas abrasive wear testing of materials and coatings with centrifugal accelerator. Standards Publishing House, Moscow, 1978. In Russian.
- [Hawk99a] J.A. Hawk, R.D. Wilson, J.H. Tylczak, Ö.N. Doğan, Laboratory abrasive wear tests: investigation of test methods and alloy correlation, *Wear* 225-229 (1999) 1031-1042.
- [Hawk01a] Jeffrey A. Hawk, R.D. Wilson, chapter 35 Tribology of Earthmoving Mining and Minerals Processing, *Modern Tribology Handbook*, editor B. Bhushan, Volumes 1-2., USA, CRC Press, 2001.
- [Heinonen00a] Mirva Heinonen, Microstructural control in the Powder Metallurgical Processing of Cr₃C₂ Reinforced Steel Matrix Composites. Master's thesis, Helsinki University of Technology, Department of Materials Science and Rock Engineering, Laboratory of Physical Metallurgy and Materials Science, Espoo, November, 17, Finland 2000.
- [Hertzberg96a] Richard W. Hertzberg, Deformation and fracture mechanics of engineering materials, fourth edition, John Wiley & Sons, Inc., United States of America 1996, 786 p.
- [Hokka04a] Mikko Hokka, Material Behavior Under Heavy Abrasion and Gouging, a thesis presented for examination for the degree of Master of Science in Engineering, Tampere, Finland 2004, p. 75.
- [Hokka04b] M. Hokka, V.-T. Kuokkala, P. Siitonen, J. Liimatainen, Experimental techniques for studying the behaviour of wear resistant materials under dynamic gouging and surface fatigue, ICEM12 – 12th International conference on Experimental Mechanics, 29 August- 2 September, 2004 Politecnico di Bari, Italy.
- [Hovis86a] S.K. Hovis, J.E. Talia, R.O. Scattergood, Erosion in multiphase systems, *Wear*, 108 (1986) 139-155.
- [Hsu01a] S.M. Hsu, M.C. Shen, Wear Maps Ch. 9 in *Modern Tribology Handbook*, ed. Bharat Bhushan, 2001 by CRC Press LCC. (electronic)
- [Hussainova01b] I. Hussainova, Some aspects of solid particle erosion of cermets, *Tribology international* 34 (2001) 89-93.

- [Hussainove03a] I. Hussainova, Effect of microstructure on the erosive wear of titanium carbide-based cermets, *Wear* 255 (2003) 121-128.
- [Hutchings92a] I.M. Hutchings, *Tribology: Friction and Wear of Engineering Materials*, Edward Arnold, Great Britain, 1992, 273 p.
- [Jacobson96a] S. Jacobson, S. Hogmark, *TRIBOLOGI Friction Smörning Nötning*, Karlebo-serien ISBN 91-634-1532-1, Liber Utbidning AB, Sverige, 1996, 260 p. In Swedish.
- [Kato01a] Koji Kato, Koshi Adachi, Chapter 7 Wear Mechanisms in *Modern Tribology Handbook*, editor B. Bhushan, Volumes 1-2., USA, CRC Press, 2001.
- [Kleis05a] Ilmar Kleis, Priit Kulu, *Solid particle erosion, Occurrence, Prognostication and Control*, ISBN 9985-59-561-0, Tallinn University Press, Estonia, 2005, 233 p.
- [Kosel92a] H. Kosel, *Solid particle erosion in ASM Handbook*, Vol. 18 Friction, Lubrication and Wear Technology, printed in USA, 1992, 942 p.
- [Kübarsepp01a] Jacob Kübarsepp, Heinrich Klaasen, Jüri Pirso, Behaviour of TiC-base cermets in different wear conditions, *Wear* 249 (2001) 229-234.
- [Kulu02a] P. Kulu, T.Phil, Selection Criteria for Wear resistant Powder Coatings Under Extreme Erosive Wear Conditions, *Journal of Thermal Spray Technology*, Volume 11 (4) December 2002, 517-522.
- [Kulu04a] P. Kulu, I. Hussainova, R. Veinthal, Solid particle erosion of thermal sprayed coatings, *Wear* 258 (2005) 488-496.
- [Kuokkala04a] V.-T. Kuokkala, M. Hokka, J. Rämö, T. Vuoristo, Dynamic scratch testing of wear resistant materials by a modified Hopkinson Split Bar device, 15th Technical meeting DYMAT, Metz 1-2 June 2004.
- [Lee02a] Gun Y. Lee, C.K.H. Dharan, R.O. Ritchie, A Physically-based abrasive wear model for composite materials, *Wear* 252 (2002) 322-331.
- [Levin 00a] B.F. Levin, J. N. DuPont, A.R. Marder, The effect of second phase volume fraction fraction on the erosion resistance of metal-matrix composites, *Wear* 238 (2000) 160-167.
- [Lim98a] S.C. Lim, Recent developments in wear-mechanisms maps, *Tribology International* Vol.31, Nos 1-3, pp. 87-97, 1998.

- [Lindqvist03a] M. Lindqvist, C. M. Evertsson, Linear wear in jaw crushers, Mineral Engineering 16 (2003) 1-12.
- [Lindqvist03b] M. Lindqvist, D. M. Evertsson, Prediction of worn geometry in cone crushers, Minerals Engineering 16 (2003) 1355-1361.
- [Lindqvist05a] M. Lindqvist, Wear in cone crusher chambers, Doctoral dissertation, Department of Applied Mechanics, Chalmers University of Technology, Göteborg, Sweden 2005, 36 p and publications.
- [Liu03a] Xuwen Liu, A study on the erosion and erosion-oxidation of metal matrix composites, Doctoral dissertation, Helsinki University of Technology, 2003, 108 p.
- [Lou02a] D. Lou, J. Hellman, O.M. Akselsen, V. Lindroos, Development of Steel Matrix Composite for Forming Tools, 44th Mechanical Working and Steel Processing Conference, September 8-10, 2002, Orlando, FL, USA.
- [Lou03a] D. Lou, J. Hellman, D. Luhulima, J. Liimatainen, V.K. Lindroos, Interactions between tungsten carbide (WC) particulates and metal matrix in WC-reinforced composites, Materials Science and Engineering A340 (2003) pp. 155-163.
- [Meng 95a] H.C. Meng, K.C. Ludema, Wear models and predictive equations: their form and content, Wear 181-183 (1995) pp. 443-457.
- [Nemat-Nasser01] S. Nemat-Nasser, Introduction to high strain rate testing, in ASM Handbook vol. 8: Mechanical Testing and Evaluation. 2001, Materials Park, Ohio, P. 427-512.
- [Osara01a] Karri Osara, Characterization of abrasion, impact-abrasion and impact wear of selected materials, Doctoral dissertation, Tampere University of Technology, Finland 2001.
- [Osara03a] K. Osara, T. Tainen, Three-body impact wear study on conventional and new P/M + HIPed wear resistant materials, Wear 250 (2001) 785-794.
- [Pagounis96a] E. Pagounis, M. Talvitie, V. K. Lindroos, Influence of reinforcement volume fraction and size on the microstructure and abrasion wear resistance on hot isostatic pressed white iron matrix composites, Met. and Mat. Transact. A, Vol. 27A, 1996, pp. 4171-4181.

- [Pagounis 98a] E. Pagounis, V.K. Lindroos, Processing and properties of particulate reinforced steel matrix composites, materials Science and Engineering A246 (1998) pp. 221-234.
- [Pirso 04a] Jüri Pirso, Sergei Letunoviš, Mart Viljus, Friction and Wear of cemented carbides, Wear 257 (2004) 257-265.
- [Roberts04a] <http://users.ox.ac.uk/~roberts/sgrgroup/lectures/engalloys/intro.pdf> 1.6.2004
<http://www-sgrgroup.materials.ox.ac.uk/lectures/engalloys/intro.pdf> 5.7.2006
- [Roberts06a] <http://www-sgrgroup.materials.ox.ac.uk/lectures/tribology/wear.pdf> 5.7.2006
- [Runkle94a] J.C. Runkle, US Patent Number 5,290,507, Date of Patent Mar.1, 1994.
- [Ruuskanen06a] Jaakko Ruuskanen, Influence of Rock Properties on Compressive Crusher Performance, Doctoral dissertation, Tampere University of Technology, Publication 585, Finland 2006, 236 p.
- [Saarinen06a] T. Saarinen, M. Hokka, V.-T. Kuokkala, SFW and Scratch Resistance of Selected Materials, Tampere University of Technology, 2006, ISBN 952-15-1556-2, ISSN 1459-4161.
- [Shin87a] Y. W. Shin, G. A. Sargent, H. Conrad, Effect of Microstructure on the Erosion of Al-Si Alloys by Solid Particles, Metallurgical Transactions A, Volume 18A, March 1987, 437-450.
- [Siipilehto04a] S. Siipilehto, Homogeneity optimization of PM steel matrix composites, a thesis presented for examination for the degree of Master of Science in Engineering, Espoo, Finland 2004, p. 89.
- [Stack97a] M.M. Stack, D. Pena, Solid particle erosion of Ni-Cr/WC metal matrix composites at elevated temperatures: construction of erosion mechanisms and process control maps, Wear 203-204 (1997) 489-497.
- [Stack99a] M.M. Stack, D. Pena, Particle size effect of the elevated temperature erosion behaviour of Ni-Cr/WC MMC-based coatings, Surface and Coating Technology 113 (1999) 5-12.
- [Stack 01a] M.M. Stack, D. Pena, Mapping erosion of Ni-Cr/WC-based composites at elevated temperatures: some recent advances, Wear 251 (2001) 1433-1443.
- [Sundararajan83a] G. Sundararajan, P.G. Shewmon, The use of dynamic impact experiments in the determination of the strain rate sensitivity of metals and alloys, Acta Metall., 1983, vol. 31, pp.101-109.

- [Sundararajan91a] G. Sundararajan, A comprehensive model for the solid particle erosion of ductile metals, *Wear*, 1991, vol, 149, pp. 111-127.
- [Söderberg81a] S. Söderberg, S. Hogmark, U. Engman, H. Swahn, Erosion classification of materials using a centrifugal erosion tester, *Tribology international*, December 1981, pp. 333-343.
- [Theisen01a] Werner Theisen, A novel PM-wear protection method to meet high comminution demands, *Wear* 250 (2001) 54-58.
- [Theisen04a] Werner Theisen, "Metal Matrix Composites" widerstehen dem Verschleiss: walzen aus pulver, <http://www.ruhr-uni-bochum.de/rubin/maschinenbau/werkstoffe.htm> 25.11.2004.
- [Tikomet06a] <http://www.tikomet.fi/tikomet.html> 14.10.2005.
- [Tirupataiah91a] Y. Tirupataiah, G. Sundararajan, A dynamic indentation technique for the characterization of the high strain rate plastic flow behaviour of ductile metals and alloys, *J. Mech. Phys. Solids* Vol. 39, No.2, pp. 243-271, 1999.
- [Tylczak92a] J.H. Tylczak, Abrasive wear in *ASM Handbook*, Vol. 18 Friction, Lubrication and Wear Technology, printed in USA, 1992, 942 p.
<http://products.asminternational.org/hbk/index.jsp> 19.10.2006
- [UTHSCSA04a] <http://ddsdx.uthscsa.edu/dig/itdesc.html> 1.6.2004
- [Veinthal05a] Renno Veinthal, Characterization and Modelling of Erosion Wear of Powder Composite Materials and Coatings, Doctoral dissertation, Tallinna University of Technology, Estonia 2005, 128 p.
- [Williams99a] J. A. Williams, Wear modelling: analytical, computational and mapping: a continuum mechanics approach, *Wear* 225-229 (1999) 1-17.
- [ZumGahr87a] Karl-Heinz Zum Gahr, *Microstructure and wear of materials*, Tribology series 10, Elsevier Science Publishers B.V., Netherlands, 1987, p. 560.